

**MITIGATING NEW YORK CITY'S HEAT ISLAND WITH  
URBAN FORESTRY, LIVING ROOFS, AND LIGHT SURFACES**

**NEW YORK CITY REGIONAL HEAT ISLAND INITIATIVE**  
Final Report

Prepared for

**THE NEW YORK STATE  
ENERGY RESEARCH AND DEVELOPMENT AUTHORITY**  
Albany, NY

Peter Savio, Project Manager

Prepared by

**COLUMBIA UNIVERSITY CENTER FOR CLIMATE SYSTEMS RESEARCH &  
NASA/GODDARD INSTITUTE FOR SPACE STUDIES**  
New York, NY

Cynthia Rosenzweig, Principal Investigator

and

**DEPARTMENT OF GEOGRAPHY, HUNTER COLLEGE – CUNY**  
New York, NY

William D. Solecki, Principal Investigator

and

**SAIC**  
Albany, NY

Ronald B. Slosberg, Principal Investigator

NYSERDA Contract # 6681

June 2006

## **NOTICE**

This report was prepared by the Columbia University Center for Climate Systems Research at the Goddard Institute for Space Studies, Hunter College – CUNY, and SAIC Corporation in the course of performing work contracted for and sponsored by the New York State Energy Research and Development Authority (hereafter “NYSERDA”). The opinions expressed in this report do not necessarily reflect those of NYSERDA or the State of New York, and reference to any specific product, service, process, or method does not constitute an implied or expressed recommendation or endorsement of it. Further, NYSERDA, the State of New York, and the contractor make no warranties or representations, expressed or implied, as to the fitness for particular purpose or merchantability of any product, apparatus, or service, or the usefulness, completeness, or accuracy of any processes, methods, or other information contained, described, disclosed, or referred to in this report. NYSERDA, the State of New York, and the contractor make no representation that the use of any product, apparatus, process, method, or other information will not infringe privately owned rights and will assume no liability for any loss, injury, or damage resulting from, or occurring in connection with, the use of information contained, described, disclosed, or referred to in this report.

## **ABSTRACT AND KEYWORDS**

This study uses a regional climate model (MM5) in combination with observed meteorological, satellite, and GIS data to determine the impact of urban forestry, living (green) roofs, and light-colored surfaces on near-surface air temperature and the urban heat island in New York City. Nine mitigation scenarios are evaluated city-wide and in six case study areas. Temperature impacts are calculated both on a per-unit area basis, as well as taking into account the available land area for implementation, and other physical constraints. The scenarios are then evaluated based on their cost-effectiveness at reducing air temperature and resulting energy demand. All the mitigation strategies have a significant temperature impact. A combined strategy that maximizes the amount of vegetation in New York City by planting trees along streets and in open spaces, as well as by building living (or green) roofs (i.e. ecological infrastructure), offers more potential cooling than any individual strategy. Among the single-strategy scenarios, light surfaces, light roofs, and living roofs can potentially reduce the summer peak electric load more than the other strategies. The choice of a strategy should consider the characteristics and priorities of the neighborhood, including benefit/cost factors and the available area for implementation of each strategy.

Keywords – urban heat island mitigation, energy demand, cost-benefit analysis, MM5

**Editors**

Cynthia Rosenzweig Columbia University Center for Climate Systems Research and  
NASA/Goddard Institute for Space Studies  
William D. Solecki Hunter College – City University of New York  
Lily Parshall Columbia University Center for Climate Systems Research  
Sara Hodges Hunter College – City University of New York

**Project Members*****Observed Data and Model Evaluation***

Richard Goldberg Columbia University Center for Climate Systems Research  
Stuart Gaffin Columbia University Center for Climate Systems Research

***Remote Sensing and GIS Analysis***

Jennifer Cox Hunter College – City University of New York and  
Regional Plan Association

***Statistical Analysis and Case Study Synthesis***

Sara Hodges Hunter College – City University of New York

***MM5 Regional Climate Model***

Barry Lynn Columbia University Center for Climate Systems Research

***Mitigation Scenarios***

Cynthia Rosenzweig Columbia University Center for Climate Systems Research and  
NASA/Goddard Institute for Space Studies  
William D. Solecki Hunter College – City University of New York  
Lily Parshall Columbia University Center for Climate Systems Research

***Air Quality and Public Health***

Patrick Kinney Columbia University Mailman School of Public Health  
Joyce Rosenthal Columbia University School of Architecture, Planning, and  
Preservation  
Rob Crauderueff Sustainable South Bronx

***NYSERDA and DEC Partners***

Peter Savio New York State Energy Research and Development Authority  
Mark Watson New York State Energy Research and Development Authority  
Elizabeth Perry New York State Energy Research and Development Authority  
Janet Joseph New York State Energy Research and Development Authority  
Frank M. Dunstan New York State Department of Environmental Conservation  
Kevin Civerolo New York State Department of Environmental Conservation

***Editorial Support***

Todd Paul New York State Energy Research and Development Authority

**Advisory Committee**

Matthew Hudson Arn	United States Department of Agriculture Forest Service
David F. Bomke	New York Energy Consumers Council, Inc.
John Dickinson	New York City Mayor's Office of Environmental Coordination
Adam W. Hinge	Sustainable Energy Partnerships
Laurie Kerr	New York City Department of Design and Construction
Edward J. Linky	United States Environmental Protection Agency – Region II
Jacqueline Lu	New York City Department of Parks and Recreation
Joseph Madia	Consolidated Edison Company of New York
Sandra Meier	Environmental Energy Alliance of New York
Stephen A. Pertusiello	Consolidated Edison Company of New York
Nicole Rodriguez	New York City Department of City Planning
Gopal Sistla	New York State Department of Environmental Conservation
Megan Sheremata	New York State Department of Environmental Conservation
Fiona Watt	New York City Department of Parks and Recreation
Michael Weil	City of New York Department of City Planning
Eva Wong	United States Environmental Protection Agency

## TABLE OF CONTENTS

<u>Section</u>	<u>Page</u>
<b>PREFACE</b> .....	<b>xiv</b>
<b>SUMMARY</b> .....	<b>S-1</b>
<b>1 INTRODUCTION</b> .....	<b>1</b>
<b>Project Objectives</b> .....	<b>3</b>
<b>Key Questions</b> .....	<b>4</b>
<b>Urban Heat Island Processes</b> .....	<b>4</b>
<b>The Urban Heat Island of New York City</b> .....	<b>6</b>
<b>Urban Heat Island Mitigation Strategies</b> .....	<b>7</b>
<b>Case Study Areas</b> .....	<b>12</b>
<b>2 DETERMINING TEMPERATURE IMPACTS: STUDY METHODS, DATA, AND MODELS</b> .....	<b>21</b>
<b>Identification of Heat-Wave Periods</b> .....	<b>21</b>
<b>Characterization of New York City’s Heat Island on Heat-Wave Days</b> .....	<b>23</b>
<b>Remote Sensing Data</b> .....	<b>23</b>
<b>NDVI and Albedo</b> .....	<b>25</b>
<b>GIS Data</b> .....	<b>27</b>
<b>Land Surface Data</b> .....	<b>28</b>
<b>Statistical Analysis</b> .....	<b>31</b>
<b>MM5 Regional Climate Model</b> .....	<b>35</b>
<b>Mitigation Scenarios</b> .....	<b>39</b>
<b>3 CITY-WIDE TEMPERATURE IMPACTS</b> .....	<b>44</b>
<b>Answers to Key Questions on Temperature Impacts</b> .....	<b>45</b>
<b>Discussion of City-Wide Results</b> .....	<b>48</b>
<b>Urban Heat Island Simulations with MM5</b> .....	<b>49</b>
<b>4 CASE STUDY TEMPERATURE IMPACTS</b> .....	<b>52</b>
<b>Mid-Manhattan West</b> .....	<b>52</b>
<b>Lower Manhattan East</b> .....	<b>53</b>
<b>Fordham Bronx</b> .....	<b>54</b>
<b>Maspeth Queens</b> .....	<b>54</b>
<b>Crown Heights Brooklyn</b> .....	<b>55</b>
<b>Ocean Parkway Brooklyn</b> .....	<b>56</b>
<b>5 ENERGY DEMAND ANALYSIS</b> .....	<b>58</b>
<b>Temperature versus kW Load Model</b> .....	<b>58</b>
<b>MM5 Temperature Impacts</b> .....	<b>62</b>

<b>Estimating Electric Load Impacts</b> .....	<b>64</b>
<b>6 COST-BENEFIT ANALYSIS</b> .....	<b>67</b>
<b>Mitigation Scenario Costs</b> .....	<b>67</b>
<b>Cost - Benefit Modeling</b> .....	<b>70</b>
<b>Analysis Assumptions and Limitations</b> .....	<b>71</b>
<b>Results</b> .....	<b>72</b>
<b>Answers to Key Questions on Costs and Benefits</b> .....	<b>73</b>
<b>7 OTHER BENEFITS OF MITIGATION STRATEGIES</b> .....	<b>78</b>
<b>Air Quality and Public Health</b> .....	<b>78</b>
<b>Greenhouse Gas Emissions</b> .....	<b>79</b>
<b>8 CONCLUSIONS</b> .....	<b>81</b>
<b>9 FURTHER RESEARCH</b> .....	<b>83</b>
<b>10 RECOMMENDATIONS</b> .....	<b>84</b>
<b>11 REFERENCES</b> .....	<b>85</b>
<b>APPENDIX A Tree Species Selection for New York City (Nowak, USFS)</b> .....	<b>93</b>
<b>APPENDIX B Evaluation of WeatherBug® Data Quality</b> .....	<b>110</b>
<b>APPENDIX C Remote Sensing Surface Temperature Algorithm</b> .....	<b>112</b>
<b>APPENDIX D Additional GIS Data</b> .....	<b>113</b>
<b>APPENDIX E Borough-Level Statistical Analysis</b> .....	<b>116</b>
<b>APPENDIX F Evaluation of MM5 v3.7+SEBM</b> .....	<b>119</b>

## FIGURES

### Figure

- S-1 Case study areas and weather stations. Grid boxes correspond to the MM5 model 1.3 km grid.
- S-2 Remotely sensed thermal satellite data. Landsat ETM, August 14, 2002, at 10:30 AM, Band 6, resolution is 60 meters.
- S-3 City-wide costs for selected mitigation scenarios (in millions).
- S-4 Costs for selected mitigation scenarios (in millions) by case study area.
- S-5 Cost per city-wide on-peak megawatt reduction (in millions).
- S-6 Cost per on-peak megawatt reduction (in millions) for case study areas.
- 1-1 Case study areas and weather stations. Grid boxes correspond to the MM5 model 1.3 km grid.
- 1-2 Diagram illustrating a typical non-urban energy balance as compared to a typical urban energy balance. Longer arrows denote a greater heat flux (e.g. latent heat flux is larger in non-urban areas than in urban areas; sensible heat flux is larger in urban areas than in non-urban areas).
- 1-3 Variability in satellite-derived surface heating between the day and night from a MODIS day-night pair. September 8, 2002, resolution is 1 km. a) 10:30 AM, b) 10:30 PM.
- 1-4 Example of a living roof. Hamilton City Apartments, Portland OR. Source: Environmental Services of Portland Brochure.
- 1-5 Mid-Manhattan West case study area. a) aerial view, b) street view, c) gridded surface temperature on September 8, 2002 with resolution of 250 meters, d) gridded NDVI with resolution of 250 meters.
- 1-6 Lower Manhattan East case study area. a) aerial view, b) street view, c) gridded surface temperature on September 8, 2002 with resolution of 250 meters, d) gridded NDVI with resolution of 250 meters.
- 1-7 Fordham Bronx case study area. a) aerial view, b) street view, c) gridded surface temperature on September 8, 2002 with resolution of 250 meters, d) gridded NDVI with resolution of 250 meters.



- 1-8 Maspeth Queens case study area. a) aerial view, b) street view, c) gridded surface temperature on September 8, 2002 with resolution of 250 meters, d) gridded NDVI with resolution of 250 meters.
- 1-9 Crown Heights Brooklyn case study area. a) aerial view, b) street view, c) gridded surface temperature on September 8, 2002 with resolution of 250 meters, d) gridded NDVI with resolution of 250 meters.
- 1-10 Ocean Parkway Brooklyn case study area. a) aerial view, b) street view, c) gridded surface temperature on September 8, 2002 with resolution of 250 meters, d) gridded NDVI with resolution of 250 meters.
- 2-1 Heat-wave days during the summer of 2002. a) Maximum, minimum, and mean daily temperature, b) Daily temperature anomaly.
- 2-2 Remotely sensed thermal satellite data. Landsat ETM, August 14, 2002 at 10:30 AM, Band 6, resolution is 60 meters.
- 2-3 Landsat July 22, 2002 image imbedded in MM5 1.3 km grid cells.
- 2-4 Normalized difference vegetation index (NDVI) derived from September 8, 2002 Landsat image. NDVI is a non-linear transformation of the visible (red) and near-infrared bands of satellite information. NDVI is defined as the difference between the red and near-infrared (nir) bands, over their sum [ $NDVI = \frac{nir - red}{nir + red}$ ]. NDVI is an alternative measure of vegetation amount and condition. It is associated with vegetation canopy characteristics such as biomass, leaf area index and percentage of vegetation cover. NDVI units are non-dimensional, a fraction with a potential range between -1 and 1.
- 2-5 Albedo proxy based on Small (2003). The albedo proxy is an integrated measure of reflected radiance at visible to near infrared wavelengths.
- 2-6 Road density network derived from Census TIGER roads from 2002.
- 2-7 Average building height derived from number of stories. Extracted from the real property database of New York City's Department of Finance, 2002.
- 2-8 Base percentages of trees, impervious surfaces, and grass within each 1.3 km MM5 grid box. Percentages were derived from a land cover classification performed by Myeong et al. (2003) on EMERGE aerial photography obtained from flyovers during 2001 – 2002.
- 2-9 Grass areas available for open-space planting. Data resolution is 3 meters.
- 2-10 Street tree inventory from New York City Department of Parks in Maspeth Queens case study area.

- 2-11 Residuals for bivariate regression analysis, 8% random sample of 250 meter pixels in New York City. Average surface temperature and NDVI both derived from September 8, 2002 Landsat image.
- 2-12 MM5 regional climate model diagram with simultaneous energy balance models (MM5 v3.7+SEBM).
- 2-13 Surface (skin) temperature in an urban setting. MM5 sees horizontal surfaces only and the 2-meter temperature is conceptually above city's rooftops.
- 2-14 Mitigation scenario percentages. a) Urban forestry/grass-to-trees (open-space planting) at 100% redevelopment of available area, b) Urban forestry/grass+street-to-trees (open-space + curbside planting) at 100% redevelopment of available area.
- 3-1 National Weather Service meteorological data spatially interpolated across the New York metropolitan region. August 14, 2002 at 6 AM.
- 3-2 Bleed-over Effect in Central Park.
- 5-1 Load model and economic cost-benefit analysis process.
- 5-2 Electric load and temperature data for New York City.
- 5-3 Electric load and temperature data for Mid-Manhattan West.
- 5-4 Electric load and temperature data for Lower Manhattan East.
- 5-5 Electric load and temperature data for Fordham.
- 5-6 Electric load and temperature data for Maspeth.
- 5-7 Electric load and temperature data for Crown Heights.
- 5-8 Electric load and temperature data for Ocean Parkway.
- 6-1 City-wide costs for selected mitigation scenarios (in millions). Note that urban forestry plus roofs represents mitigation scenario 9: 50% open space planting plus 50% curbside planting + 25% living roofs plus 25% light roofs.
- 6-2 Costs for selected mitigation scenarios (in millions) by case study area.
- 6-3 Cost per city-wide on-peak megawatt reduction (in millions).
- 6-4 Cost per on-peak megawatt reduction (in millions) for case study areas.

## Appendix Figures

- A-1 Relative transpiration factors corresponding to tree species' water use classification.
- A-2 Range of overall leaf scores and the development of their associated relative particle deposition rates ( $V_d$ ).
- A-3  $\text{NO}_2$  removal rates based on relative transpiration rate.
- A-4  $\text{O}_3$  removal rates based on relative transpiration rate.
- A-5  $\text{SO}_2$  removal rates based on relative transpiration rate.
- A-6 California ambient air quality standards. Weight was based on referencing against the 1-hour ozone standard.
- A-7 Weighting of tree functions by NYSERDA/DEC for park trees.
- A-8 Weighting of tree functions by NYSERDA/DEC for street trees.
- A-9 Ranked tree species list for NYC based on weighting factors by NYSERDA/DEC.
- D-1 Building square footage.
- D-2 Average year built.
- D-3 Energy map by parcel land use.
- D-4 Population density.
- E-1 Borough study areas with 250 meter grid cells.
- F-1 MM5 36 km, 12 km, 4 km, and 1.3 km domains.
- F-2 Observed Central Park data and MM5 base weighted average near-surface air temperatures.

## **TABLES**

### Table

- S-1 Available area for implementing heat island mitigation strategies in each case study area.
- S-2 Mitigation scenarios.
- S-3 Absolute differences in near-surface air temperature between difference surface-cover types, averaged over all MM5 grid boxes within New York City and all three heat waves.
- S-4 MM5 weighted average near-surface air temperature reductions for selected mitigation scenarios averaged over all times of day and at 3 PM, and assuming implementation in 100% of the available area.
- 1-1 Base percentages for each land surface type.
- 1-2 Available area for implementing heat island mitigation strategies in each case study area.
- 2-1 Mean temperature and relative humidity during each of the three heat-wave periods.
- 2-2 Remotely-sensed satellite images.
- 2-3 Variables included in GIS data library.
- 2-4 Descriptive statistics for each case study area. 0 – 10K is low population density, 10 – 45K is medium population density and 45 – 350K is high population density.
- 2-5 Average surface temperature during the summer of 2002 derived from four remotely-sensed satellite images.
- 2-6 Bivariate analysis with an 8% random sample of New York City.
- 2-7 Regression results for the case study areas using surface temperatures from the July 22, 2002 Landsat images as the dependent variable.
- 2-8 Definitions of surface temperature and 2-meter temperature for each land surface type in MM5.
- 2-9 Mitigation scenarios.

- 3-1 Absolute temperature differences in near-surface air temperature between difference surface-cover types averaged over all three heat waves.
- 4-1 MM5 weighted average near-surface air temperature reductions for selected mitigation scenarios averaged over all times of day, at 3 PM, and at 6 PM.
- 5-1 Summary of electric load and weather data for study period days.
- 5-2 Summary of regression models for electric load and temperature.
- 5-3 Selected mitigation scenarios.
- 5-4 Maximum on-peak temperature reduction.
- 5-5 Average temperature reduction.
- 5-6 Average on-peak temperature reduction.
- 5-7 Energy and demand reduction.
- 5-8 Percentage reduction on peak electric load from mitigation scenarios.
- 6-1 Costs for tree planting mitigation scenarios (\$millions).
- 6-2 Cost for living roof and light surfaces mitigation scenarios (\$millions).
- 6-3 Costs for combination mitigation scenarios (\$millions).
- 6-4 Net mitigation scenario benefits (\$millions).
- 6-5 Benefit-to-cost ratio for mitigation scenarios.

#### Appendix Table

- B-1 NWS and WeatherBug® stations with data quality ratings. Tier I indicates the data is from an NWS station. Tier II indicates high confidence in a WeatherBug station. Tier III indicates some confidence in a WeatherBug station and Tier IV indicates that the data were not useable.
- E-1 Descriptive statistics for New York City and the five boroughs.
- E-2 Bivariate OLS regression results – New York City and boroughs derived from September 8, 2002 Landsat ETM+ image.
- F-1 MM5 vegetation specification.

- F-2 Evaluation of MM5 results for HW1, July 2-4, 2002.
- F-3 Evaluation of MM5 results for July 29<sup>th</sup> – August 3<sup>rd</sup>, 2002 heat-wave period.
- F-4 Evaluation of MM5 results for August 11<sup>th</sup> – August 18th, 2002 heat-wave period.

## **BOXES**

### Box

- 3-1 Does cooling potential change as a heat-wave progresses?
- 3-2 Do mitigation benefits tend to remain localized or spread to adjacent areas?

Figure B3-2. Central Park bleed-over effect.

- 4-1 Are potential benefits greater when trees are planted curbside or in open spaces?

## PREFACE

The New York State Energy Research and Development Authority (NYSERDA) is pleased to publish “Mitigating New York City’s Heat Island with Urban Forestry, Living Roofs, and Light Surfaces.” The report was prepared by principal investigators Cynthia Rosenzweig of the Columbia University Center for Climate Systems Research and the NASA/Goddard Institute for Space Studies, William D. Solecki of Hunter College – City University of New York, and Ronald Slosberg of SAIC. It is a product of a longstanding collaboration between researchers at Columbia University and Hunter College to improve scientific understanding of the urban heat island.

This project was funded as part of two **New York Energy \$mart<sup>SM</sup>** programs, the Peak-Load Reduction Program (PLRP) and Environmental Monitoring, Evaluation, and Protection (EMEP) Program. Funding support was also provided by the United States Department of Agriculture, Forest Service, in collaboration with the New York State Department of Environmental Conservation (DEC). This represents one of several air quality modeling studies underway in New York State. Summaries of findings and policy implications from this and other studies are available on NYSERDA’s website at: [www.nysERDA.org/programs/environment/emep/](http://www.nysERDA.org/programs/environment/emep/).

The project began in the summer of 2004 and was completed during the spring of 2006. The Columbia team was responsible for meteorology and climate modeling, and the Hunter team was responsible for remote sensing, GIS analysis, and statistical analysis. The Columbia/Hunter results were used by SAIC to estimate the impact of heat island mitigation strategies on energy demand. SAIC also performed a Benefit/Cost analysis on a range of mitigation strategies, based on wholesale energy and demand benefits.

The research team met monthly to present interim findings and held biweekly teleconferences to discuss progress. Project Advisory Committee members contributed frequently to the meetings and teleconferences, providing guidance on methods, results, and deliverables along the way. Advisory Committee members also participated in several steering meetings, at which they met with the research team leaders. Throughout the year, Peter Savio and Mark Watson from NYSERDA, and Frank Dunstan and Kevin Civerolo from the DEC, provided invaluable guidance.

Preliminary findings from this study were incorporated into a Request for Proposals issued by NYSERDA in collaboration with DEC, for a pilot urban tree planting project in New York City (Manhattan, Lower East Side). This study has also informed the large scale urban reforestation program: “Greening the Bronx.”

Findings from this study will also be incorporated into an EPA-funded study on an integrated modeling approach to local energy use and environmental planning in Lower Manhattan. This study is led by John Lee and Vatsal Bhatt of the Brookhaven National Laboratory and Owen Carroll of the State University of New York at Stonybrook. The EPA Region II liaison is Edward Linky. This group participated in many of the research meetings to achieve integration across the two projects.





## **SUMMARY**

New York City, like other large cities, is warmer than surrounding areas due to the urban heat island effect, which occurs when impervious built surfaces such as roads and buildings absorb solar radiation and re-radiate it in the form of heat. The development of a heat island has regional-scale impacts on energy demand, air quality, and public health. Heat island mitigation strategies, such as urban forestry, living (green) roofs, and light-colored surfaces, could be implemented at the community level within New York City, but their effects need to be tested with comparable methodologies. Although the heat island effect occurs throughout the year, its occurrence during the summer months is of particular public policy concern because of the association of higher temperatures with increases in electric demand due to air conditioning, elevated air pollution and heat-stress related mortality and illness.

This study uses a regional climate model (MM5) in combination with observed meteorological, satellite, and GIS data to determine the impact of urban forestry, living roofs, and light surfaces on near-surface air temperature in New York City. Nine mitigation scenarios are evaluated city-wide and in six case study areas. Temperature impacts are calculated on a per-unit area basis, as well as taking into account the available land area for implementation, and other physical constraints. The scenarios are then evaluated based on their cost-effectiveness at reducing air temperature and consequent lower demand for electrical energy for air conditioning.

## **PROJECT OBJECTIVES**

The overall goal of this project is to provide information about urban heat island mitigation to policy-makers based on study results. The specific objectives are to:

1. Analyze and model the heat island effect in New York City;
2. Test urban forestry, living roofs, and light surfaces as potential heat island mitigation strategies city-wide and in six case study areas;

3. Improve scientific understanding of how urban heat island mitigation strategies affect New York City's surface and near-surface air temperatures;
4. Evaluate potential interactive consequences associated with heat island mitigation strategies with particular attention to land use, electric loads, and potential air quality and/or health impacts;
5. Test the impact of temperature reduction on energy demand; and
6. Determine the cost-effectiveness of each strategy.

## **KEY QUESTIONS**

The project is designed to answer the following key questions:

1. What are the dominant climate factors, land-use patterns, and geographic conditions that affect New York City?
2. Are there viable options for reducing elevated near-surface air temperature associated with the urban heat island?
3. Which mitigation strategies offer the potential to reduce near-surface air temperature on a per unit area basis?
4. Taking into consideration available land area and other physical constraints, which mitigation strategies provide potential for reducing temperature city-wide and in the six case study areas?
5. What are the costs associated with each mitigation strategy?
6. Which mitigation strategies provide greater benefits in terms of reduced air temperature and demand for electrical energy for cooling at lower costs?

## **CASE STUDY AREAS**

In addition to the city-wide study, six smaller case study (sub-regional) areas were selected according to several criteria: (1) location within an area with potential electric distribution constraints (anticipated possible load pocket), as defined by Con Edison;



Table S-1. Available area for implementing heat island mitigation strategies in each case study area.

Case Study Area	Grass-to-Trees Open-space Planting (%)	Street-to-Trees Curbside Planting (%)	Impervious Roofs to Living or Light Roofs (%)	Impervious Roadways and Sidewalks to Light Street-Level Surfaces (%)
New York City	10.8	6.7	13.6	34.4
Mid-Manhattan West	1.9	8.0	33.8	37.0
Lower Manhattan East	5.8	8.8	26.6	36.2
Fordham Bronx	8.7	9.9	16.1	35.3
Maspeth Queens	15.9	6.2	16.5	28.7
Crown Heights Brooklyn	7.8	14.4	21.8	34.2
Ocean Parkway Brooklyn	5.2	13.4	21.7	38.1

## DETERMINING TEMPERATURE IMPACTS: STUDY METHODS, DATA, AND MODELS

The summer of 2002 was chosen as the time period for the study. A remote sensing and geographic information system (GIS) data library was developed to characterize the multiple dimensions of New York City’s heat island. Satellite-derived surface temperatures (Figure S-2) were regressed on other satellite-derived and/or GIS-based environmental variables to determine the extent to which surface temperature is related to vegetation, albedo and other land-surface characteristics city-wide and within each case study area.

Landsat Surface Temperature August 14 2002 10:30am

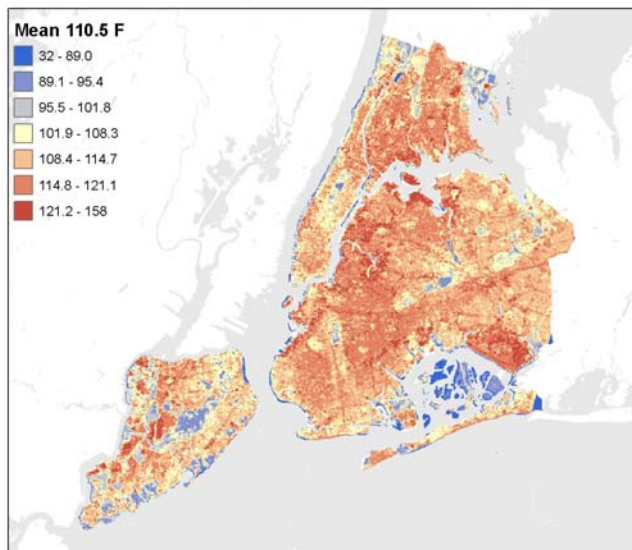


Figure S-2. Remotely sensed thermal satellite data. Landsat ETM, August 14, 2002 at 10:30 AM, Band 6, resolution is 60 meters.

Three heat-wave periods during 2002 were selected using observed meteorological data. The Penn State/NCAR MM5 dynamic regional climate model was used to test the effects of the mitigation scenarios on temperature in the region. MM5 base runs were compared with meteorological data from National Weather Service (NWS) and WeatherBug®<sup>1</sup> stations for the three heat-wave periods; comparison showed that the model simulations represent regional climate adequately. However, the model may underestimate near-surface air temperature because the effect of shading is not represented by the regional climate model and because atmospheric mixing tends to dampen the effects of land-surface-cover changes. MM5 was then used to determine potential reductions in simulated near-surface air temperature with each mitigation scenario during the three heat-wave periods. The mitigation scenarios are listed in Table S-2.

Table S-2. Mitigation scenarios.

<b>Strategy</b>	<b>Mitigation Scenario</b>
Urban Forestry	1) Urban Forestry/Grass-to-Trees (open space planting)
	2) Urban Forestry/Street-to-Trees (curbside planting)
	3) Urban Forestry/Grass + Street-to-Trees (open space + curbside planting)
Light Surfaces	4) Light Surfaces/Roof-to-High Albedo (light roofs)
	5) Light Surfaces/Impervious-to-High Albedo (roofs + sidewalks/streets)
Living Roofs	6) Living Roofs/Roof-to-Grass
Ecological Infrastructure	7) Urban Forestry/Grass + Street-to-Trees and Living Roofs
Urban Forestry + Light Roofs	8) Urban Forestry/Grass + Street-to-Trees and Light Roofs
Combination of All	9) 50% Open Space + 50% Curbside + 25% Living Roofs + 25% Light Roofs

A statistical model of the electric load and its relationship to ambient weather conditions was developed to assess the economic feasibility of each mitigation scenario. A benefit-to-cost ratio based on wholesale energy and demand impacts was developed to evaluate the cost effectiveness of selected mitigation scenarios based on the net benefit and cost. The benefit was based on reduced wholesale electric energy and capacity requirements correlated with the MM5-derived temperature impact; costs were obtained from literature review, as well as materials vendors and other professionals involved with the technologies and materials needed to achieve the temperature impact of each mitigation

<sup>1</sup> WeatherBug data are available commercially through AWS Convergence Technologies.  
[http://www.aws.com/aws\\_2005/default.asp](http://www.aws.com/aws_2005/default.asp).

scenario. The cost-benefit analysis assumes 50% implementation of strategies 1-6 and 9 in Table S-2, and 100% implementation of strategies 7 and 8.

## **RESULTS: ANSWERS TO KEY QUESTIONS**

### **1. What are the dominant climate factors, land-use patterns, and geographic conditions that affect New York City?**

New York is a coastal city and thus is subject to sea-breezes. However, during heat waves, when the sea-breeze tends to be small, the urban heat island tends to intensify. In general, high temperature, low cloud cover, and low wind speed lead to more intense heat island conditions.

Our results indicate that vegetation plays a more important role than albedo or other features of the urban physical geography (e.g. building heights, road density) in determining heat island potential in New York City. Therefore, the redevelopment of urban surfaces to increase vegetation cover should help to reduce New York City's surface temperature. Since elevated surface temperatures are expected to lead to elevated air temperatures, land-cover modification could in turn affect the city's near-surface air temperature.

### **2. Are there viable options for reducing elevated near-surface air temperature associated with the urban heat island?**

Yes. Results show that significant reductions in New York City's near-surface air temperature, generally defined as the air temperature 2 meters (6 feet) above the street or surface level, can be achieved by implementing heat island mitigation strategies. Effects vary in magnitude across scenarios, case study areas, and heat-wave days. A combined strategy that maximizes the amount of vegetation in New York City by planting trees

along streets and in open spaces, as well as by building living (green) roofs (i.e. ecological infrastructure), offers more potential cooling than any individual strategy.

### 3. Which mitigation strategies offer the potential to reduce near-surface air temperature on a per unit area basis?

Model results indicate that the most effective mitigation strategy per unit area redeveloped is curbside planting (Table S-3). The average difference in simulated near-surface air temperature between impervious surfaces and trees was 3.5°F (1.9°C), higher than the differences between other surface-cover types. Therefore, street trees – which involve redevelopment of impervious surfaces – have the largest cooling potential per unit area, followed by living roofs, light-colored surfaces, and open space planting. This can also be thought of as the upper limit of mitigation potential if New York City were completely covered with impervious surfaces and then these surfaces were all replaced with trees, averaged over all times of day and ignoring feedbacks between the surface-cover alteration and regional meteorology.

Table S-3. Absolute differences in near-surface air temperature between different surface-cover types, averaged over all MM5 grid boxes within New York City and all three heat waves.

<b>Weighted Average Near-Surface Air Temperature (°F)</b>	<b>Grass-to-Trees</b>	<b>Impervious-to-Trees</b>	<b>Impervious-to-Grass</b>	<b>Impervious-to-Light</b>
Average	-1.1	-3.5	-2.5	-2.0
Maximum	-3.0	-8.7	-5.8	-4.6

Note: These values were derived from the MM5 base run, which assumes that New York City's land surface has its present configuration of trees, grass, and impervious surfaces (i.e. no mitigation). The difference in near-surface air temperature between impervious surfaces and trees represents the potential cooling from replacing a unit of impervious surface with a unit of trees. Considering these differences independent of the amount of available area for redevelopment allows for direct comparison of the cooling potential of each mitigation strategy, all else being equal. The actual city-wide cooling potential of each mitigation strategy depends on the number of units that can be redeveloped and the percent of the City's total surface area these units represent.



**4. Taking into consideration available land area and other physical constraints, which mitigation strategies provide potential for reducing temperature city-wide and in the six case study areas?**

**City-Wide**

Ecological infrastructure, a combined strategy of urban forestry and living roofs, has the greatest city-wide temperature impact. The city-wide simulated temperature impact of the mitigation scenarios ranges from 0.1°F (<0.1°C) for open space planting to 0.7°F (0.4°C) for ecological infrastructure if 100% of the available area is redeveloped, averaged over all heat-wave days and times. At the 3 PM peak, the impact ranges from 0.2°F (0.1°C) for open space planting to 1.2°F (0.7°C) for ecological infrastructure. Of the single strategy scenarios, light surfaces has the greatest modeled temperature impact, 0.4°F (0.3°C), averaged over all heat-wave days and times. At the 3 PM peak, both light surfaces and living roofs have a simulated city-wide temperature impact of 0.7°F (0.4°C).

Although curbside planting has only half the temperature impact, it involves redeveloping only 6.7% of the city's surface area as compared to 48.0% for light surfaces. In addition, even though there is more available area city-wide for open space planting (10.8%) compared to curbside planting, the temperature impact of open space planting is less than the temperature impact of curbside planting.

**Case Study Areas**

The differences in cooling potential across the case studies are primarily driven by differences in their available area for redevelopment. The simulated temperature impact of the mitigation scenarios in the six case study areas range from 0.0°F (0.0°C) for open space planting in Mid-Manhattan West, to 1.2°F (0.7°C) for ecological infrastructure in Crown Heights, averaged over all heat-wave days and times (Table S-4). At the 3 PM peak, the impact ranges from 0.0°F (0.0°C) for open space planting in Mid-Manhattan West, to 1.9°F (1.2°C) for ecological infrastructure in several of the case study areas.

Mitigation strategies in Mid-Manhattan West and Lower Manhattan East have a greater temperature impact compared to their application in other case study areas. Location, existing configuration of surface-cover types, and baseline surface and near-surface air temperatures appear to play a lesser role. Although the magnitude of the temperature impact varies between the different heat-wave days, the same case studies usually have the greatest temperature impact on all heat-wave days.

Of the single strategy scenarios, living roofs produces the greatest temperature impact in all case study areas. Although curbside planting has a smaller impact than living roofs, it requires less space. In Mid-Manhattan, for example, there is more than four times the available area for living roofs (33.8%) than for curbside planting (8.0%), but the temperature impact of living roofs is only three times that of curbside planting.

Table S-4. MM5 weighted average near-surface air temperature reductions for selected mitigation scenarios averaged over all times of day and at 3 PM, and assuming implementation in 100% of the available area.

Average reduction over all times of day	Open Space Planting (°F)	Curbside Planting (°F)	Living Roofs (°F)	Light Roofs (°F)	Light Surfaces (°F)	Ecological Infrastructure (°F)	Urban Forestry + Light Roofs (°F)
New York City	-0.1	-0.2	-0.3	-0.3	-0.4	-0.7	-0.6
Mid-Manhattan West	0.0	-0.3	-0.9	-0.6	-0.7	-1.1	-0.9
Lower Manhattan East	-0.1	-0.3	-0.7	-0.5	-0.6	-1.1	-0.9
Fordham Bronx	-0.1	-0.4	-0.4	-0.3	-0.4	-0.8	-0.8
Maspeth Queens	-0.2	-0.2	-0.4	-0.3	-0.4	-0.8	-0.7
Crown Heights Brooklyn	-0.1	-0.5	-0.5	-0.4	-0.5	-1.2	-1.0
Ocean Parkway Brooklyn	-0.1	-0.5	-0.6	-0.4	-0.5	-1.1	-1.0
<b>Average 3 PM Reduction</b>							
New York City	-0.2	-0.4	-0.6	-0.5	-0.6	-1.2	-1.1
Mid-Manhattan West	0.0	-0.5	-1.4	-1.0	-1.2	-1.9	-1.5
Lower Manhattan East	-0.1	-0.5	-1.1	-0.9	-1.1	-1.8	-1.5
Fordham Bronx	-0.2	-0.6	-0.7	-0.5	-0.6	-1.3	-1.2
Maspeth Queens	-0.3	-0.4	-0.7	-0.6	-0.7	-1.4	-1.2
Crown Heights Brooklyn	-0.1	-0.9	-0.9	-0.7	-0.9	-1.9	-1.8
Ocean Parkway Brooklyn	-0.1	-0.9	-1.0	-0.8	-1.0	-1.9	-1.7

## 5. What are the costs associated with each mitigation strategy?

### City-Wide

Given the cost assumptions of the study, the cost for combination mitigation scenarios implemented in all available areas ranges from \$2,927 million for urban forestry + light roofs to \$12,793 million for ecological infrastructure (Figure S-3). Implementing the single strategy scenarios in 50% of the available area ranges in estimated cost from \$199 million for open space planting to \$5,855 million for living roofs.

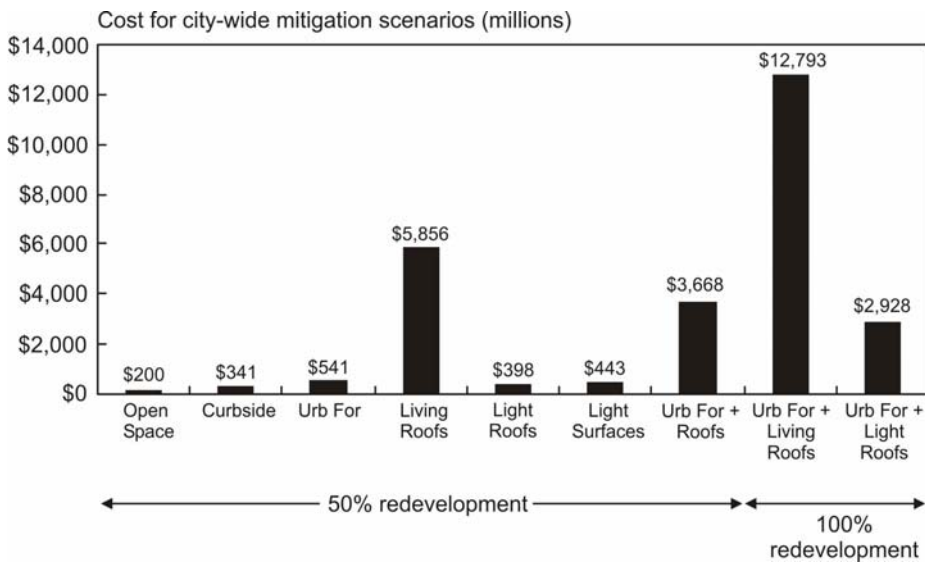


Figure S-3. City-wide costs for selected mitigation scenarios (in millions). Note that urban forestry plus roofs represents mitigation scenario 9: 50% open space planting plus 50% curbside planting + 25% living roofs plus 25% light roofs.

### Case Study Areas

The estimated costs vary across mitigation scenarios and case study areas (Figure S-4). Across all case study areas and all mitigation scenarios, the cost ranges from \$0.3 million for 50% open space planting in Mid-Manhattan West to \$588 million for ecological infrastructure in Maspeth.

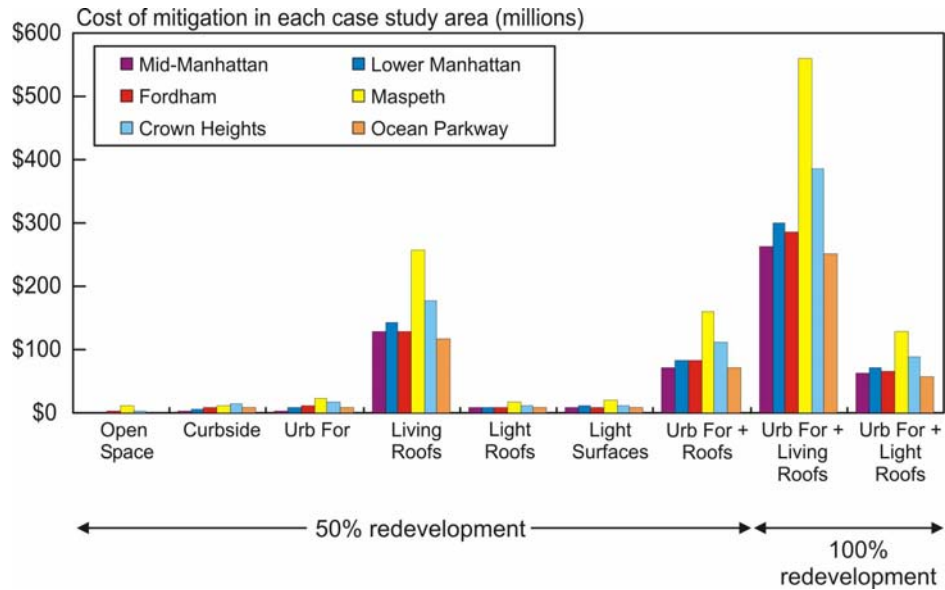


Figure S-4. Costs for selected mitigation scenarios (in millions) by case study area

## 6. Which mitigation strategies provide greater benefits in terms of reduced air temperature and demand for electrical energy for cooling at lower costs?

### City-Wide

Light surfaces, light roofs, and curbside planting are more cost-effective than the other strategies. The estimated cost per 0.1°F (0.06°C) temperature reduction ranges from \$233 million for 50% light surfaces to \$3,904 million for 50% living roofs.

The peak load megawatt (MW) impacts of the mitigation scenarios are moderate. The largest city-wide impacts are seen for the measures that combine 100% urban forestry with either living roofs or light roofs. The two scenarios that include 100% urban forestry average peak demand reductions of approximately 2% (MW), over all heat-wave days. The maximum on-peak demand reduction (single largest value of demand between 12 and 6 PM on non-holiday weekdays) was 3.2% (MW) for both of these scenarios.

While all of the measures reduce summer peak demand, for individual scenarios the average summer peak demand reduction over all heat-wave days was less than 1%. Among these scenarios, light surfaces, light roofs, and living roofs can potentially reduce

the summer peak electric load more than the other strategies. At 50% redevelopment of the available area, light surfaces can potentially reduce peak load by 0.51%, light roofs by 0.37%, and living roofs by 0.36%. Given cost and benefit assumptions (see Section 6 for details), the cost per MW reduction ranges \$8.4 for light surfaces to \$154 million for living roofs (Figure S-5).

Tree-planting may have a greater impact on energy demand than was estimated by this study because the effect of shading the sides of buildings was not included in the MM5 simulated temperature impacts.

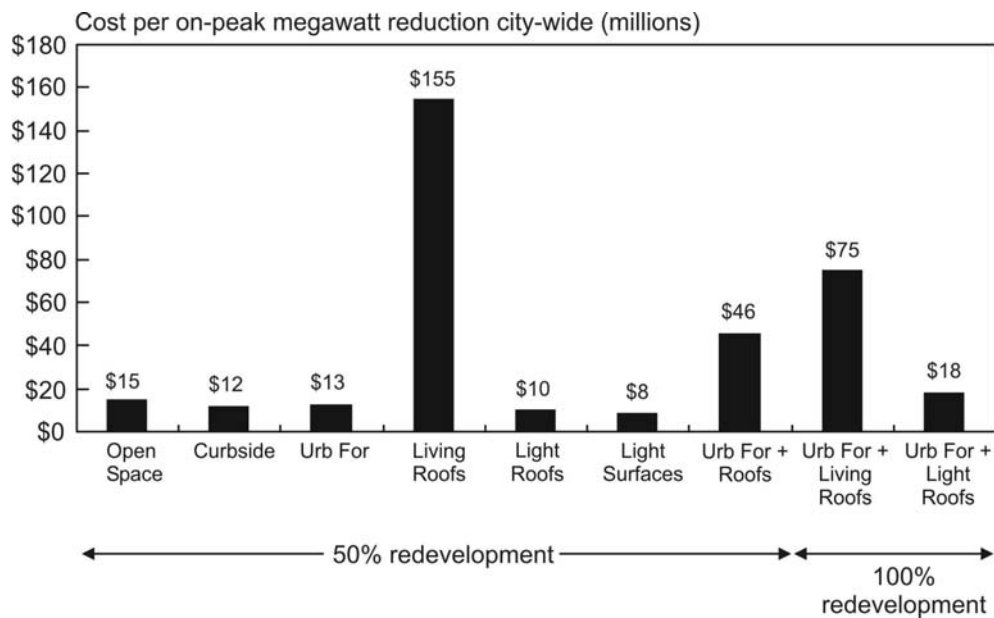


Figure S-5. Cost per city-wide on-peak megawatt reduction (in millions).

**Case Study Areas**

The cost per 0.1°F (0.06°C) temperature reduction is greater in Fordham, Maspeth, and Crown Heights and lower in Mid-Manhattan West, Lower Manhattan East, and Ocean Parkway. Differences are mainly result of the amount of redevelopment necessary to achieve comparable levels of cooling. The costs range from \$1 million per 0.1°F (0.06°C) temperature reduction for 50% open space planting in Mid-Manhattan West to \$143 million per 0.1°F (0.06°C) reduction for 50% living roofs in Maspeth.

The energy demand benefit exceeds the cost of implementation for all individual scenarios in Lower Manhattan, Mid-Manhattan West and Ocean Parkway. Although costs exceed the benefit in the remaining case study areas, as well as city-wide, it is likely that if additional benefits such as air quality, public health, reduction in the City’s contribution to greenhouse gas emissions, and reduction in stormwater runoff were also taken into account, in many cases the benefit-cost ratio city-wide and for all case study areas would be positive. This is an important area for further study.

For all case study areas, 50% living roofs is the most expensive strategy per on-peak MW reduction (Figure S-6). All other 50% implementation scenarios have approximately equal costs per on-peak MW reduction. Maspeth, Crown Heights, and Fordham have higher costs per on-peak MW reduction, partly because these case study areas tend to have more available area for open space planting, which has a lesser temperature impact, and less available area for living roofs.

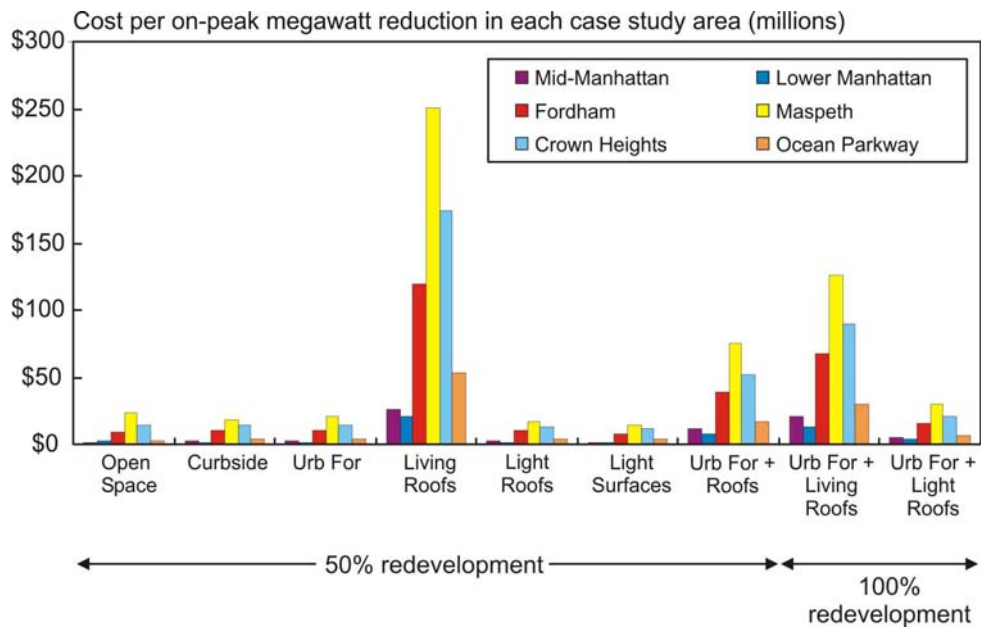


Figure S-6. Cost per on-peak megawatt reduction (in millions) for case study areas.

## **MAIN FINDINGS**

Results of this study show that all mitigation strategies have a significant temperature impact, but there is substantial variability in the magnitude of their effects across scenarios, case study areas, and heat-wave days. A combined strategy that maximizes the amount of vegetation in New York City by planting trees along streets and in open spaces, as well as by building living (or green) roofs (i.e. ecological infrastructure), offers more potential cooling than any individual strategy. The choice of a strategy should consider the characteristics and priorities of the neighborhood, including benefit/cost factors and the available area for implementation of each strategy.

There is potential for cooling in all case study areas; however, Mid-Manhattan West, Lower Manhattan East, and Ocean Parkway have greater potential for both temperature and cost-effective energy reduction.

From a standpoint of *per-unit area impacts*, vegetation cools more effectively than changes in albedo and the street trees scenarios have the greatest temperature impact per unit area.

From a standpoint of *available areas or opportunities* in the city for each strategy, curbside planting, living roofs, and light roofs and surfaces have comparable cooling effects. (Note that the area for light surfaces is many times greater than the area for street trees needed to achieve comparable cooling.)

From a standpoint of *cost-effectiveness and MW impacts*, light surfaces, light roofs, and curbside planting tend to have lower costs per 0.1°F (0.06°C) temperature reduction as well as per on-peak MW reduction.

## **OTHER BENEFITS OF MITIGATION STRATEGIES**

It is important to note that our assessment of benefits and costs did not address non-energy benefits. It is likely that if additional benefits such as air quality, public health,

reduction in the city's contribution to greenhouse gas emissions, and reduction in stormwater runoff were also taken into account, the benefit-cost ratio would be positive in all case study areas. The benefit/cost analysis does not account for market price effects due to price dampening, effects of reduced energy demand, or possible deferral of need for and cost of utility distribution upgrades. Furthermore, planting trees and building living roofs can be expected to have a positive impact on quality of life in New York City resulting from neighborhood beautification and enhanced wildlife habitat.

## **RECOMMENDATIONS**

Results of this study indicate that policy-makers should consider the following measures:

- 1) Develop urban heat island mitigation strategies appropriate to priorities and conditions in individual neighborhoods and communities.
- 2) Implement urban heat island strategies at large enough spatial extents to be temperature and cost-effective.
- 3) Maximize the temperature impact of urban heat island mitigation through combination strategies, and particularly by planting trees along streets and in open spaces, as well as by building living roofs (i.e. ecological infrastructure).
- 4) Develop and implement cost-effective strategies for light-colored surfaces, light roofs, and curbside planting for reducing on-peak energy use.
- 5) Conduct ongoing analyses and monitoring of tree-planting programs, living roofs, and light surfaces to observe actual mitigation levels over time and use results to improve calibration and validation of regional climate models for further documentation of heat island mitigation.
- 6) Conduct additional analyses to value benefits of the mitigation scenarios, and include appropriate non-energy benefits of mitigation strategies in cost-benefit analyses.





## Section 1

### INTRODUCTION

New York City, like other large cities, is warmer than surrounding areas due to the urban heat island effect, which occurs when impervious built surfaces such as roads and buildings absorb solar radiation and re-radiate it in the form of heat. The development of a heat island has regional-scale impacts on energy demand, air quality, and public health. Heat island mitigation strategies, such as urban forestry, living (green, vegetated) roofs, and light-colored surfaces, could be implemented at the community level within New York City, but their effects need to be tested with comparable methodologies. This study uses a regional climate model (MM5) in combination with observed meteorological, satellite, and GIS data to determine the impact of urban forestry, living roofs, and light surfaces on near-surface air temperature in New York City. Nine mitigation scenarios are evaluated city-wide and in six case study areas. Temperature impacts are calculated on a per-unit area basis, as well as taking into account the available land area for implementation, and other physical constraints. The scenarios are then evaluated based on their cost-effectiveness at reducing air temperature and consequent lower demand for electrical energy for air conditioning.

The case study areas are: Mid-Manhattan West, Lower Manhattan East, Fordham Bronx, Maspeth Queens, Crown Heights Brooklyn, and Ocean Parkway Brooklyn (Figure 1-1). These areas were selected according to several criteria: (1) location within an area with potential electric distribution constraints (anticipated possible load pocket), as defined by Con Edison<sup>2</sup>; (2) measurement of warmer than average near-surface air temperatures (i.e., a “hot spot”); and (3) presence of available area for testing a range of urban heat island mitigation strategies. In addition, an effort was made to include low-income and minority neighborhoods to potentially allow the results to be used to address environmental equity concerns. All case study areas met the criteria, with the exception

---

<sup>2</sup> A load pocket is an area with anticipated potential power transmission constraint(s) in distribution capacity.

of Lower Manhattan, which is not in a designated load pocket.<sup>3</sup> Crown Heights and Fordham are low-income, high-minority neighborhoods.

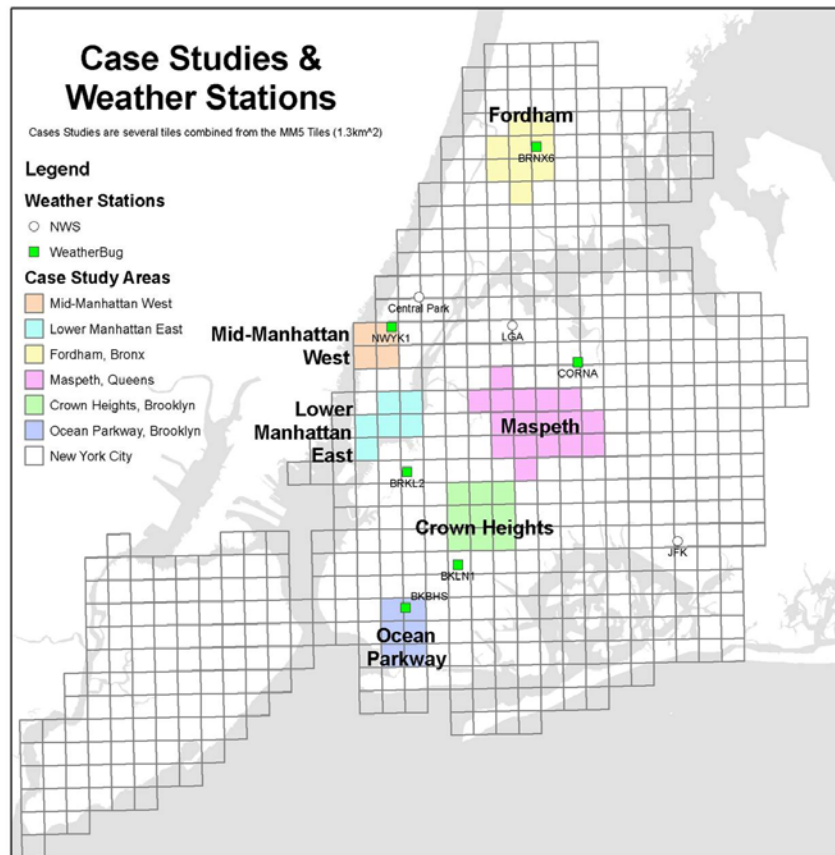


Figure 1-1. Case study areas and weather stations. Grid boxes correspond to the MM5 model 1.3 km grid.

Heat island mitigation strategies were tested within these case studies during three heat-wave periods in the summer of 2002: July 2<sup>nd</sup> – 4<sup>th</sup> (HW1), July 28<sup>th</sup> – August 7<sup>th</sup> (HW2), and August 11<sup>th</sup> – August 18<sup>th</sup> (HW3). A heat-wave period is defined as at least three consecutive days with maximum temperatures above 90°F (32.2°C) in Central Park.

Evaluation of the performance of MM5 over New York City at 1.3 km grid resolution lays the foundation for further high-resolution climate modeling in urban areas.

<sup>3</sup> The Lower Manhattan case study was chosen to link this project to an EPA Region II-funded project investigating the effect of heat island mitigation on building-level energy demand.

However, climate modeling on a regional scale in New York is complicated by complex urban land use, building and street geometry, and dynamic drivers such as the sea-breeze. Thus, considerable uncertainty regarding model assumptions and land surface-atmosphere interactions remains.

The data library assembled for the project is a large compilation of climatic and geographical variables related to the New York metropolitan region. The library includes remotely-sensed satellite images, meteorological station data, and GIS databases that incorporate land surface and urban morphology information. The spatial and temporal resolution of these datasets, as well the extent of their incorporation into modeling efforts have led to improvement in scientific understanding of heat island processes and mitigation potential in New York City.

## **PROJECT OBJECTIVES**

The overall goal of this project is to provide information about urban heat island mitigation to policy-makers based on study results. The specific objectives are to:

1. Analyze and model the heat island effect in New York City;
2. Test urban forestry, living roofs, and light surfaces as potential heat island mitigation strategies city-wide and in six case study areas;
3. Improve scientific understanding of how urban heat island mitigation strategies affect New York City's surface and near-surface air temperatures;
4. Evaluate potential interactive consequences associated with heat island mitigation strategies with particular attention to land use, electric loads, and potential air quality and/or health impacts;
5. Test the impact of temperature reduction on energy demand; and
6. Determine the cost-effectiveness of each strategy.

## **KEY QUESTIONS**

The project is designed to answer the following key questions:

1. What are the dominant climate factors, land-use patterns, and geographic conditions that affect New York City?
2. Are there viable options for reducing elevated near-surface air temperature associated with the urban heat island?
3. Which mitigation strategies offer the potential to reduce near-surface air temperature on a per unit area basis?
4. Taking into consideration available land area and other physical constraints, which mitigation strategies provide potential for reducing temperature city-wide and in the six case study areas?
5. What are the costs associated with each mitigation strategy?
6. Which mitigation strategies provide greater benefits in terms of reduced air temperature and demand for electrical energy for cooling at lower costs?

## **URBAN HEAT ISLAND PROCESSES**

An urban heat island is created when naturally vegetated surfaces – e.g., grass and trees – are replaced with non-reflective, impervious surfaces that absorb a high percentage of incoming solar radiation (Taha, 1997). The development of an urban heat island is a time-varying process involving the physical geography and built environment of a metropolitan region (Grimmond and Oke, 1999). Figure 1-2 illustrates a typical urban energy balance compared to a non-urban energy balance.

In the presence of high moisture levels, vegetation plays a dominant role in surface cooling through evaporation and latent heat removed from soils and evaporation from plants (known as transpiration) (Taha et al, 1991). In urban areas, where the fraction of the surface covered by vegetation is particularly low and surfaces tend to be water-resistant, potential surface cooling due to the loss of latent heat from vegetation and soil is reduced.

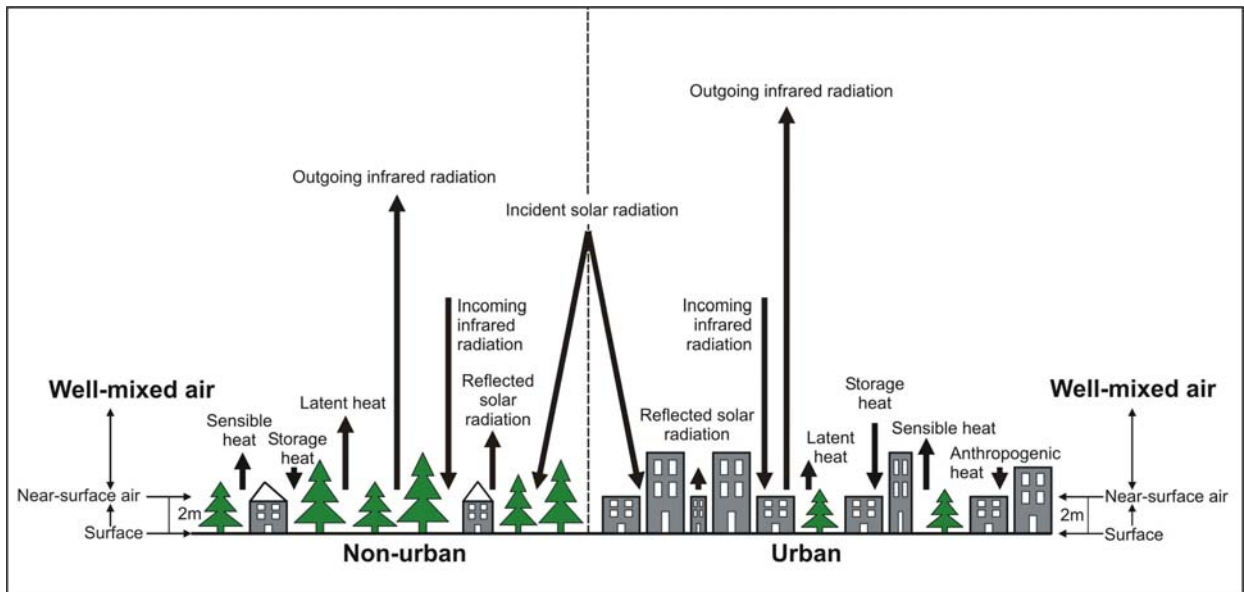


Figure 1-2. Diagram illustrating a typical non-urban energy balance as compared to a typical urban energy balance. Longer arrows denote a greater heat flux (e.g. latent heat flux is larger in non-urban areas than in urban areas; sensible heat flux is larger in urban areas than in non-urban areas).

The rate at which solar energy is absorbed and re-radiated depends not only on the physical properties of different surface types, but also on their configuration within the urban landscape, regional meteorology, and localized microclimate (Oke, 1987; Sailor, 1995). This can lead to the formation of local ‘hot spots’, which may shift in space with diurnal and seasonal cycles, under particular meteorological conditions, and with land-use changes (Unwin, 1980). Thus, the complex temperature variation in New York City could better be described as an “urban heat island archipelago.”

Interactions between patterns of surface heating and regional meteorology determine the overall intensity of the heat island over space and time. In general, the intensity is greatest on calm, clear days in the summer and fall.

On clear days, incoming short-wave radiation has a direct path to the surface. In this case, internal surface properties, such as heat capacity, play the dominant role in spatial surface-heating differences. On cloudy days, a much larger percentage of incoming radiation is reflected, reducing surface heating. In this case, meteorological conditions

tend to outweigh surface properties and the potential for urban heat island development will likely not be realized (Rosenzweig et al., 2005).

The addition of anthropogenic heat and pollutants from power plants, industrial processes, and vehicles into the urban atmosphere can further contribute to the intensity of the urban heat island effect (Taha, 1997). Anthropogenic heat can directly raise near-surface air temperatures while air pollution increases absorption of radiation in the lower troposphere, often contributing to the creation of an inversion layer. The inversion layer not only prevents rising air from cooling at the normal rate, but also limits dispersion of pollutants that are produced in the urban area.

Although the heat island effect occurs throughout the year, its occurrence during the summer months is of particular public policy concern because of the association of higher temperatures with increases in electric demand due to air conditioning (Rosenfeld et al., 1995), elevated air pollution (Hogrefe et al., 2004) and heat-stress related mortality and illness (Sailor et al., 2002; Kunkel et al., 1996; Knowlton et al., 2004).

### **THE URBAN HEAT ISLAND IN NEW YORK CITY**

Urban heat island conditions have been observed in New York City for more than a century (Rosenthal et al., 2003). Currently, New York City's summertime nocturnal heat island averages ~7°F (~4°C). This means that during the summer months the daily minimum temperature in the city is on average ~7°F (~4°C) warmer than surrounding suburban and rural areas (Gedzelman et al., 2003, Kirkpatrick and Shulman, 1987).

Satellite imagery shown in this report suggests that during the day, the hotter neighborhoods tend to be in northwestern Brooklyn, eastern Queens (Long Island City), and the South Bronx (Figure 1-3). At night, Midtown Manhattan tends to be hottest, and this pattern is observed during other seasons as well (Childs and Raman, 2005).

New York City's heat island can be particularly pronounced during heat-wave periods, which are often characterized by low wind speeds and a reduced sea-breeze, in addition to high temperatures. During heat-wave periods, heat island impacts also tend to be further amplified (Rosenzweig et al., 2005).

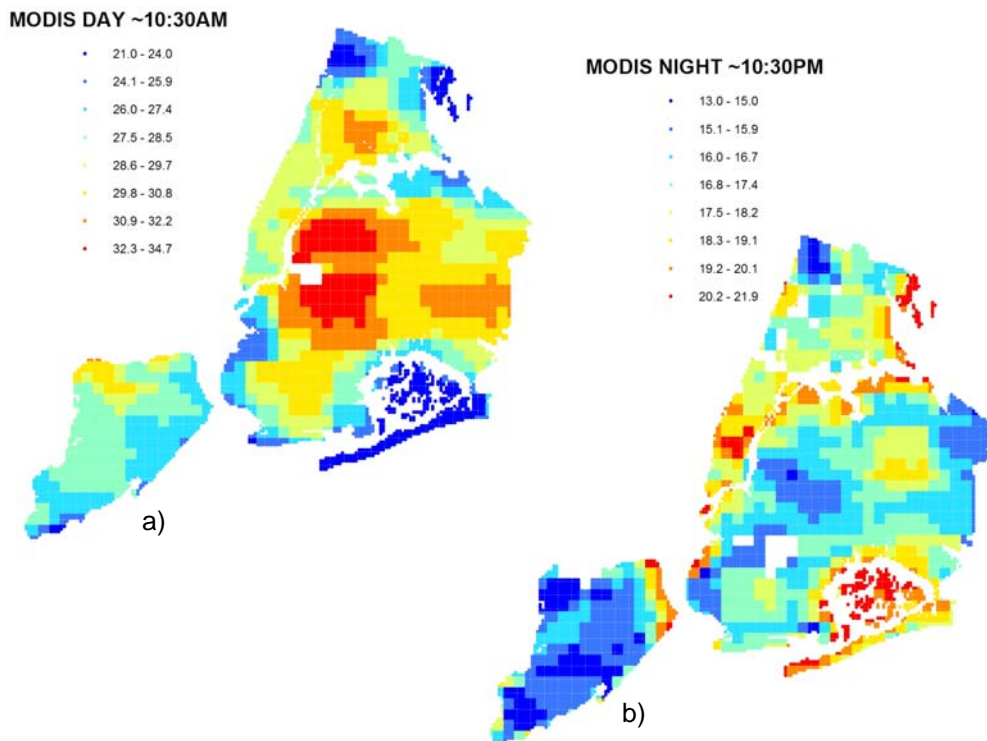


Figure 1-3. Variability in satellite-derived surface heating between the day and night from a MODIS day-night pair. September 8, 2002, resolution is 1 km. a) 10:30 AM, b) 10:30 PM.

## **URBAN HEAT ISLAND MITIGATION STRATEGIES**

Urban forestry, light surfaces, and living roofs were evaluated as possible mitigation approaches. These strategies operate by directly lowering surface temperatures through shading, evapotranspiration and reflection of radiation (Taha, 1997). The reduced surface temperatures, in turn, lower the sensible heat fluxes from the ground during the day and, similarly, the amount of heat stored in dense urban surfaces at night, both of which can lower near-surface air temperatures, thus contributing to reduction of the urban heat



island. Each mitigation strategy has relative advantages and disadvantages related to function and cost.

### **Urban Forestry**

Surface and near-surface air temperatures in New York City are coolest in areas with deciduous trees because tree canopies shade built surfaces and also cool the air through evapotranspiration. Trees can decrease energy use in three ways. First, trees planted beside buildings shade windows, preventing solar radiation from entering. Second, trees block radiation that would otherwise be absorbed by a building's roof and walls and thus reduce the amount of heat conducted into the building. Finally, trees cool the air through transpiration (Davis et al., 1992).

In cities, there are two types of locations in which trees can be planted: *on sidewalks* or "*curbside*," where they shade impervious surfaces, and *in open spaces*, where they shade grass. A previous study showed that replacing all urban grass with trees could reduce Manhattan's air temperature by up to 1.8°F (1°C) in the afternoon (Luley and Bond, 2002).

Of the three heat island mitigation strategies considered in this study, urban forestry, and particularly planting curbside street trees, contributes additional non-energy benefits such as fostering environmental equity in poorer neighborhoods that tend to have hotter temperatures and fewer street trees, and bringing cooling benefits to areas where people live and work.

In addition to reduced energy demand, benefits of urban forestry include improvements in air quality, both through the direct uptake of pollutants and through urban cooling that slows the rate of ozone-producing photochemical reactions (Taha, 1996). However, a disadvantage is that some trees, known as high-emitting trees, release volatile organic compounds (VOCs), an ozone precursor, into the atmosphere. The Recommended Tree Species List attached in Appendix A was developed by the United States Department of

Agriculture, Forest Service (David J. Nowak) as an aid to urban foresters for optimizing the potential to reduce temperature while minimizing negative trade-offs such as emissions of VOCs.

### **Living Roofs**

A “living” or “green” roof allows for the propagation of vegetation across a building’s upper surface (Figure 1-4). Living roofs mitigate the heat island by cooling the roof surface of a building through evaporation from soil media and transpiration from plants. This can reduce air temperatures above the roof. The cooler air then mixes locally, potentially affecting the urban heat island and energy demand at the neighborhood level (Akbari, 2002; Bass, 2003; Solecki et al., 2005; Rosenzweig, Gaffin, and Solecki, 2006).



Figure 1-4. Example of a living roof. Hamilton City Apartments, Portland OR. Source: Environmental Services of Portland Brochure.

Living roofs offer a number of additional advantages that are not quantified by this study. For example, a living roof can also reduce energy demand by lowering the surface temperature and thus the amount of solar energy that is conducted into a building. Living roofs can also reduce stormwater runoff and improve air quality. In a city with limited available space for street-level planting, living roofs provide a good opportunity for the re-introduction of vegetation into the urban environment.

Modeling work has shown that living roofs provide greater cooling potential than light roofs (Gaffin et al., 2005). However, in their current state of development, living roofs tend to be expensive to install and they only reduce conduction through the roof, which may represent a small fraction of a building's total surface area.

### **Light Surfaces**

Urban surfaces such as buildings, roads, sidewalks, and rooftops tend to have low albedos (i.e., low reflectivities) and high heat capacities, and are thus good at absorbing and later re-radiating the sun's energy. To mitigate the heat island effect, pavements can be lightened by using lighter-colored aggregate in asphalt, light-colored resurfacing material, or concrete instead of asphalt (Davis et al., 1992). At the roof level, lighter-colored roof materials can be used or roof surfaces can be coated with lighter colors. A case study of Los Angeles showed that increasing citywide albedo by 15% could reduce 3 PM temperatures in the downtown area by up to 3.6°F (2°C) (Taha et al., 1997).

However, it is important that appropriate light-colored surface materials be chosen. Materials such as unpainted steel that are light in color, but that are good at storing and conducting absorbed radiation will not be effective (Rosenzweig et al., 2005).

The major advantages of employing light surfaces as a heat island mitigation strategy are a large available area for implementation (e.g., all impervious streets, sidewalks, and roofs) and a relatively low cost per unit area. However, light surfaces are difficult to keep clean and may lose up to one-third of their reflectivity in a few years. This is due to

normal staining, weathering and soot deposition that occurs in urban areas (Bretz and Pon, 1994). Light surfaces also scatter radiation to other surfaces, resulting in a lower net effect on the energy budget than urban forestry or living roofs.

### **Surface and Near-Surface Air Temperature Influences on Energy Demand**

*Surface temperature* is defined as the “skin” temperature of a surface (e.g., the temperature of asphalt when it is touched), and *near-surface air temperature* is generally defined as the air temperature two meters (~6 ft.) above the street level.

Energy demand for air-conditioning in buildings is affected by both surface temperature and near-surface air temperature through interrelated processes. Reductions in surface temperature on building walls and roofs directly reduce the conductive heat flow, partially driving energy demand. Rooftop summer surface temperatures are dramatically lowered by living and light-colored roof surfaces, and this tends to reduce heat conduction in a downward direction. Conduction of heat through the walls of buildings is also reduced when urban tree canopies shade the walls. Reductions in near-surface air temperature can reduce the temperature of air entering buildings through ventilation and infiltration into buildings, one of the primary determinants of air-conditioning loads. Since all building surfaces are affected by air temperature – not just the surfaces that are directly shaded or have modified roofs – this can have a large effect on energy demand.

Currently, most building energy models calculate surface temperatures based on a given ambient air temperature. However, it is not clear how well these models calculate surface temperatures affected by latent heat fluxes from vegetated surfaces. To the extent that building energy models do not fully simulate latent heat fluxes, they may underestimate the impact of urban vegetation on building energy demands.

## CASE STUDY AREAS

The case studies are thermal hot spots within an area that may face electric constraints in the future and that have available area in which to implement heat island mitigation strategies. Case studies were characterized according to their remotely-sensed surface temperature, microclimate, land-surface types, and socioeconomic profile. Table 1-1 lists baseline area percentages of impervious surfaces (roofs and street-level), grass, trees, and the estimated available space for street trees (Myeong et al., 2003). Table 1-2 lists mitigation potential for each land surface type. Among many factors, configuration of different land surface types within the case study areas affects where mitigation strategies can be applied.

Table 1-1. Base percentages for each land surface type.

<b>Case Study Area</b>	<b>Grass (%)</b>	<b>Trees (%)</b>	<b>Impervious (%)</b>	<b>Total Area (%)</b>
New York City	14.1	21.9	64.1	100
Mid-Manhattan West	2.6	3.1	94.3	100
Lower Manhattan East	8.3	8.1	83.6	100
Fordham Bronx	9.2	22.1	68.7	100
Maspeth Queens	17.5	22.3	60.2	100
Crown Heights	8.1	17.2	74.7	100
Ocean Parkway	5.5	14.8	79.6	100

Table 1-2. Available area for implementing heat island mitigation strategies in each case study area.

<b>Case Study Area</b>	<b>Grass-to-Trees Open-space Planting (%)</b>	<b>Street-to-Trees Curbside Planting (%)</b>	<b>Impervious Roofs to Living or Light Roofs (%)</b>	<b>Impervious Roadways and Sidewalks to Light Street-Level Surfaces (%)</b>
New York City	10.8	6.7	13.6	34.4
Mid-Manhattan West	1.9	8.0	33.8	37.0
Lower Manhattan East	5.8	8.8	26.6	36.2
Fordham Bronx	8.7	9.9	16.1	35.3
Maspeth Queens	15.9	6.2	16.5	28.7
Crown Heights	7.8	14.4	21.8	34.2
Ocean Parkway	5.2	13.4	21.7	38.1

### **New York City**

New York City is a large, densely populated urban area that is approximately 309 square miles (800 square kilometers). New York City is composed of five boroughs with extensive shorelines on the Atlantic Ocean, the New York Bay, the Hudson River, the East River, and Long Island Sound. The land use of New York City is very heterogeneous, with a complex assemblage of business districts with office buildings that have high daytime energy use as well as densely populated residential areas with high evening energy use, less dense residential areas with one and two-family detached homes, vegetated open spaces, industrial areas, and many mixed residential/commercial areas.

### **Mid-Manhattan West**

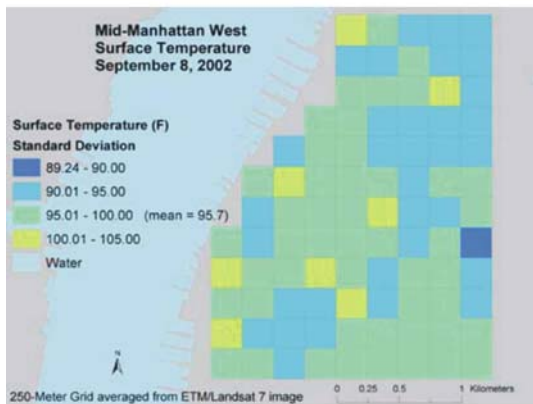
The Mid-Manhattan West case study area, located in western Manhattan from 35<sup>th</sup> street to the southern end of Central Park at 59<sup>th</sup>, is approximately 2.5 square miles (7 square kilometers) running along the coast of the Hudson River (Figure 1-5). Mid-Manhattan West has a population density of ~45,000 people per square mile. The central portion of the Mid-Manhattan West case study area is a commercial and business district with high-rise buildings and street-level commercial space with a daytime population that is much higher than the night time residential population. The northern and southern areas have a high residential population density. There is a gridded street pattern with very few vegetated areas and many industrial areas.



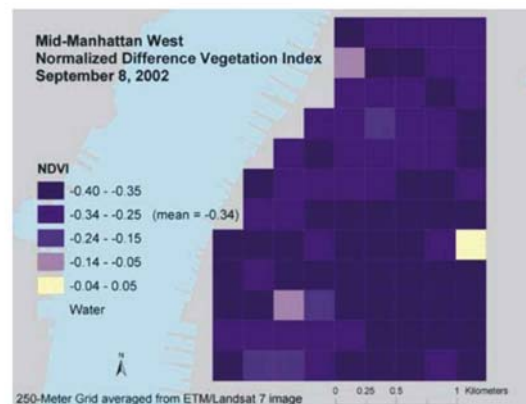
a)



b)



c)



d)

Figure 1-5. Mid-Manhattan West case study area. a) aerial view, b) street view c) gridded surface temperature on September 8, 2002 with resolution of 250 meters, d) gridded NDVI with resolution of 250 meters.

### **Lower Manhattan East**

The Lower Manhattan East case study area, which includes parts of the downtown Manhattan business district, Chinatown, and the East Village, is approximately four square miles (10 square kilometers) at the southern tip of Manhattan up to 14<sup>th</sup> St, surrounded by water on three sides (Figure 1-6). Overall, it has the highest population density of all case study areas (~79,000 people per square mile). The Lower Manhattan case study area can be divided into two sections: the downtown business district, characterized by low-to-medium residential population density, high daytime population and high daytime energy use with very tall buildings; and Chinatown/East Village,



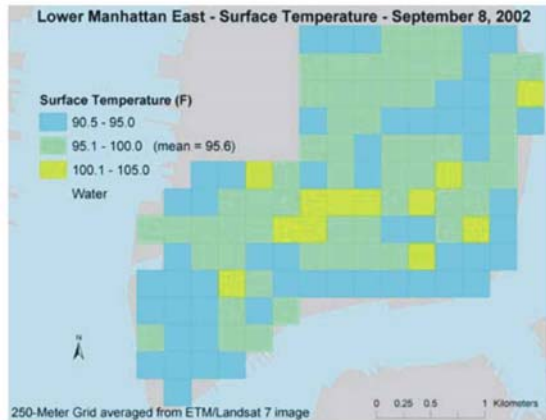
characterized by high population density and commercial spaces with relatively high energy-use during the day and the evening. The street pattern is less uniformly gridded than Mid-Manhattan West; the streets are mostly straight, but there are also many diagonal streets that intersect the grid. There are very few open spaces other than along the coastline and few industrial areas.



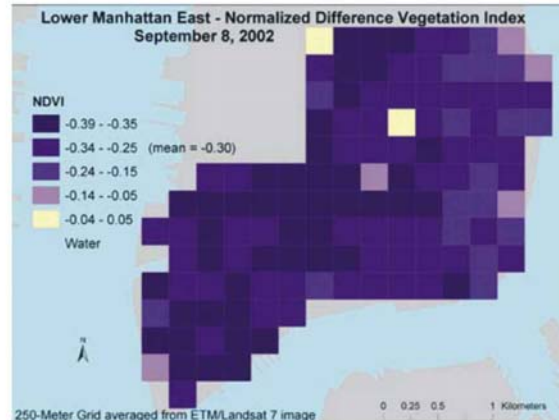
a)



b)



c)



d)

Figure 1-6. Lower Manhattan East case study area. a) aerial view, b) street view, c) gridded surface temperature on September 8, 2002 with resolution of 250 meters, d) gridded NDVI with resolution of 250 meters.



## **Fordham Bronx**

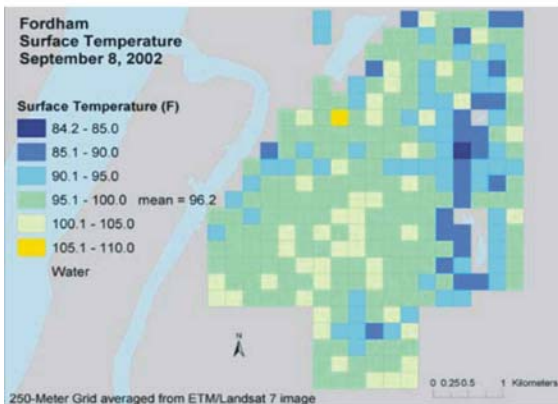
The Fordham case study area, located in the west-central part of the Bronx, is approximately 6 square miles (15 square kilometers) (Figure 1-7). Fordham is a heterogeneous site that contains Bronx Park, Fordham University, and a mixed-use neighborhood of one-to-four family homes, high rises, commercial spaces, transportation hubs and some industry. Fordham has a population density of ~55,000 people per square mile, is predominantly low-income (average median household income is \$22,770), is high-minority (77% of the residents identify themselves as people of color) and has a dense population. Implementation of the mitigation strategies in this neighborhood could contribute to improving environmental equity.



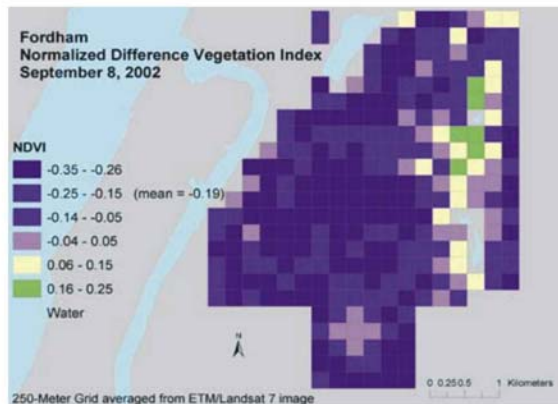
a)



b)



c)



d)

Figure 1-7. Fordham Bronx case study area. a) aerial view, b) street view, c) gridded surface temperature on September 8, 2002 with resolution of 250 meters, d) gridded NDVI with resolution of 250 meters.

## Maspeth Queens

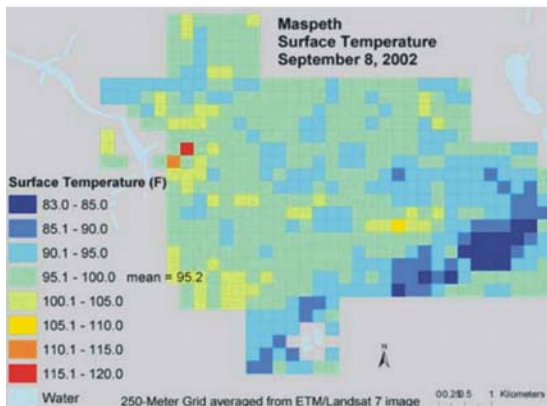
The Maspeth Queens case study area, located in west-central Queens, is approximately 11 square miles (29 square kilometers) and has relatively low base surface temperatures. (Figure 1-8). It contains Forest Park, many cemeteries, a large industrial area, and several residential areas with a mix of detached homes and high-rise apartment buildings. The population density in the Maspeth case study is the lowest of all areas (~ 25,000 people per square mile), although it ranges from relatively low in the industrial areas to relatively high in the residential areas. The industrial areas and the large parks and cemeteries are characterized by large tracts and few roads, while the residential areas have a fairly gridded street pattern.



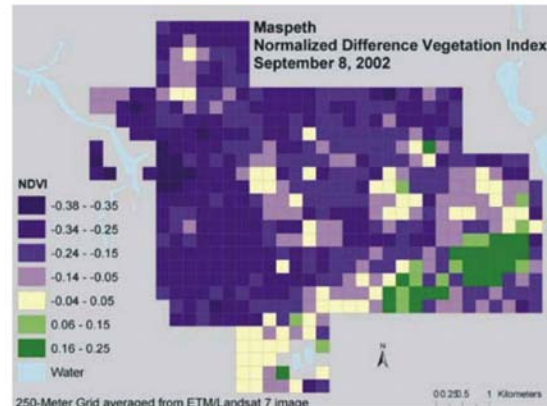
a)



b)



c)

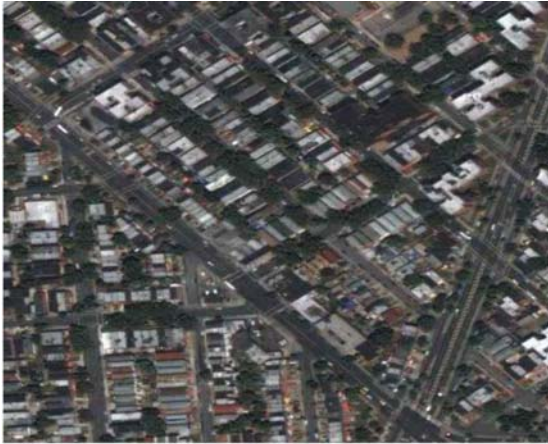


d)

Figure 1-8. Maspeth Queens case study area. a) aerial view, b) street view, c) gridded surface temperature on September 8, 2002 with resolution of 250 meters, d) gridded NDVI with resolution of 250 meters.

### **Crown Heights Brooklyn**

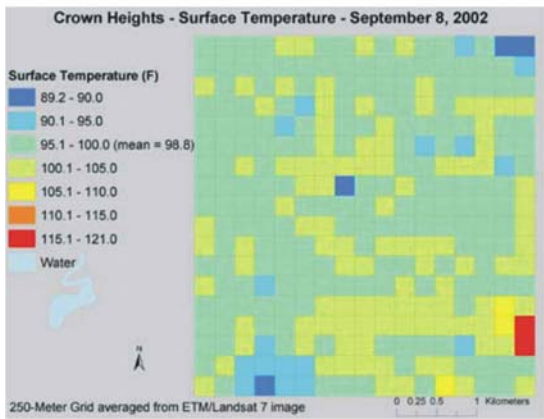
The Crown Heights case study area is one of the hotter case study areas in terms of base surface temperature. It is located in central Brooklyn and is approximately 6 square miles (15 square kilometers) (Figure 1-9). The housing is predominantly mixed residential and commercial with two-to three-story attached homes and multi-story pre-war apartment buildings. The vegetation varies significantly across the study area, with some residential areas having a large number of street trees, while other areas have very little vegetation. The average population density is ~ 47,000 people per square mile, but much lower in the industrial areas. The vegetation varies significantly across the study area, with some residential areas having a large number of street trees, while other areas have very little vegetation. There are several large industrial areas and few open spaces. Crown Heights has a predominantly low-income population, with an average median household income of \$28,371. Crown Heights also has a high minority population, with 90% of the residents identifying themselves as people of color. Therefore, reducing this neighborhood's summertime temperature could improve environmental equity.



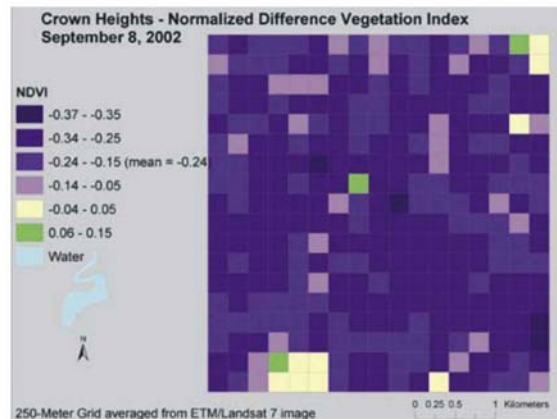
a)



b)



c)



d)

Figure 1-9. Crown Heights Brooklyn case study area. a) aerial view, b) street view, c) gridded surface temperature on September 8, 2002 with resolution of 250 meters, d) gridded NDVI with resolution of 250 meters.



### Ocean Parkway Brooklyn

The Ocean Parkway Brooklyn case study area, located on and near the coast in southern Brooklyn, is approximately 4 square miles (10 square kilometers) (Figure 1-10). It is a predominantly two-story post-WWII residential community characterized by wide boulevards and tree-lined sidewalks. The average population density is ~41,000 people per square mile, with the highest population density in the western portion of the area. Although there is some high-rise housing, the average building height is just 1.5 floors. There are few open spaces and few industrial areas.

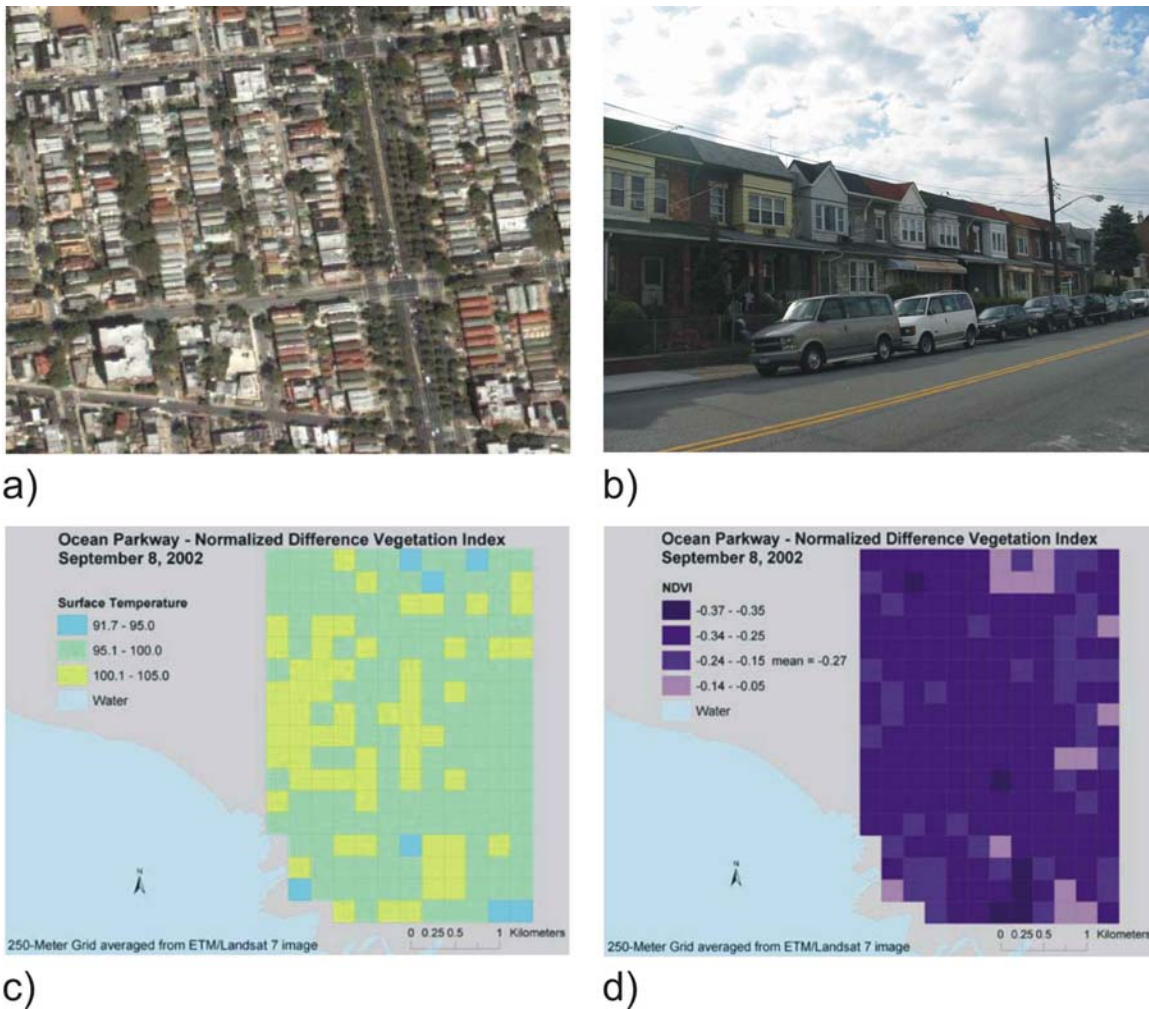


Figure 1-10. Ocean Parkway Brooklyn case study area. a) aerial view, b) street view, c) gridded surface temperature on September 8, 2002 with resolution of 250 meters, d) gridded NDVI with resolution of 250 meters.

## **Section 2**

### **DETERMINING TEMPERATURE IMPACTS: STUDY METHODS, DATA, AND MODELS**

The project used a combination of methods, data types, and models to study the mitigation of the urban heat island in the New York Metropolitan Region. The summer of 2002 was chosen as the time period for this study. A remote sensing and geographic information system (GIS) data library was developed to characterize the numerous dimensions of New York City's heat island. Satellite-derived surface temperatures were regressed on other satellite-derived and/or GIS-based environmental variables to evaluate factors that affect the surface temperature within each case study area. Three heat waves during the study period were selected using observed meteorological data. The Penn State/NCAR MM5 regional climate model was used to test the mitigation scenarios. MM5 base runs were compared with meteorological data from National Weather Service (NWS) and WeatherBug®<sup>4</sup> stations for the three heat-wave periods. (For more information about WeatherBug stations, see Appendix A.) Comparison showed that the model simulation represented regional climate adequately. MM5 was then used to determine potential reductions in surface temperature and near-surface air temperature with each mitigation scenario during the three heat-wave periods.

#### **IDENTIFICATION OF HEAT-WAVE PERIODS**

National Weather Service data from Central Park were used to identify three heat-wave periods during the summer of 2002 (Figure 2-1). The three heat-wave periods are July 2<sup>nd</sup> – 4<sup>th</sup> (HW1), July 28<sup>th</sup> – August 7<sup>th</sup> (HW2), and August 11<sup>th</sup> – August 18<sup>th</sup> (HW3). For this analysis, a heat-wave period is defined as at least three consecutive days with maximum temperatures above 90°F (32.2°C) in Central Park.

---

<sup>4</sup> WeatherBug data are available commercially through AWS Convergence Technologies.  
[http://www.aws.com/aws\\_2005/default.asp](http://www.aws.com/aws_2005/default.asp).

HW1 was the hottest and driest of the three heat-wave periods, but lasted only a few days (Table 2-1). HW2 and HW3 were about equally hot, but during HW3 John F. Kennedy Airport (JFK) was considerably cooler than Central Park, in part due to winds blowing from the south across the water. Conditions during HW3 were also more humid than during HW2. During HW2 and HW3, scattered showers punctuated the overall dryness.

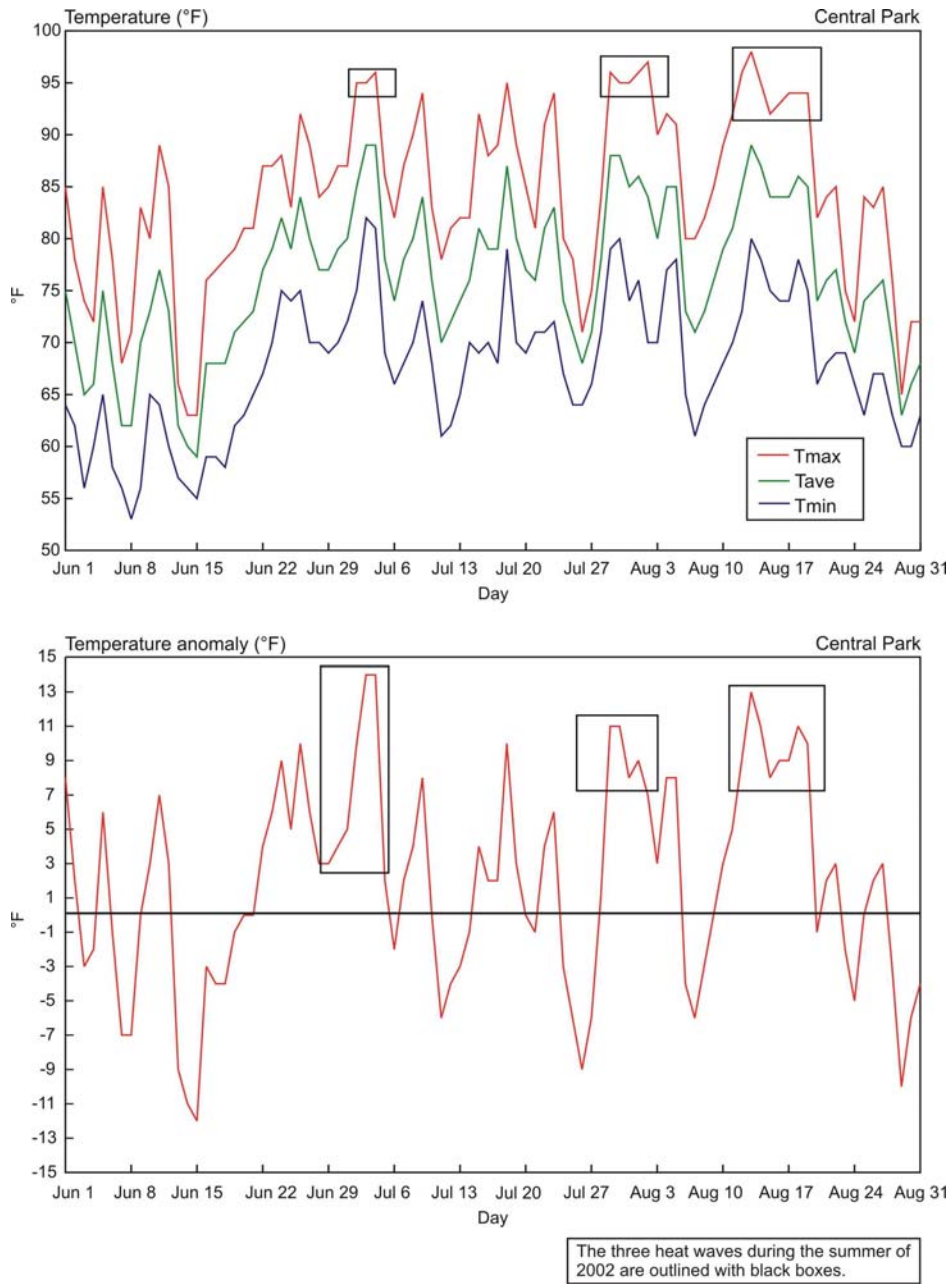


Figure 2-1. Heat wave days during the summer of 2002. a) Maximum, minimum, and mean daily temperature, b) Daily temperature anomaly.

Table 2-1. Mean temperature and relative humidity during each of the three heat waves.

Heat Wave	Mean Near-Surface Air Temperature (F)		Mean Relative Humidity (%)	
	Central Park	JFK	Central Park	JFK
NWS Station	Central Park	JFK	Central Park	JFK
July 2 – 4	87.8	86.0	58.8	62.9
July 29 – Aug 3	84.2	82.9	58.4	64.4
Aug 11 – Aug 19	83.3	79.2	60.7	72.7

### **CHARACTERIZATION OF NEW YORK CITY’S HEAT ISLAND ON HEAT-WAVE DAYS**

Observed meteorological data and remotely-sensed satellite data for the New York metropolitan region were used to characterize the spatial and temporal dimensions of the city’s heat island on August 14, 2002, one of the hottest heat-wave days during the summer of 2002. The NWS data were spatially interpolated across the region to determine spatial patterns in near-surface air temperatures over the course of the day. Landsat data from the same day were used to characterize the spatial dimensions of New York City’s surface heat island. The Landsat thermal data have a spatial resolution of 60 meters, and thus reveal surface heating differences at a finer scale than the NWS data. These surface-heating differences contribute to the development of the heat island effect by creating conditions for local hot spots where energy is retained.

### **REMOTE SENSING DATA**

A remote sensing and geographic information system (GIS) data library was developed to characterize the numerous dimensions of New York City’s heat island. Five remotely-sensed images were obtained. Three are Landsat images with a resolution of 30 meters in the visible and near-infrared bands and 60 meters in the thermal-infrared band; one is an ASTER image with a resolution of 90 meters; and one is a MODIS day-night pair with a resolution of 1 kilometer (Table 2-2). Figure 2-2 shows surface temperatures derived from the August 14 image; Figure 2-3 shows the Landsat July 22 image mapped to the MM5 grid boxes. Remotely-sensed surface temperatures are skin temperatures of surfaces exposed to the satellite sensor. These include unobstructed roads, roofs, grassy



surfaces, tree canopies, etc. However, it is not possible to distinguish between individual surfaces – which may be at different heights – from the remotely-sensed data. Appendix C describes the algorithm used to derive surface temperature from the remotely-sensed images.

Table 2-2. Remotely sensed satellite images.

Satellite	Date	Time	Resolution in Thermal Band
Landsat 7 ETM+	July 22, 2002	10:30 AM	60 meters
Landsat 7 ETM+	August 14, 2002	10:30 AM	60 meters
Landsat 7 ETM+	September 8, 2002	10:30 AM	60 meters
ASTER	September 8, 2002	10:30 AM	90 meters
MODIS day-night pair	September 8, 2002	10:30 AM & 10:30 PM	1 kilometer

Landsat Surface Temperature August 14 2002 10:30am

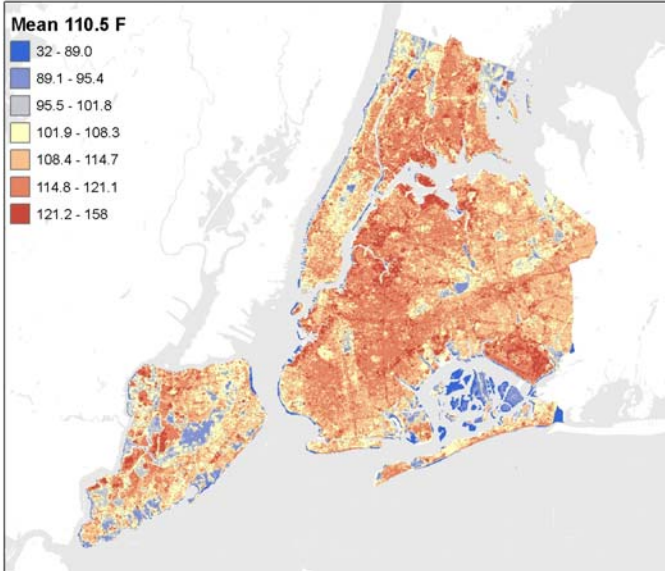


Figure 2-2. Remotely sensed thermal satellite data. Landsat ETM, August 14, 2002 at 10:30 AM, Band 6, resolution is 60 meters.

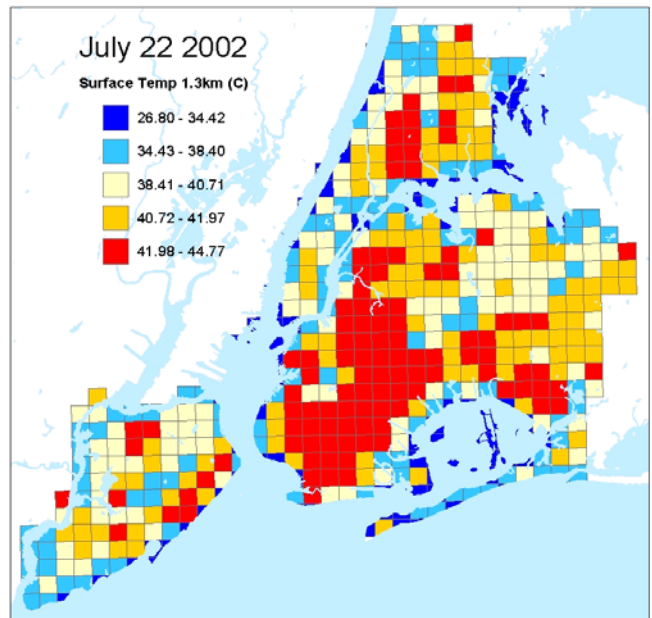


Figure 2-3. Landsat July 22, 2002 image imbedded in MM5 1.3 km grid cells.

The remote sensing data are limited to three days and, with the exception of the MODIS night time image, to the morning. The Landsat satellite pass does not coincide with the hour of occurrence of the daily maximum temperature, nor the time of peak energy demand. Also, only one of the images corresponds to a summer 2002 heat-wave day.

Nevertheless, although the magnitude of surface temperatures differs, the relative distribution of temperatures is similar across all images and thus representative of summertime surface-heating patterns. The August 14 image also has the highest surface temperatures of the set, supporting an association between elevated surface temperatures and elevated near-surface air temperatures.

## NDVI AND ALBEDO

The GIS databases incorporate land surface and urban morphology information as well as streets, hydrology, open space, block groups, and land cover (Table 2-3). Descriptive statistics for land surface and urban morphology data are given in Table 2-4.

Table 2-3. Variables included in GIS data library.

<b>Variable</b>	<b>Description (source)</b>	<b>Assumed Influence on Surface Temperature</b>
Albedo Proxy	Reflectivity measure calculated by Small (2003).	Negative
Normalized Difference Vegetation Index (NDVI)	Calculated from RS image for each day 60 meter resolution	Negative
Road Density	Calculated from Census TIGER 2003 Roads	Positive
Population Density	Calculated from Census 2000 Block Groups	Positive
Building Square Footage	Calculated from Tax Parcel Database of NYC	Positive
Average Building Height	Calculated from Tax Parcel Database of NYC	Positive
Average Year Built	Calculated from Tax Parcel Database of NYC, The more recent the construction of individual buildings the greater the negative influence on heat island conditions (especially pre-1980 construction); derived from the year built	Negative

Two land-surface parameters of particular interest are normalized difference vegetation index (NDVI) and albedo (Figures 2-4 and 2-5). NDVI is a measure of vegetation amount and condition calculated for each pixel on the image and associated with vegetation canopy characteristics such as biomass, leaf area index and percentage of vegetation cover.

Table 2-4. Descriptive statistics for each case study area.

Variable	NDVI		Albedo Proxy (% reflected)		Population Density* (people per sq mile)		Building Height (number of floors)	
	Mean	Stan Dev	Mean	Stan Dev	Mean	Stan Dev	Mean	Stan Dev
New York City	-0.16	0.16	11.0	3.0	27,634	34,601	1.8	3.4
Mid-Manhattan West	-0.34	0.06	10.9	3.2	44,224	46,110	5.3	9.3
Lower Manhattan East	-0.30	0.08	10.8	2.3	78,930	54,022	6.3	9.6
Fordham Bronx	-0.18	0.14	10.3	2.9	55,558	50,254	2.0	2.9
Maspeth Queens	-0.17	0.14	11.5	3.1	24,870	27,155	1.4	1.5
Crown Heights Brooklyn	-0.24	0.08	11.5	2.5	47,026	29,070	1.9	3.1
Ocean Parkway Brooklyn	-0.27	0.06	13.1	2.5	40,771	19,039	1.4	1.8

\* 0 – 10K is low population density, 10-45K is medium population density and 45-350K is high population density.

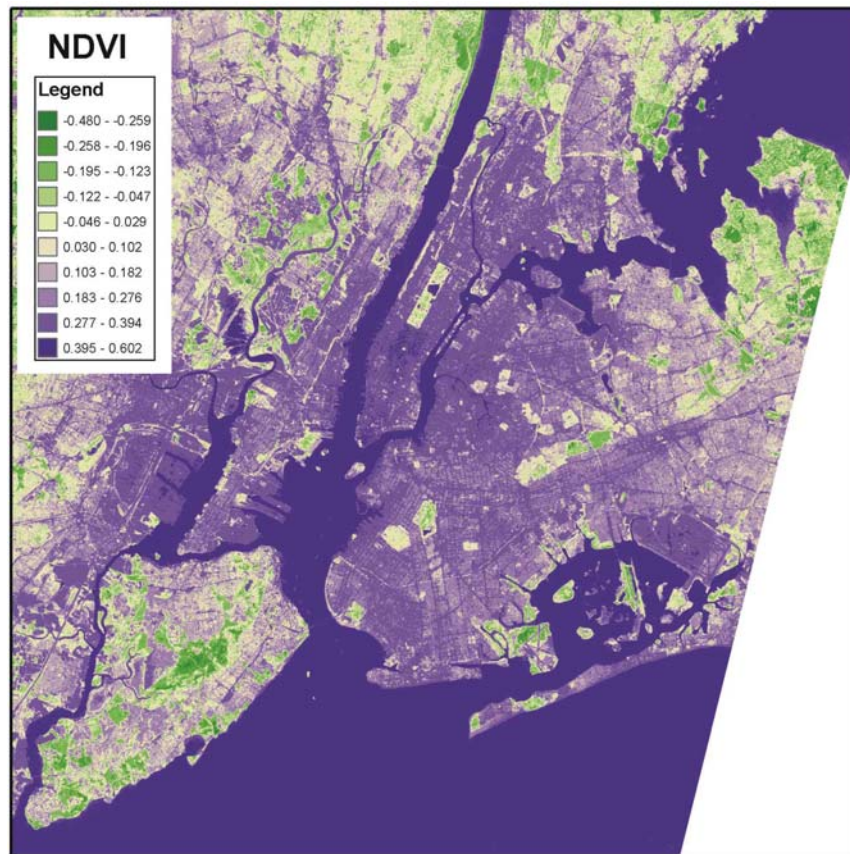


Figure 2-4. Normalized difference vegetation index (NDVI) derived from September 8, 2002 Landsat image. NDVI is a non-linear transformation of the visible (red) and near-infrared bands of satellite information. NDVI is defined as the difference between the red and near-infrared (nir) bands, over their sum [ $NDVI = \frac{nir - red}{nir + red}$ ]. NDVI is an alternative measure of vegetation amount and condition. It is associated with vegetation canopy characteristics such as biomass, leaf area index and percentage of vegetation cover. NDVI units are non-dimensional, a fraction with a potential range between -1 and 1.

Albedo proxy, a measure of the reflectivity of an illuminated surface, was derived from Landsat 7 panchromatic imagery following Small (2003). The Landsat 7 panchromatic band is an integrated measure of reflected radiance at visible to near-infrared wavelengths (Small, 2003). This band is considered a good proxy for albedo because most of the solar emission is in the very near infrared range (Small, 2003). Overall, albedo in and around New York City tends to be low, seldom reaching more than 0.13 (i.e., no more than 13% of the energy incident on a surface is reflected).

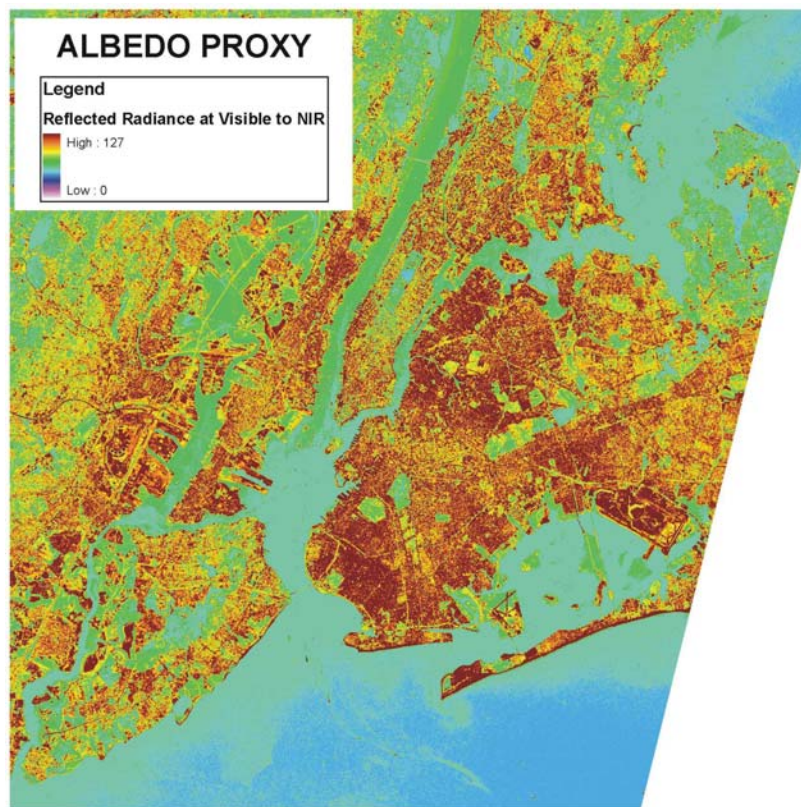


Figure 2-5. Albedo proxy based on Small (2003). The albedo proxy is an integrated measure of reflected radiance at visible to near infrared wavelengths.

## GIS DATA

Key urban morphology parameters in New York City are road density and average building height (Figures 2-6 and 2-7). Other parameters include building square footage and average building age. To derive road density, Census TIGER (Topologically Integrated Geographic Encoding and Referencing) road data from 2002 were used in the



ArcGIS Spatial Analyst extension to calculate the total amount of road length for 60-meter grid cells. The 60-meter cell size was selected to match the resolution of the remotely-sensed surface temperature data.

Average building heights were derived from the number of stories – a proxy for building height – in the real property database of New York City’s Department of Finance. The data are attached to the tax parcel database maintained by the Department of City Planning. New York City’s Regional Plan Association generated a 10-meter RASTER data layer of average building heights for the urban heat island data library. Information on additional data in the GIS-based heat island data library can be found in Appendix D.

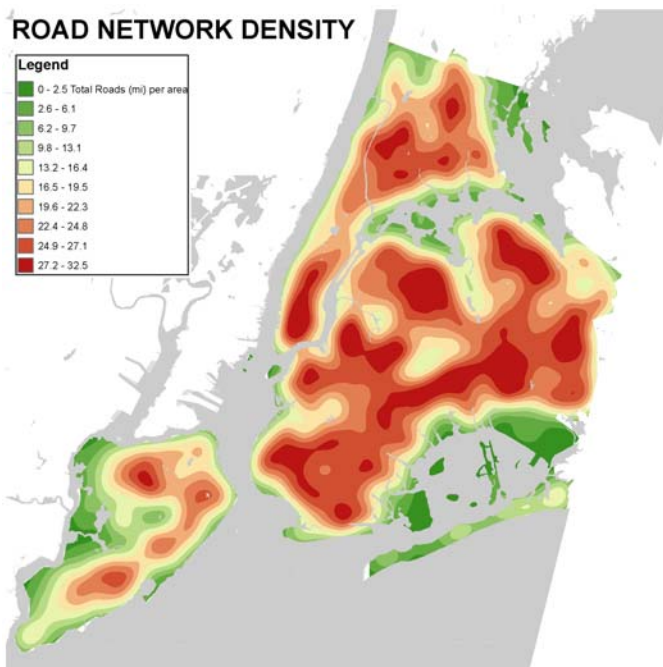


Figure 2-6. Road density network derived from Census Tiger roads from 2002.

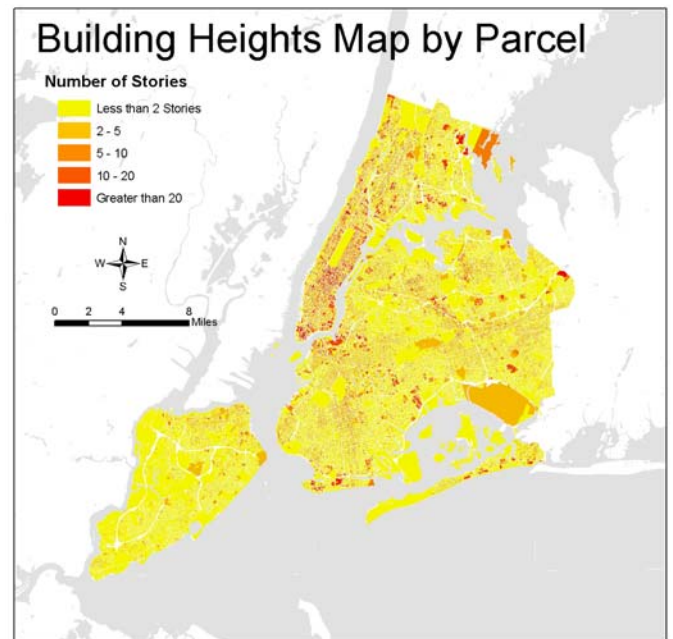


Figure 2-7. Average building height derived from number of stories. Extracted from the real property database of New York City’s Department of Finance, 2002.

## LAND SURFACE DATA

The land-cover data were derived from a database developed by Myeong et al. (2003). Land-cover classification was based on EMERGE aerial photography obtained from flyovers during 2001 – 2002 (Myeong et al., 2003). The database was used to develop a

GIS layer classifying all surface area as either impervious, grass, or trees. Base land cover is shown in Figure 2-8. Open space that is currently grassy but could be planted with trees is shown in Figure 2-9.<sup>5</sup> The available area for planting street trees was defined using a GIS layer created by the New York City Department of Parks and Recreation based on the same aerial photography. The available area for planting street trees in the Maspeth case study area is shown in Figure 2-10 (Myeong et al., 2003).

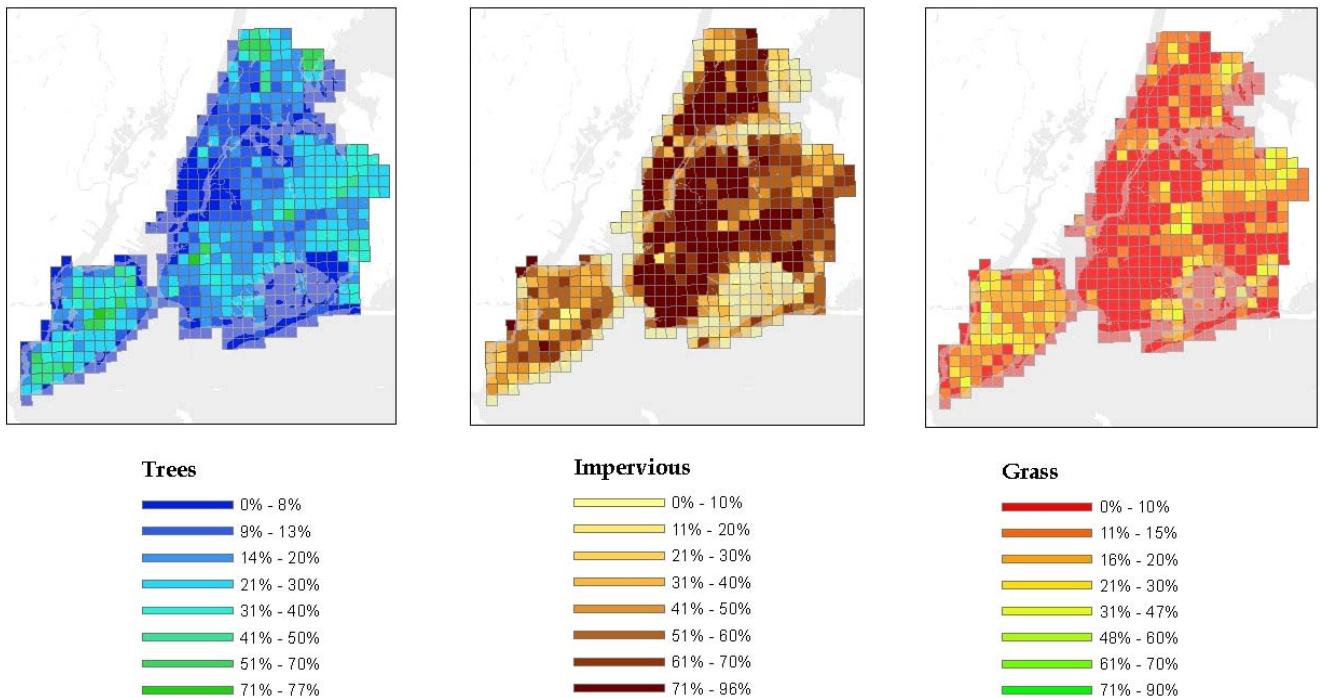


Figure 2-8. Base percentages of trees, impervious surfaces, and grass within each 1.3 km MM5 grid box. Percentages were derived from a land cover classification performed by Myeong et al. (2003) on EMERGE aerial photography obtained from flyovers during 2001 – 2002.

<sup>5</sup> Note that some of this open space area was filtered out during the mitigation scenario analysis to account for the fact that playgrounds, athletic tracks, cemeteries, etc. cannot actually be planted with trees. More information on this can be found in the section on Mitigation Scenario Assumptions.



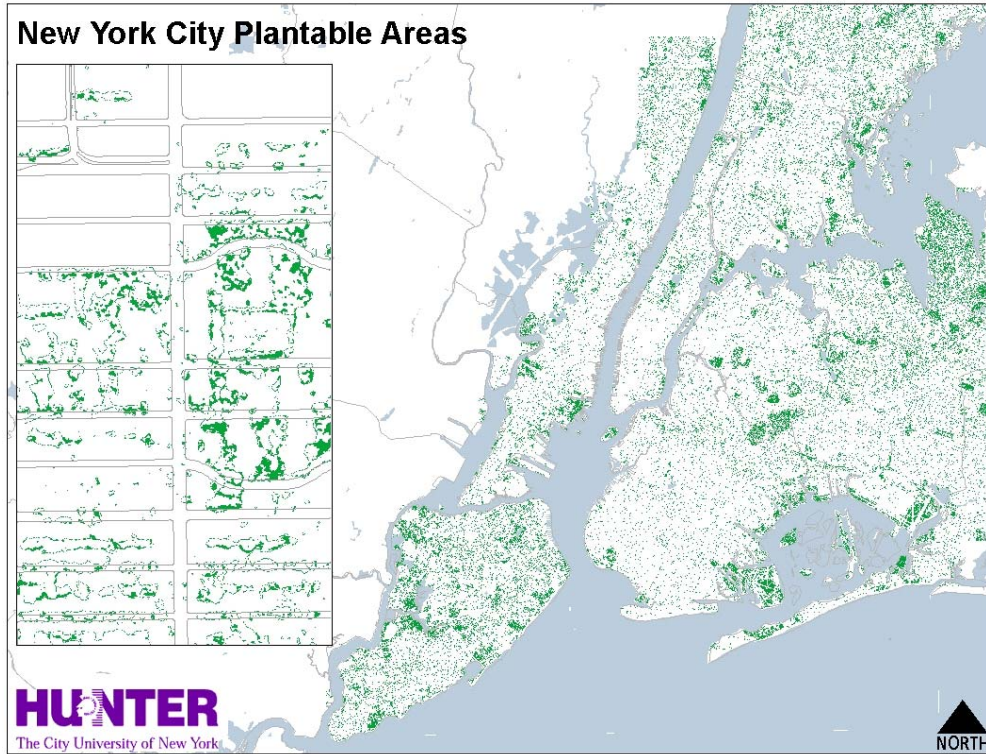


Figure 2-9. Grass areas available for open space planting. Data resolution is 3 meters.

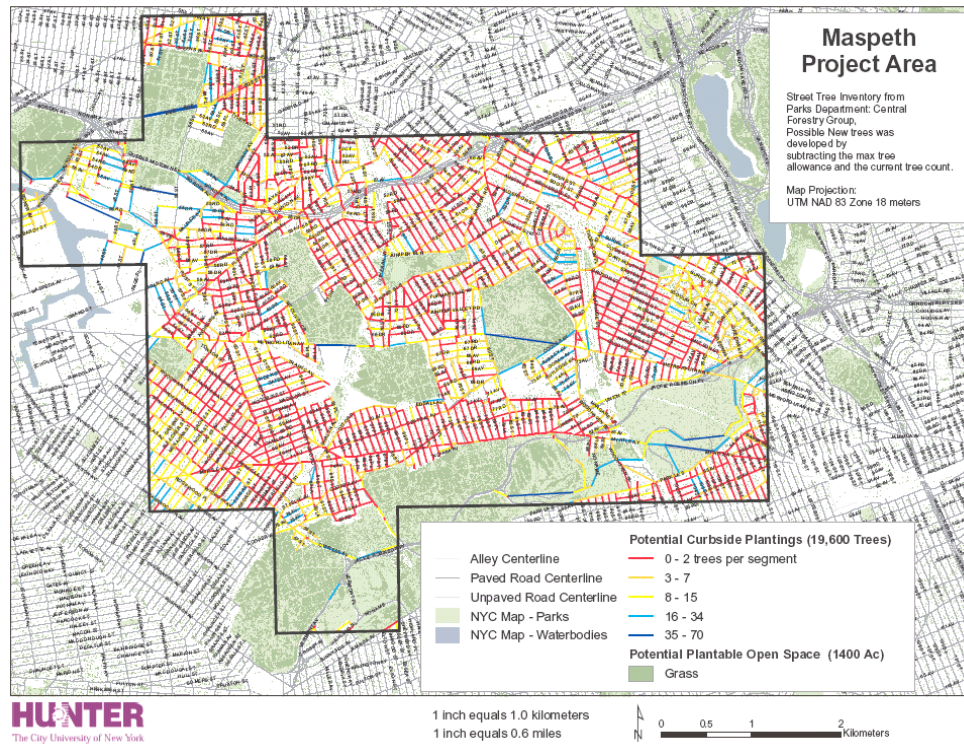


Figure 2-10. Street tree inventory from New York City Department of Parks in Maspeth Queens case study area.

## STATISTICAL ANALYSIS

Exploratory data analysis and ordinary least squares (OLS) regressions were conducted to evaluate how well environmental variables predict the surface temperature city-wide and in each case study area. The unit of analysis is a 250-meter grid coupled to a Geographic Information System (GIS) for both spatial mapping and statistical analysis. Significance was established at the 0.05 level where significance indicates a rejection of the null hypothesis that there is no relationship between surface temperature and the environmental variable(s). As suggested by Mertens and Lambin (2000), random spatial sampling was used to filter out the scale effect and the spatial autocorrelation in the residuals where necessary. Some grid cells were removed for city-wide analysis because preliminary results showed that in these areas, a single variable drives their surface temperature, skewing the results. These areas included the two major airports (JFK and LaGuardia), areas within 328 feet (100 meters) of large water bodies (e.g. Hudson River, Atlantic Ocean), and areas that are within open spaces larger than 10 acres (4 hectares).

The dependent variables in the analyses are remotely-sensed surface temperatures, averaged over the 250-meter grid, derived from four of the remotely sensed images described previously.<sup>6</sup> Three primary sets of independent variables are defined; land surface (NDVI and albedo proxy), urban form (road density, average year built, and average building height), and urban density (population density, energy use, and building square footage) (see Table 2-3).

Exploratory data analysis revealed surface temperature variation between the different days and across the case study areas. Average remotely-sensed surface temperatures range from 76.1 – 105.6°F (24.5 – 40.9°C) across the four images, with variability across the case studies (Table 2-5). At 10:30 AM, Crown Heights is the hottest case study area in all four images, followed closely by Ocean Parkway. The coolest case study areas are Mid-Manhattan West, Lower Manhattan East, and Maspeth Queens, which are between 2.7 and 4.5°F (1.5 – 2.5°C) cooler than Crown Heights.

---

<sup>6</sup> The three Landsat images acquired on July 22<sup>nd</sup>, August 14<sup>th</sup>, and September 8, 2002 as well as the ASTER image acquired on September 8 were used. The MODIS day-night pair was excluded from the statistical analysis because of its coarser spatial resolution.



Table 2-5. Average surface temperatures during the summer of 2002 derived from four remotely-sensed satellite images.

Case Study Area	Surface Temperature (°F)
Mid-Manhattan West	105.6
Lower Manhattan East	105.4
Fordham Bronx	106.3
Maspeth Queens	105.1
Crown Heights Brooklyn	109.8
Ocean Parkway Brooklyn	109.8
New York City	105.6

In the New York City-wide study area, the regression analysis showed that NDVI is the strongest predictor of surface temperature for all four images. NDVI has a negative relationship with surface temperature, so as vegetation increases, remotely-sensed surface temperature decreases (Table 2-6). On the September 8 image, NDVI accounts for 30% of the variability in surface temperature (Figure 2-11).

Table 2-6. Bivariate analysis with an 8% random sample of New York City.\*

Independent Variable	RS Image	R <sup>2</sup> (S.E)	Regression Equation	Moran's I (sig)
Normalized Difference Vegetation Index (NDVI)	ETM072202	.30 (2.01)	$E(Y) = 39.74 - 10.51 X + e$	I = .08 (.02)
	ETM081402	.32 (1.25)	$E(Y) = 27.80 - 7.44 X + e$	I = .09 (.01)
	ETM090802	.30 (1.52)	$E(Y) = 34.47 - 7.92 X + e$	I = .07 (.20)
	AST090802	.33 (1.74)	$E(Y) = 23.29 - 9.91 X + e$	I = .03 (.32)
Albedo Composite	ETM072202	.15 (2.22)	$E(Y) = 37.62 + .37 X + e$	I = .04 (.20)
	ETM081402	.13 (1.41)	$E(Y) = 27.02 + .22 X + e$	I = .05 (.10)
	ETM090802	.15 (1.67)	$E(Y) = 32.88 + .27 X + e$	I = .04 (.20)
	AST090802	.11 (2.00)	$E(Y) = 22.29 + .26 X + e$	I = .08 (.01)
Road Density	ETM072202	.07 (2.32)	$E(Y) = 39.07 + .12 X + e$	I = .02 (.47)
	ETM081402	.08 (1.46)	$E(Y) = 27.72 + .08 X + e$	I = .05 (.11)
	ETM090802	.07 (1.75)	$E(Y) = 33.97 + .09 X + e$	I = .02 (.46)
	AST090802	.08 (2.03)	$E(Y) = 22.91 + .11 X + e$	I = .09 (.01)

\*Excluding cells that are open space, coastal, or airports.

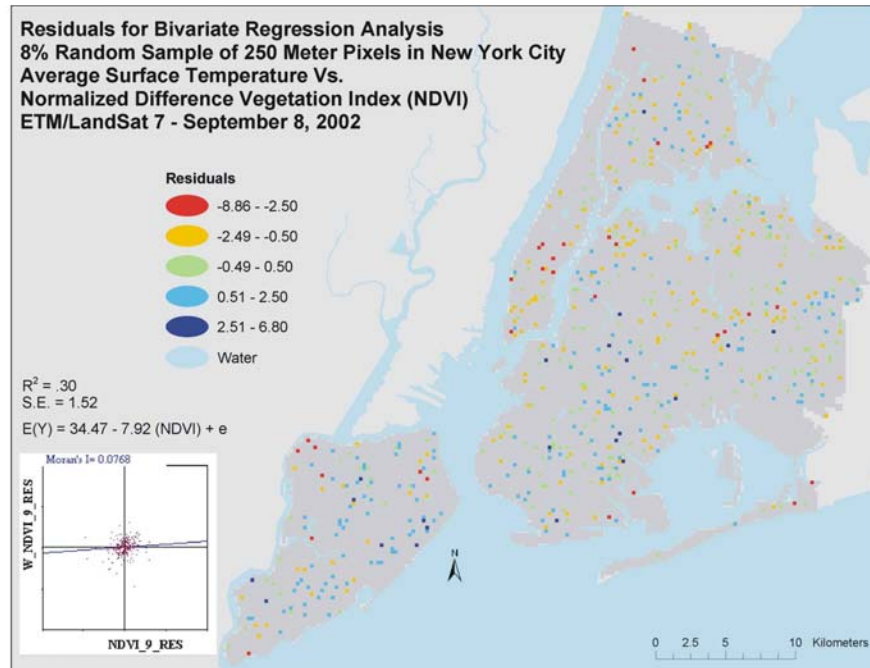


Figure 2-11. Residuals for bivariate regression analysis, 8% random sample of 250 meter pixels in New York City. Average surface temperature and NDVI both derived from September 8, 2002 Landsat image.

Albedo proxy is the second strongest explanatory variable, accounting for 15% of the variability in surface temperature city-wide on the September 8 image. However, albedo is lower in vegetated suburban areas than in New York City. Thus, impervious surfaces are associated with both higher surface temperatures and higher albedo; this is the opposite of the expected relationship in which more reflective surfaces are cooler. There are a number of possible explanations for this. It could be that the albedo proxy is not an adequate proxy for albedo in the New York Metropolitan region; or it could be related to the very small range of values on the albedo proxy image; or to the role that evapotranspiration, higher shading, and/or lower heat capacity of vegetated surfaces play in the suburbs, which might outweigh the effect of the higher albedo. The relationship between albedo and remotely-sensed surface temperature is stronger in Fordham and Maspeth, the two case study areas that have the most existing vegetation, as compared to the other case study areas (Table 2-7).

Finally, road density has a slight positive relationship with surface temperature, accounting for 8% of its variability city-wide on the September 8 image. In Fordham, road density, population density, and distance to large open spaces also contribute to the variation in surface temperature; however these factors are not significant for the other case study areas. Such differences highlight the spatial complexity of the urban heat island archipelago within New York City. A borough-scale statistical analysis is discussed in Appendix E.

Table 2-7. Regression results for the case study area using surface temperatures derived from the July 22, 2002 Landsat image as the dependent variable.

	Crown Heights 40% sample n = 121	Ocean Parkway 60% sample n = 122	Fordham 45% sample n = 126	Maspeth 20% sample n = 111	Lower Manhattan East 40% sample n = 50	Mid- Manhattan West n = 93
	Adj R <sup>2</sup> (S.E.)	Adj R <sup>2</sup> (S.E.)	Adj R <sup>2</sup> (S.E.)	Adj R <sup>2</sup> (S.E.)	Adj R <sup>2</sup> (S.E.)	Adj R <sup>2</sup> (S.E.)
	Moran's I (Sig.)	Moran's I (Sig.)	Moran's I (Sig.)	Moran's I (Sig.)	Moran's I (Sig.)	Moran's I (Sig.)
NDVI	<b>.34</b> (1.45)	<b>.28</b> (.75)	<b>.67</b> (1.77)	<b>.74</b> (1.59)		<b>.08</b> (1.77)
	.08 (.23)	.12 (.04)	-.02 (.90)	.03 (.67)		.07 (.14)
Albedo Composite	<b>.13</b> (1.66)		<b>.25</b> (2.67)	<b>.35</b> (2.49)	<b>.16</b> (1.82)	
	.16 (.03)		.07 (.30)	.22 (.03)	.08 (.41)	
Road Density			<b>.18</b> (2.78)	<b>.07</b> (2.99)	<b>.08</b> (1.90)	
			.15 (.03)	.31 (.00)	.02 (.63)	
Population Density			<b>.22</b> (2.71)			
			.15 (.03)			
Average Building Height					<b>.08</b> (1.91)	<b>.08</b> (1.76)
					-.04 (.87)	.00 (.83)

## MM5 REGIONAL CLIMATE MODEL

The MM5 regional climate model is a state-of-the-art three-dimensional, non-hydrostatic model that dynamically simulates the interactions among a range of land-surface cover and climate variables (Grell et al., 1994).<sup>7</sup> MM5 and similar regional atmospheric models use a fluid dynamics approach to simulate the flows of heat, moisture and momentum over different land surface types including urban areas. Therefore, although buildings are not explicitly represented in the model, their presence is assumed through the boundary layer structure, which controls the surface transport of heat and moisture. This was represented by a global urban roughness of one meter, applied uniformly city-wide.<sup>8</sup> Although surface properties in the boundary layer can alter the near-surface energy budget and thus the temperature of near-surface air, MM5 is primarily driven by regional circulation processes that tend to dampen near-surface effects through atmospheric mixing.

MM5 version 3.7 was run with high-resolution land-surface data and simultaneous energy balance models for impervious, grass, tree, and water surfaces (MM5 v3.7+SEBM) for each of the three heat-wave periods. Version 3.7 is a recent model release; in the course of the project, MM5 version 3.6 was replaced with version 3.7 to improve the sensitivity of near-surface air temperature to different surface types. A key difference between the two versions is the incorporation of a new horizontal diffusion scheme that improves MM5 results in regions with complex topography (e.g., urban areas), especially when MM5 is run at fine grid resolutions (Zaengl, 2002). Version 3.7 also includes an improved upper radiative boundary condition.

Model performance was evaluated by comparing hourly near-surface air temperatures simulated by the MM5 model to National Weather Service and WeatherBug weather station data using the average error, root mean square error (RMSE), and correlation coefficients. Wind speed, wind direction, and sea-level pressures simulated by the MM5

---

<sup>7</sup> For more information about MM5, see <http://www.mmm.ucar.edu/mm5/overview.html>.

<sup>8</sup> Buildings in urban areas create a thicker boundary layer due to greater turbulent mixing in canyons as compared to rural areas. Global roughness length, a user-defined model parameter, influences the thickness of the simulated urban boundary layer.

were also compared to observations. Further details on the model evaluation can be found in Appendix F.

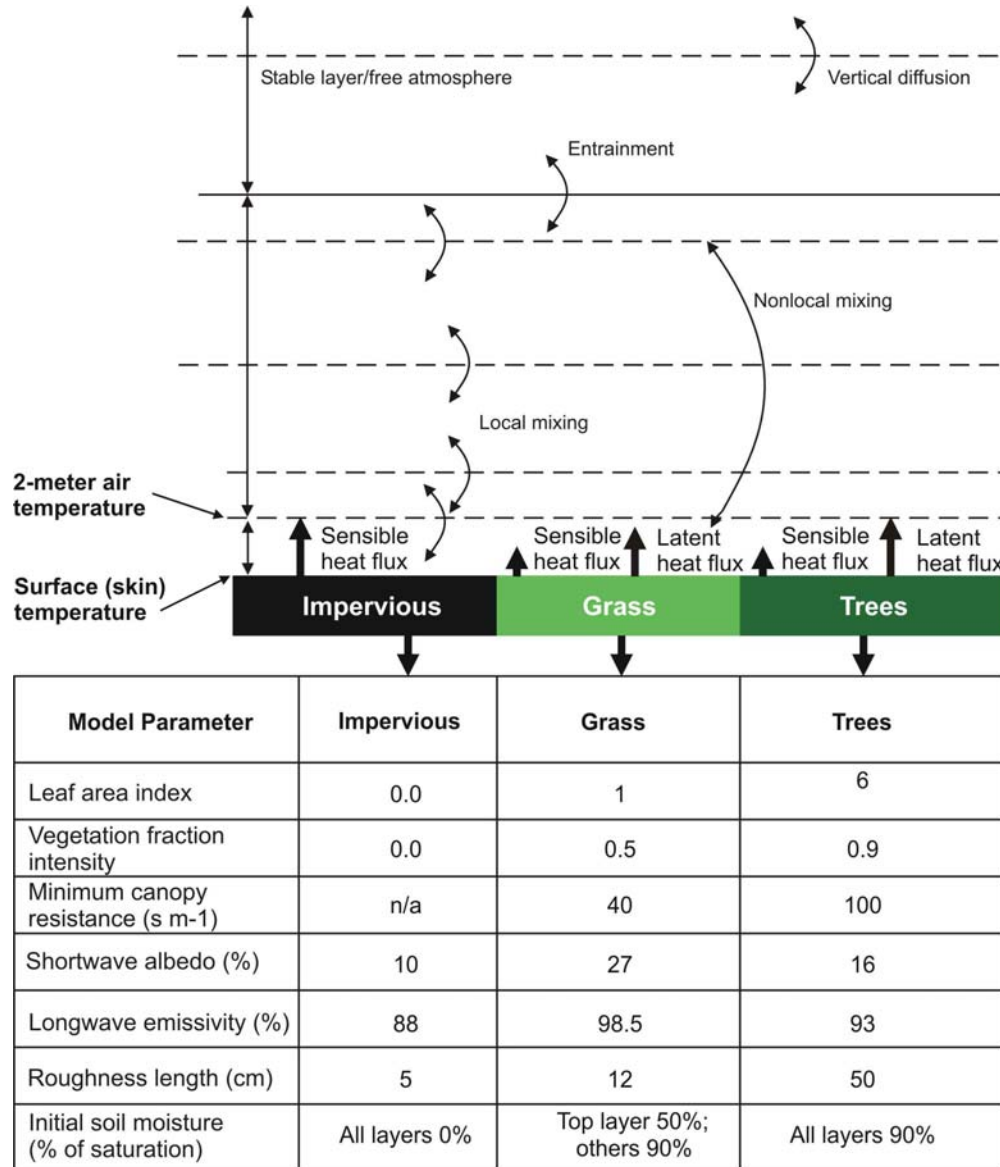


Figure 2-12. MM5 regional climate model diagram with simultaneous energy balance models (MM5 v3.7+SEBM) and model parameters for each land-surface cover type.

Within New York City, MM5 was run at 1.3 km grid resolution (initialized and forced with input from a 4-km domain; for more information see Appendix F). The Myeong et al. (2003) database of land-cover in New York City was used to specify a percent area *impervious*, a percent area *grass*, a percent area *trees*, and a percent area *water* within each grid box to achieve sub-grid scale resolution of the different land-surface types.

MM5 results for the 3 PM institutional/business energy peak and the 6 PM residential energy peak were used in the mitigation scenario analysis. In MM5, peak surface temperatures tend to occur in the mid-afternoon around 3 PM. Energy use in certain residential areas is of particular concern during the evening peak demand time represented by 6 PM (and later).

### **Modeled Base Case**

The MM5 base case was developed by simulating sensible and latent heat fluxes based on the configuration of land-surface cover within New York City and meteorological conditions (Figure 2-12). Air temperatures were calculated based on the simulated fluxes and then used to simultaneously solve four energy balance models, one each for *grass*, *trees*, *impervious*, and *water*, at each time step. Gridbox temperatures were aggregated by weighting the temperature of each land surface type according to its percent area within the case study. Additional methodology related to the MM5 modeling can be found in Appendix F.

The energy balance models were solved for surface and 2-meter air temperature. The surface temperature represents the horizontal surface of the various land-surface cover types exposed to the air including rooftops, streets, parks, and the tops of tree canopies (Figure 2-13). Therefore, shading by tree canopies is a process that is not well-captured by MM5, and as a result the cooling effect of trees is likely underestimated.

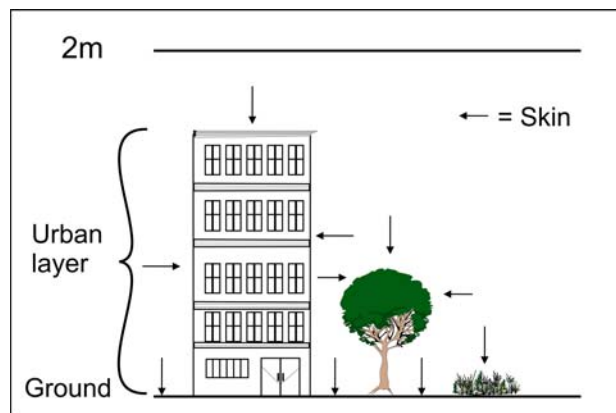


Figure 2-13. Surface (skin) temperature in an urban setting. MM5 sees horizontal surfaces only and the 2-meter temperature is conceptually above city rooftops.

Definitions of these temperatures for each land type of land surface are in Table 2-8. However, there is some ambiguity in the actual elevation represented by the 2-meter temperature above surfaces with different heights (e.g., tree canopy, streets, roofs) in MM5. Two-meter air temperatures in the MM5 are model-derived estimates<sup>9</sup> conceptually situated 2 meters above each of the surface types and therefore may better represent the well-mixed air “above” the city, rather than the air near the city’s hot urban surfaces. Impervious surfaces are present on the sides of tall buildings as well as on roofs, and at the ground surface in the form of streets and pavements. If fully represented in the regional climate model, these surfaces would have the effect of warming the air between the surface and 2-meter air that the mitigation scenarios aim to cool.

Table 2-8. Definitions of surface temperature and 2-meter temperature for each land surface type in MM5.

<b>Surface Type</b>	<b>Definition</b>
<b>Impervious</b>	
Surface Temperature	Model-calculated skin temperature of concrete, asphalt, etc.
2-meter Temperature	Model-calculated air temperature 2 meters above street level
<b>Grass</b>	
Surface Temperature	Model-calculated skin temperature of grass and bare ground between grass patches
2-meter Temperature	Model-calculated air temperature 2 meters above a grass surface
<b>Trees</b>	
Surface Temperature	Model-calculated canopy leaf temp (with small contribution from ground surface below)
2-meter Temperature	Model-calculated air temperatures two meters above a ground surface with trees. Note that the 2-meter temperature for a tree surface is not well-defined since the canopy itself is located at 2-meter height.

In addition, previous work has suggested that the MM5 scheme for interpolating 2-meter temperatures from model-derived 10-meter and ground temperatures is prone to error and that there was a cool bias when simulating Phoenix summertime temperatures with MM5 (Zehnder, 2002).

Because the 2-meter air temperatures calculated with MM5 do not capture the full effect of New York City’s highly heterogeneous surfaces on the city’s heat island, a weighted

<sup>9</sup> MM5 explicitly solves for the ground temperature and the temperature associated with the midpoint of the lowest model layer. The MM5 2-meter temperature is a model-derived estimate of the temperature based on the ground temperature and the first-layer temperature.

average of MM5 calculated surface and 2-meter air temperatures was calculated to better represent New York City’s near-surface air temperature. The weighting function was  $T_{\text{near-surface air}} = 0.3 * \text{surface temperature} + 0.7 * \text{2-meter temperature}$ . This function was arrived at by optimizing the fit of the linear weighting function to the observed data by minimizing the root mean square error (RMSE) over all the case study areas. The near-surface air temperatures calculated using the weighting function are closer in magnitude to the observed temperatures and also better simulate the observed diurnal range.

To calculate mitigation potential, the new series of base near-surface air temperatures for each land-surface type were weighted according to the percentage of each land-surface type with each mitigation scenario.

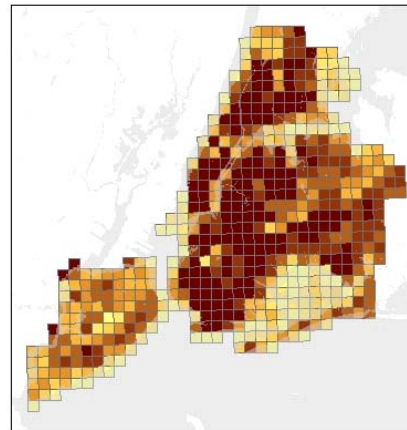
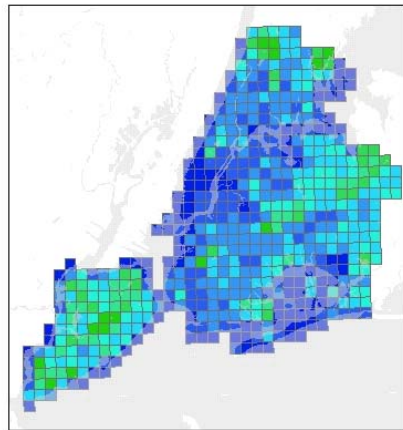
### MITIGATION SCENARIOS

Potential cooling citywide and within each case study area was investigated by testing a set of mitigation scenarios with MM5. The main strategies are urban forestry (curbside planting, open-space planting, or both), living roofs, and light roofs and surfaces. The scenarios are listed in Table 4-9 and two of the urban forestry scenarios are illustrated in Figure 2-14. The scenarios were tested at 100% intensity by assuming that all available area for redevelopment from one surface type to another would be changed to that surface type. The relationship between intensity of redevelopment and cooling potential was assumed to be linear. Therefore, 50% redevelopment would have half the cooling potential of 100% redevelopment. Additional model runs testing various intensities of redevelopment would be needed to test the validity of this assumption.

Table 2-9. Mitigation scenarios.

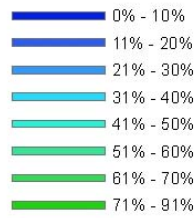
Strategy	Mitigation Scenario
Urban Forestry	1) Urban Forestry/Grass-to-Trees (open space planting)
	2) Urban Forestry/Street-to-Trees (curbside planting)
	3) Urban Forestry/Grass + Street-to-Trees (open space + curbside planting)
Light Surfaces	4) Light Surfaces/Roof-to-High Albedo (light roofs)
	5) Light Surfaces/Impervious-to-High Albedo (light surfaces)
Living Roofs	6) Living Roofs/Roof-to-Grass
Ecological Infrastructure	7) Urban Forestry/Grass + Street-to-Trees and Living Roofs
Urban Forestry + Light Roofs	8) Urban Forestry/Grass + Street-to-Trees and Light Roofs
Combination of All	9) 50% Open Space + 50% Curbside + 25% Living Roofs + 25% Light Roofs



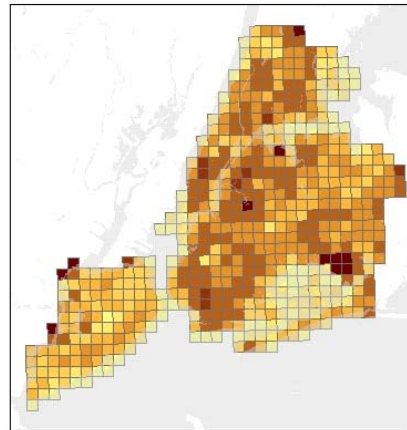
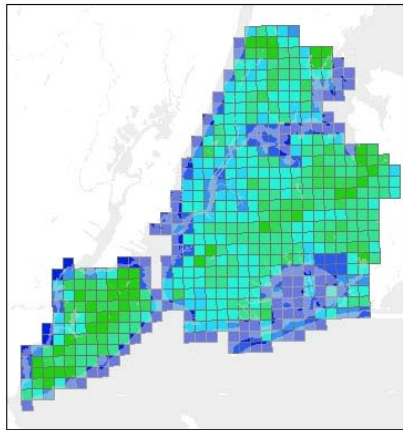
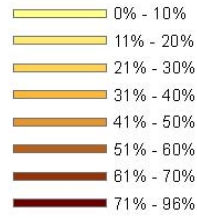


a)

**Trees**

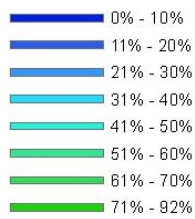


**Impervious**



b)

**Trees**



**Impervious**

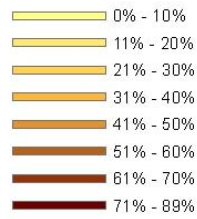


Figure 2-14. Mitigation scenario percentages. a) Urban forestry/grass-to-trees (open space planting) at 100% intensity, b) Urban forestry / grass+street-to-trees (curbside planting) at 100% intensity.

### **Mitigation Scenario Assumptions**

A number of simplifying assumptions were made in the mitigation scenario tests. In both urban forestry scenarios, all planted trees were assumed to be deciduous and mature from the date of planting.

In the urban forestry/grass-to-trees (open space planting) scenario, it was assumed that any area that is currently grassy could be planted with trees unless it has been delineated in the database as a cemetery, ball field, playground, athletic track, or tennis courts. In addition, areas within parks that are designated as beaches, gardens, recreational centers, playgrounds, or athletic areas were filtered out. However, areas like the Great Lawn in Central Park that are not delineated remained in the analysis, as did backyards. This scenario assumes that all open space plantings replace grass, but some newly planted trees would replace impervious surfaces in parks rather than grass.

In the urban forestry/street-to-trees (curbside planting) scenario, the available area for street trees is an estimate based on existing inventories subtracted from a hypothetical maximum carrying capacity for each city street, where city streets are represented as line segments (Lu, J., 2005). The estimate is adjusted for highways, bridges, and tunnels and subtraction of intersection widths and tree setbacks from corners, and other infrastructure that could limit street tree density. Carrying capacity estimates assumed an optimum tree spacing of 25 feet (8 meters), however for this analysis spacing of one tree every 75 feet (23 meters) was applied in an attempt to account for the impact of limited sites due to existing infrastructure. This scenario further assumed that trees would replace impervious surfaces; under actual conditions, street trees shade impervious surfaces, but the impervious surfaces still exist beneath them.

In the urban forestry/street-to-trees (curbside planting) scenario, a canopy diameter of 37.7 feet (11.5 meters), corresponding to an estimated canopy of the average New York City street tree, was used to calculate an area multiplier equal to 1116 square feet (104 square meters) per tree. Absent detailed data regarding the age of street trees in New York City, it was necessary to estimate canopy width from assumed growth rate

calculations. It is possible that street trees in New York City grow at a slower rate. The estimate for the average canopy width of a New York City street tree was calculated using projected canopy growth for a healthy tree growing in park like conditions (open, non-competitive, non-forest conditions). Planting of a 2.5 inch (6.4 cm) diameter at breast height (dbh) tree after 30 years is calculated to attain a dbh of 18.7 inches (47.5 cm) (growth rate of 0.27 inches/year (0.67 cm/year)) (Nowak, D., personal communications). The above 30 year estimated dbh of 18.7 inches (47.5 cm) was used to select the 17-19 inch (43 – 48 cm) dbh range (n=78) from the New York city-wide sample inventory that measured an average crown diameter of 37.7 feet (11.5 meters) (Lu, J., personal communication).

For the living roofs and light roofs scenarios, a flat-roof data layer was created by determining which land-use categories in New York City are most likely to have flat-roof architecture. In these scenarios, it was assumed that all flat roofs were available to receive 75% coverage with a living or light roof. It is unlikely that the total area of any individual flat roof would be available for redevelopment due to rooftop equipment and infrastructure. It was further assumed that all green roofs were planted with grass and that this grass would have the same surface temperature as the street-level grass currently present in parks and other areas. On the one hand, roof surfaces tend to be hotter than street-level surfaces, so rooftop grass might have a greater cooling effect on surface temperature than street-level grass (Solecki et al., 2005). On the other hand, rooftop grass affects air temperatures at the top of the urban canyon, where air temperatures are generally cooler than at its bottom. Additionally, air-conditioning intakes are often at the rooftop level, affecting energy demand calculations.

In the light roofs scenario, a clean bright surface with albedo of 0.5 (as opposed to an estimated average albedo of 0.15 for impervious surfaces in New York City) was assumed. An albedo of 0.5 was chosen because it is significantly higher than the typical urban rooftop albedo and thus was expected to yield a significant cooling effect. New bright white coatings can have an albedo greater than 0.5, but these are unlikely to be

sustainable for very long considering the weather, staining, and soot deposition that occurs in urban areas (Heat Island Group, 2006a).

In the light surfaces scenario, an albedo of 0.2 was used for street-level impervious surfaces such as sidewalks and roadways in combination with the 0.5 albedo for light roofs. Although it is not difficult to achieve an albedo of 0.5 using available roofing materials, it is a significant technical and cost challenge to achieve such a high albedo with the available paving materials. Asphalt pavement typically consists of 7/8 volume rock aggregate bound by 1/8 volume dark asphalt (bitumen). The bitumen binder has very low albedo (in the range of 0.04) and freshly laid pavement starts out with this dark color. After a few months, the pavement weathers exposing the lighter-colored aggregate, so the overall albedo of the surface tends to increase to a value in the range of 0.08-0.16 (Heat Island group, 2006b). A Los Angeles model study of albedo increases assumed that pavement albedo could be raised to 0.3 (Rosenfeld et al., 1996). Although lighter-colored aggregate may be able to achieve a higher albedo, data supporting this are lacking (Heat Island Group, 2006c), and materials remain experimental. Therefore, an albedo of 0.2 was selected to represent high-albedo roadways and sidewalks.

### Section 3

## CITY-WIDE RESULTS

New York City surface temperatures manifest as a heat island archipelago, with hot spots and cool spots within the overall zone of elevated surface temperature. The NWS data showed that a classic heat island – concentric circles radiating outward from the urban core – is present at 6 AM on August 14, 2002 (Figure 3-1). However, this pattern is more difficult to see at other times and on other heat-wave days. The particularly high area of built surfaces – including streets, roofs, and walls – in New York City as compared to other cities may delay the time of the peak heat island from the typical 2 – 3 AM to 6 AM.

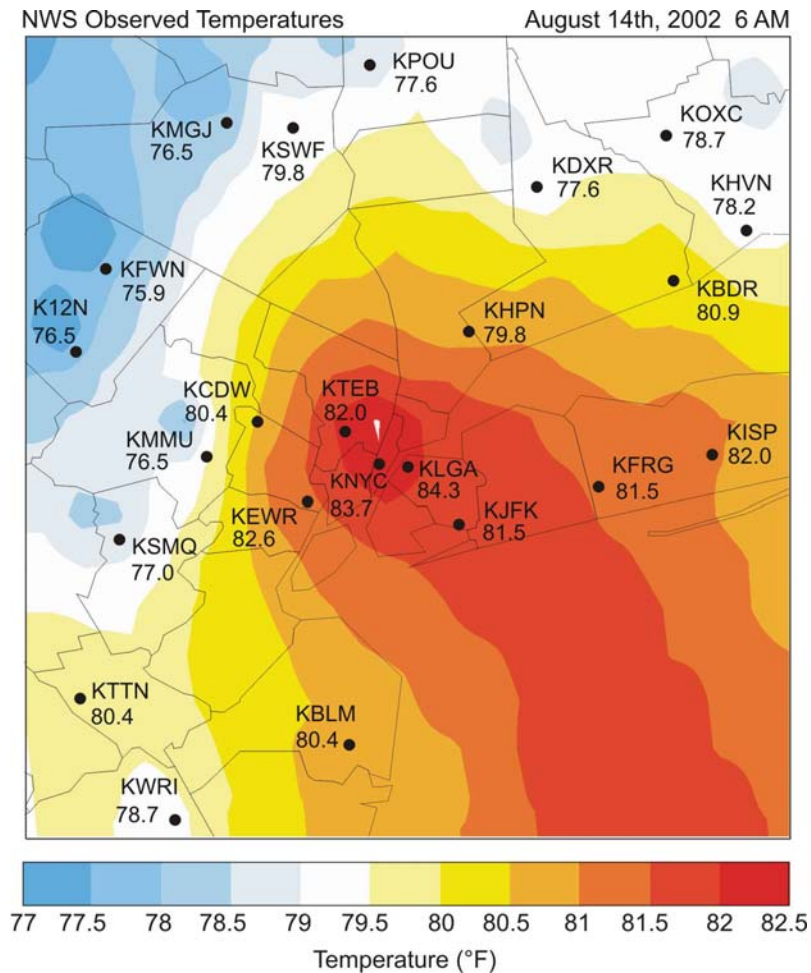


Figure 3-1. National Weather Service observed meteorological data spatially interpolated across the New York metropolitan region. August 14, 2002 at 6 AM.

## **ANSWERS TO KEY TEMPERATURE IMPACT QUESTIONS**

### **1. What are the dominant climate factors, land-use patterns, and geographic conditions that affect New York City?**

New York is a coastal city and thus is subject to sea-breezes. The sea-breeze often inhibits temperature over land from rising and can even cool it significantly. On days with a sea-breeze, the Manhattan case study areas would likely benefit the most from the mitigation scenarios and Ocean Parkway would benefit the least because areas nearer the coast are more influenced by the sea-breeze. However, during heat waves, when the sea-breeze tends to be small, the urban heat island tends to intensify. In general, high temperature, low cloud cover, and low wind speed lead to more intense heat island conditions.

Our results indicate that vegetation plays a more important role than albedo or other features of the urban physical geography (e.g. building heights, road density) in determining heat island potential in New York City. Therefore, the redevelopment of urban surfaces to increase vegetation cover should help to reduce New York City's surface temperature. Since elevated surface temperatures are expected to lead to elevated air temperatures, land-cover modification could in turn affect the city's near-surface air temperature.

### **2. Are there options for reducing elevated near-surface air temperature associated with the urban heat island?**

Yes. Results show that significant reductions in New York City's near-surface air temperature can be achieved by implementing heat island mitigation strategies. There is variability in the magnitude of their effects across scenarios, case study areas, and heat-wave days. A combined strategy that maximizes the amount of vegetation in New York City by planting trees along streets and in open spaces, as well as by building living

(green) roofs (i.e. ecological infrastructure), offers more potential cooling than any individual strategy.

### **3. Which mitigation strategies offer the most potential to reduce temperature per unit area?**

To answer this question, differences between the scenarios are considered independently of the amount of available area for redevelopment and pre-existing land surface conditions. The answer depends only on how differences in the energy balance of each of the surface-cover types interact with regional meteorology to determine the temperature above the surface.

Model results indicate that the most effective mitigation strategy per unit area redeveloped is curbside planting (Table 3-1). The average difference in simulated near-surface air temperature between impervious surfaces and trees was 3.5°F (1.9°C), higher than the differences between other surface-cover types. Therefore, street trees – which involve redevelopment of impervious surfaces – have the largest cooling potential per unit area, followed by living roofs, light-colored surfaces, and open space planting. This can also be thought of as the upper limit of mitigation potential if New York City were completely covered with impervious surfaces and then these surfaces were all replaced with trees, averaged over all times of day and ignoring feedbacks between the surface-cover alteration and regional meteorology. The largest difference between impervious surfaces and trees was 8.7°F (4.8°C), across all times of day. This can be thought of as the upper limit of mitigation potential at a particular point in time (e.g., time of peak surface heating).

Table 3-1. Absolute temperature differences in near-surface air temperature between different surface-cover types averaged over all three heat waves.

<b>Weighted-average Near-Surface Air Temperature (°F)</b>	<b>Grass-to-Trees</b>	<b>Impervious-to-Trees</b>	<b>Impervious-to-Grass</b>	<b>Impervious-to-Light</b>
Average	-1.1	-3.5	-2.5	-2.0
Maximum	-3.0	-8.7	-5.8	-4.6

Note: These values were derived from the MM5 base run, which assumes that New York City's land surface has its present configuration of trees, grass, and impervious surfaces (i.e. no mitigation). The difference in near-surface air temperature between impervious surfaces and trees represents the potential cooling from replacing a unit of impervious surface with a unit of trees. Considering these differences independent of the amount of available area for redevelopment allows for direct comparison of the cooling potential of each mitigation strategy, all else being equal. The actual city-wide cooling potential of each mitigation strategy depends on the number of units that can be redeveloped and the percent of the city's total surface area these units represent.

**4. Taking into consideration available land area and other physical constraints, which mitigation strategies provide the greatest overall potential for reducing temperature city-wide?**

The answer to this question depends on the amount of each surface-cover type that is already in the case study areas as well as the amount that could be added. Ecological infrastructure, a combined strategy of urban forestry and living roofs, has the greatest city-wide temperature impact. The city-wide simulated temperature impact of the mitigation scenarios ranges from 0.1°F (<0.1°C) for open space planting to 0.7°F (0.4°C) for ecological infrastructure if 100% of the available area is redeveloped, averaged over all heat-wave days and times.

At the 3 PM peak, the impact ranges from 0.2°F (0.1°C) for open space planting to 1.2°F (0.7°C) for ecological infrastructure. If ecological infrastructure was implemented in 50% of the available area, the simulated temperature impact would be 0.6°F (0.3°C) at 3 PM.

Of the single strategy scenarios, light surfaces has the greatest modeled temperature impact, 0.4°F (0.3°C), averaged over all heat-wave days and times. At the 3 PM peak, both light surfaces and living roofs have a simulated city-wide temperature impact of 0.7°F (0.4°C). Most of the temperature impact of the light surfaces scenario comes from



the light roofs because light roofs are assumed to have an albedo of 0.5, whereas light roadways and sidewalks are assumed to have an albedo of 0.2. Since the temperature impact of the light surface scenario is 0.3°F (0.2°C), the additional impact of lightening street-level impervious surfaces is relatively small.

Although curbside planting has only half the temperature impact of light surfaces averaged over all times of day, at 6 PM curbside planting and light surfaces both have cooling potential of 0.3°F (0.2°C). However, a major difference between these two scenarios is that curbside planting involves redeveloping 6.7% of the city's surface area to street trees, whereas the light surfaces scenario involves redeveloping 48.0% of the city's surface area.

## **DISCUSSION OF CITY-WIDE RESULTS**

Results show that substantial reductions in New York City's near-surface air temperature can be achieved by implementing heat island mitigation strategies. Vegetation cools surfaces more effectively than increases in albedo. Maximizing the amount of vegetation in New York City by planting trees along streets and in open spaces, as well as by building living roofs (ecological infrastructure), offers more potential cooling than any individual strategy.

Model results indicate that the most effective mitigation strategy per unit area redeveloped is curbside planting. Because there is limited available area for planting street trees, living roofs could have a potentially greater temperature impact city-wide.

The greatest temperature reductions tend to occur in early-to-mid-afternoon, often peaking around 3 PM; however, there is some variability in the time of peak reduction across the case studies and mitigation strategies. In addition, curbside planting and light surfaces have a second peak in the evening because of differences in the cooling rates of different land-surface types.

**Box 3-1: Does cooling potential change as a heat-wave progresses?**

In general, the mitigation strategies have greater cooling potential on hotter days. During the third heat wave, the coolest days were August 15, 16, and 17 and these were also the days with the least cooling potential. On August 16 and 17, peak daily reductions in surface temperature with 50% redevelopment to street trees were less than 2°F (1°C), whereas during the rest of this heat-wave peak daily reductions in surface temperature exceeded 2°F (1°C).

During all the heat-waves, mitigation potential was small at night compared to during the day. The patterns observed with each of the mitigation strategies were similar. Among the case study areas, Mid-Manhattan has the hottest base surface temperatures during all three heat-waves, and Maspeth has the coolest surface temperatures due to the amount of trees present.

Overall, it appears that cooling potential does not change systematically as a heat-wave progresses, but further research is needed to clarify these processes.

**URBAN HEAT ISLAND SIMULATIONS WITH MM5**

The application of coupled regional scale atmospheric and surface energy balance models to urban settings is still a challenging research area. The current generation of such models, including the MM5 model used in this study, does not yet offer perfect tools for studying all the key features of urban heat islands and their mitigation. Cool biases – i.e. modeled air temperatures consistently lower than observed air temperatures – have been reported in applications of MM5 to urban settings (Zhender, 2002). These were diagnosed as due to the parameterizations for building effects on low level circulation and temperature gradients, and also due to the ground level energy balance fluxes. Other urban simulations have reported similar issues (Martelli et al, 2003, Dandou et al, 2005). Given the vast heterogeneous and structural composition of urban surfaces, superimposed with dynamic anthropogenic activities, such shortcomings are to be expected. This is especially true in New York City, a city with a particularly dense urban structure surrounded by water.

To date there have been a limited number of simulations of New York City’s urban heat island and even fewer of the effectiveness of mitigation strategies for the city. Luley and

Bond (2002), following on the modeling of Civerolo et al (2000), simulated UHI mitigation for NYC considering both “maximum” and “realistic” vegetation cover scenarios for the NY metropolitan region. The MM5 model was used but the default single urban land use category was modified to three separate categories. Using a method similar to our report, they averaged ground and lowest model air temperature changes for the scenarios to be more representative of temperature at the surface (vegetated) level. The maximum scenario produced air temperature reductions of 1.8 °F (1 °C) in Manhattan, greater reductions downwind of Manhattan, and relative humidity increases of a few percent. The authors further simulated the effects of these changes and scenarios on air pollution levels.

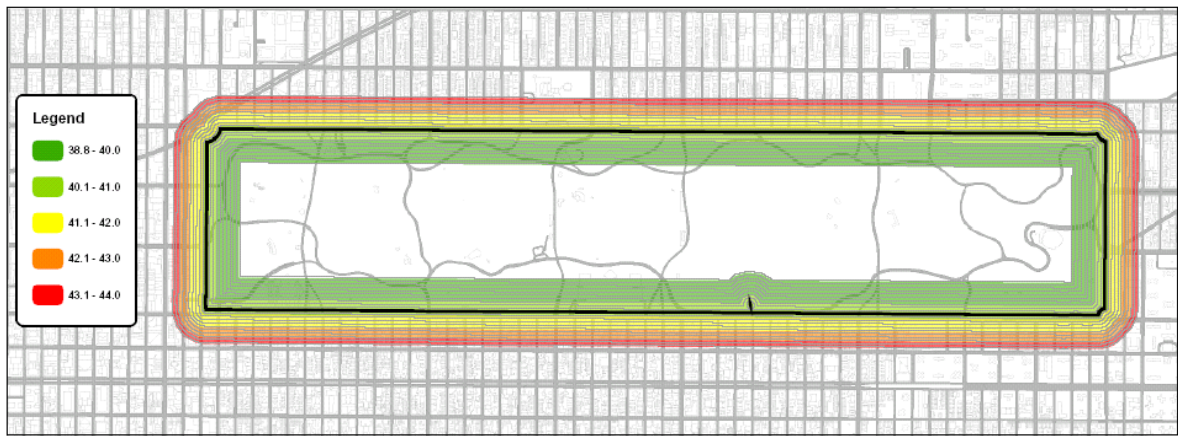
Childs and Raman (2005) simulated NYC’s UHI using the Advanced Regional Prediction System (ARPS) model developed at the Center for Analysis and Prediction of Storms in Oklahoma. Primary goals of this study were to integrate the model with regional Sonic Detection and Ranging (SODAR) and weather station data and to estimate appropriate roughness lengths for the city as a function of wind direction. UHI mitigation was not included.

Other U.S. urban centers have a somewhat longer history of modeling UHI mitigation, especially the Los Angeles basin. Using the CSUMM mesoscale model from Colorado State University, Sailor (1995) and Taha et al (1997) demonstrated significant urban heat island and air quality improvements from albedo and vegetation enhancement strategies. However, our review suggests the more complex urban fabric of New York City requires continuing research to estimate key mesoscale modeling parameters (roughness lengths, thermal conductivities and capacities, boundary layer representations) to best simulate the city’s complex urban canopy and micro-climate.

**Box 3-2: Do mitigation benefits tend to remain localized or spread to adjacent areas?**

The cooling effect of trees on surface temperature tends to be localized rather than to spread to adjacent areas. In principle, regions near areas with trees are cooler than regions near areas with a large percentage of impervious surfaces. Sensible heat fluxes in the MM5 drop in areas covered with trees and grass. The air above these surfaces does spread into neighboring areas. However, remotely-sensed data around Central Park (850 acres) shows that spreading tends to be limited to ~200 feet (61 meters) (See Figure 3-2). Around Bryant Park (~ 5 acres) cooling was limited to ~50 feet (~15 meters) outside the park.

Forest Park, a 510-acre open space in Queens, is surrounded by four-to-ten story post-war apartment buildings, and the blocks are lined with street trees. In this neighborhood, cooling could be observed 3-4 blocks away from the park. However, further research is needed to determine the degree to which this is a result of street trees as compared to cooling from trees inside the park. See Appendix G for an analysis of the surface temperature around street tree corridors.



## **Section 4**

### **CASE STUDY RESULTS**

Case study results are summarized in Table 4-1, which gives potential cooling if 100% of the available area is redeveloped. Among the individual strategies, living roofs has the greatest temperature impact in all case study areas, if the available area for redevelopment is taken into account; however in some cases the results for different strategies show comparable levels of cooling (see Table 1-2). A two-tailed t-test was performed for each case study area to determine whether the mean results for different strategies (from Table 4-1 at 100% intensity) were statistically different from one another. Each pair of strategies in each case study area were compared (1) over all times (408 observations), (2) at 3 PM only (17 observations), and (3) at 6 PM only (17 observations). All differences were statistically significant at the 0.05 level with one exception. In Crown Heights, the difference between curbside planting and living roofs was not statistically significant over all times, with the 3 PM data, and with the 6 PM data.

#### **MID-MANHATTAN WEST**

MM5 results showed that Mid-Manhattan West has higher cooling potential than the other case study areas, mainly because this case study area has the most impervious surface area – and particularly rooftops – that could be redeveloped to light surfaces. The mitigation scenario results showed that living roofs could reduce near-surface air temperature by 1.4°F (0.8°C) on average at 3 PM if 100% of the available area was redeveloped. However, because only 8.0% of Mid-Manhattan West’s surface area could be redeveloped to street trees, the 3 PM average temperature reduction with curbside planting is just 0.5°F (0.3°C).

Table 4-1. MM5 weighted-average near-surface air temperature reductions for selected mitigation scenarios averaged over all times of day, at 3 PM, and at 6 PM, and assuming implementation in 100% of the available area.

Average reduction over all times of day	Open Space Planting (°F)	Curbside Planting (°F)	Living Roofs (°F)	Light Roofs (°F)	Light Surfaces (°F)	Ecological Infrastructure (°F)	Urban Forestry + Light Roofs (°F)
New York City	-0.1	-0.2	-0.3	-0.3	-0.4	-0.7	-0.6
Mid-Manhattan West	0.0	-0.3	-0.9	-0.6	-0.7	-1.1	-0.9
Lower Manhattan East	-0.1	-0.3	-0.7	-0.5	-0.6	-1.1	-0.9
Fordham Bronx	-0.1	-0.4	-0.4	-0.3	-0.4	-0.8	-0.8
Maspeth Queens	-0.2	-0.2	-0.4	-0.3	-0.4	-0.8	-0.7
Crown Heights Brooklyn	-0.1	-0.5	-0.5	-0.4	-0.5	-1.2	-1.0
Ocean Parkway Brooklyn	-0.1	-0.5	-0.6	-0.4	-0.5	-1.1	-1.0
<b>Average 3 PM Reduction</b>							
New York City	-0.2	-0.4	-0.6	-0.5	-0.6	-1.2	-1.1
Mid-Manhattan West	0.0	-0.5	-1.4	-1.0	-1.2	-1.9	-1.5
Lower Manhattan East	-0.1	-0.5	-1.1	-0.9	-1.1	-1.8	-1.5
Fordham Bronx	-0.2	-0.6	-0.7	-0.5	-0.6	-1.3	-1.2
Maspeth Queens	-0.3	-0.4	-0.7	-0.6	-0.7	-1.4	-1.2
Crown Heights Brooklyn	-0.1	-0.9	-0.9	-0.7	-0.9	-1.9	-1.8
Ocean Parkway Brooklyn	-0.1	-0.9	-1.0	-0.8	-1.0	-1.9	-1.7
<b>Average 6 PM Reduction</b>							
New York City	-0.1	-0.3	-0.4	-0.2	-0.3	-0.8	-0.6
Mid-Manhattan West	0.0	-0.3	-0.9	-0.5	-0.6	-1.2	-0.8
Lower Manhattan East	0.0	-0.4	-0.8	-0.4	-0.5	-1.2	-0.9
Fordham Bronx	-0.1	-0.4	-0.5	-0.3	-0.3	-1.0	-0.8
Maspeth Queens	-0.2	-0.3	-0.5	-0.3	-0.4	-1.0	-0.7
Crown Heights Brooklyn	-0.1	-0.6	-0.7	-0.4	-0.4	-1.4	-1.1
Ocean Parkway Brooklyn	-0.1	-0.5	-0.7	-0.4	-0.4	-1.3	-0.9

### LOWER MANHATTAN EAST

Lower Manhattan East, like Mid-Manhattan West, has more impervious surface area and more flat roof area than the case study areas outside of Manhattan. However, the temperature impact of the mitigation scenarios are consistently lower than in Mid-Manhattan West because, with the exception of open-space planting, there is slightly less available area in which to implement each strategy. At 3 PM, the average temperature impact is 1.1°F (0.6°C) if 100% of the available area is redeveloped to living roofs. With light roofs, the analogous temperature impact is 0.9°F (0.5°C). Though none of the variables used in the statistical analysis account for a large percentage of the variability of

the surface temperature in Lower Manhattan East, the results tell a similar story. Due to the large amount of impervious surfaces, albedo composite accounts for the most variability in the surface temperature (16%).

### **FORDHAM BRONX**

Fordham has a moderate amount of available area in which to implement each of the mitigation strategies. There is more available area for curbside planting and less available area for rooftop redevelopment compared to the Manhattan case study areas. Within Fordham there is less available area for curbside trees (9.9% of surface area) than for living or light roofs (16.1% of surface area) or for light street-level surfaces (35.3% of surface area), but all scenarios offer comparable levels of cooling, both on average and at the 3 PM and 6 PM peaks, with the exception of open-space planting which offers lesser cooling potential. At the 3 PM peak, average cooling is 0.7°F (0.4°C) with living roofs, 0.6°F (0.3°C) with curbside planting, and 0.5°F (0.3°C) with light roofs if 100% of the available area is redeveloped. The statistical analysis corroborates; it shows a complex blend of contributors to the surface temperature in Fordham with vegetation, which accounts for 67% of the variability in surface temperature in Fordham, contributing the most.

### **MASPETH QUEENS**

Maspeth has the highest estimated percent trees (22.3% of the surface area) and grass (17.5% of the surface area) but the vegetation is mostly confined to the large parks and cemeteries in the area. Overall, the mitigation scenario results show that Maspeth tends to have less cooling potential than the other case study areas because there is already more vegetation in this case study area. However, because Maspeth has more available open space than the other case study areas (15.9% of total surface area), the temperature impact of open-space planting is comparable to planting street trees (with 6.2% of the case study's total surface area available). At 3 PM, the average reduction with open-space planting is 0.3°F (0.2°C) compared to an average reduction of 0.4°F (0.2°C) with

street trees if 100% of the available area is redeveloped. At the 3 PM peak, the average cooling is 0.7°F (0.4°C) with living roofs (16.5% of surface area) and light surfaces (28.7% of surface area), and 0.6°F (0.3°C) for light roofs (16.5% of surface area). Results from the statistical analysis show that vegetation intensity accounts for 74% of the variability of surface temperature. Comparable cooling is achieved by increasing the albedo of street-level impervious surfaces and roofs as with curbside planting, but with a larger area available for impervious surface mitigation scenarios.

**Box 4-1: Are potential benefits greater when trees are planted curbside or in open spaces?**

Planting street trees has greater cooling potential than open-space planting because of the greater temperature differential between impervious surfaces and trees compared to that between grass and trees. Therefore, the per-tree benefit of planting street trees is greater than the per-tree benefit of open-space planting. Further, the project database shows that there is more available space to plant street trees in New York City. Both these factors contribute to the greater temperature reductions seen with the Urban Forestry/Street-to-Trees mitigation scenarios as compared to the Urban Forestry/Grass-to-Trees scenarios. Since impervious surface temperatures are higher than both tree and grass surface temperatures, replacing an impervious surface with trees leads to a greater temperature reduction than converting from one vegetation type (e.g., grass) to another (e.g., trees). Impervious areas are represented in the models as dark surfaces that absorb a high percentage (~85%) of solar radiation without any latent heat loss, a cooling process that occurs during the evaporation from vegetation.

**CROWN HEIGHTS BROOKLYN**

The satellite data revealed that Crown Heights has hotter surface temperatures than the other case study areas. Crown Heights has the largest percentage of surface area available for curbside planting (14.4%). The mitigation scenario results show that the temperature impact of curbside planting is equivalent to the temperature impact of living roofs (21.8% of surface area) and light surfaces (34.2% of surface area including roofs, sidewalks, and roadways), on average at 3 PM: 0.9°F (0.5°C) for all three strategies if 100% of the available area is redeveloped. The statistical analysis showed that, of the



available variables, surface temperature is driven the most by vegetation, with NDVI accounting for 34% of the variability.

### **OCEAN PARKWAY BROOKLYN**

Ocean Parkway, like Crown Heights, has high base surface temperatures and a large percentage of surface area available for curbside planting (13.4%). Ocean Parkway also has the greatest percentage of impervious surface area (79.6%) among the case studies outside Manhattan. The mitigation scenario results show that, like Crown Heights, the temperature impact of curbside planting, living roofs (with 21.7% of surface area), and light surfaces (with 38.1% of surface area) is comparable: 1.0°F (0.6°C) on average at 3 PM for living roofs and light surfaces and 0.9°F (0.5°C) for curbside planting. Vegetation is the only variable with a significant statistical relationship with surface temperature in Ocean Parkway; NDVI accounts for 34% of the variability of surface temperature.

### **DISCUSSION OF CASE STUDY RESULTS**

Mid-Manhattan West and Lower Manhattan East have higher cooling potential compared to the other case study areas; however, the statistical analysis did not find a significant relationship between surface temperature and vegetation in these case study areas. More research is needed to determine what drives surface temperature in these areas, but it is likely due to the fact that there is less existing vegetation in these case study areas compared to the amount of vegetation – and particularly trees – in the other case study areas. In addition, it is possible that shade from buildings and sea-breezes have a large effect on the surface temperature in these areas.

The differences in cooling potential across the case studies are mostly driven by differences in their available area for redevelopment. Location, existing configuration of surface-cover types, and baseline surface and near-surface air temperatures appear to play a lesser role. Although the magnitude of potential cooling varies between the different heat-wave days, the same case studies tend to have the greatest potential cooling on all

heat-wave days. Also, the mitigation strategies have greater cooling potential on hotter days.

The Manhattan case study areas have the most flat roof space (33.8% in Mid-Manhattan West and 26.6% in Lower Manhattan East). However, in these case study areas, the roofs tend to be at higher elevations above street level so rooftop redevelopment may have less of an effect on energy demand in the Manhattan case study areas as compared to the case study areas in other boroughs.

Although the Manhattan case study areas have the greatest cooling potential and the highest night time surface temperatures (See Figure 1-3), the remotely-sensed data reveal that the Brooklyn case study areas have the highest daytime surface temperature. The meteorological data reveal that these two case study areas also have the highest afternoon air temperatures. Therefore, the benefit of cooling the two Brooklyn case study areas may be greater, especially if the mitigation strategies are considered on a per-unit-area basis rather than on a percent-available-area basis.

## Section 5

### ENERGY DEMAND ANALYSIS

An analysis of the wholesale energy and demand impacts of reducing near-surface air temperature city-wide and in the six case study areas was performed to contribute to a cost-benefit analysis of the mitigation scenarios. A summary flowchart is presented in Figure 5-1.

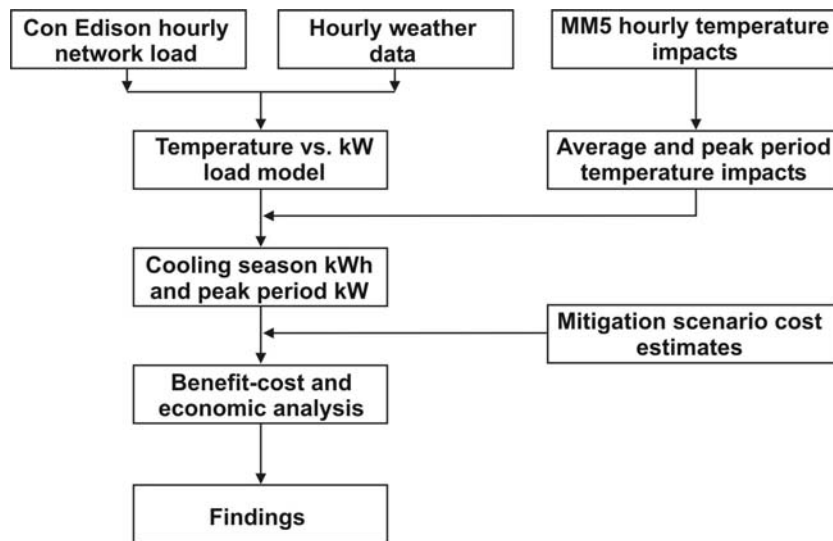


Figure 5-1. Load model and economic cost-benefit analysis process.

#### TEMPERATURE VERSUS kW LOAD MODEL

A model of the electric load and its relationship to ambient weather conditions was developed to assess the economic feasibility of various mitigation scenarios. Note that variations in electric load are due to many factors such as ambient weather, building occupancy (time-of-day and day-of-week), and load distribution amongst users. While these are not the only factors that influence electric load, they are commonly accepted as the most significant factors.

For this study, Consolidated Edison Company of New York, Inc. (Con Edison) provided hourly electric load (kW) data for the case study areas for selected heat-wave periods during the summer of 2002 (case study year). Con Edison provided 19 days of data across the July and August timeframe (with a small amount of missing data), which is summarized in Table 5-1. On August 14, 2002, a curtailment event was issued through the New York Independent System Operator (NYISO)'s Emergency Demand Response Program (EDRP) and Special Case Resources (SCR) ICAP programs from 1pm to 6pm.<sup>10</sup> The data for this period were removed from our analysis, as the electric load measured by Con Edison would have been lowered to the extent that customers participated in the NYISO program.

Table 5-1. Summary of electric load and weather data for study period days.

<b>Area</b>	<b>Average Load (MW)</b>	<b>Peak Load (MW)</b>	<b>Day of Peak Load</b>	<b>Peak Day Energy (MWh)</b>	<b>Hourly Average during Peak Day (MWh)</b>	<b>Peak Day Max Temp (F)</b>
New York City	7,896.0	10,406.0	7/3/2002	216,651	9,027.0	96.0
Mid-Manhattan West	428.7	664.4	8/13/2002	12,019	500.8	97.1
Lower Manhattan East	691.0	1,035.0	8/16/2002	19,822	825.9	96.0
Fordham Bronx	191.3	245.4	7/3/2002	5,323	221.8	101.0
Maspeth Queens	172.7	235.0	7/2/2002	4,497	187.4	98.4
Crown Heights Brooklyn	140.6	177.0	7/3/2002	3,813	158.9	96.7
Ocean Parkway Brooklyn	176.7	255.8	7/3/2002	5,176	215.7	101.4

Statistical correlations were calculated between the hourly Con Edison MW load data and ambient temperature for each case study area using drybulb temperature alone, because the MM5 model runs did not analyze the impacts of ambient humidity. Other independent variables considered in the development of the regression models were day-of-week, and off-peak versus on-peak periods. Due to the limited number of on-peak observations and normal diversity in load, a statistical correlation could not be calculated for these independent variables. The strongest regression relationships were obtained

<sup>10</sup> For additional information see <http://www.nyiso.com>.

when the independent variable was ambient drybulb temperature (Table 5-2). Figures 5-2 through 5-8 show the load and temperature data, and the best-fit regression.

Table 5-2. Summary of regression models for electric load and temperature.

Area	Regression fit	Std Error (on total fit)	Std Error (on Temperature dependency)
Mid-Manhattan West	$MW = 6.32 \cdot T_{\text{ambient}} - 90.1$	101.2	8.6%
Lower Manhattan East	$MW = 11.76 \cdot T_{\text{ambient}} - 177.6$	121.0	5.6%
Fordham Bronx	$MW = 2.80 \cdot T_{\text{ambient}} - 42.1$	17.5	3.5%
Maspeth Queens	$MW = 3.06 \cdot T_{\text{ambient}} - 74.4$	22.1	4.0%
Crown Heights Brooklyn	$MW = 2.10 \cdot T_{\text{ambient}} - 28.9$	12.3	3.3%
Ocean Parkway Brooklyn	$MW = 4.22 \cdot T_{\text{ambient}} - 178.0$	21.9	4.5%
New York City	$MW = 133.5 \cdot T_{\text{ambient}} - 2,996$	887.6	3.7%

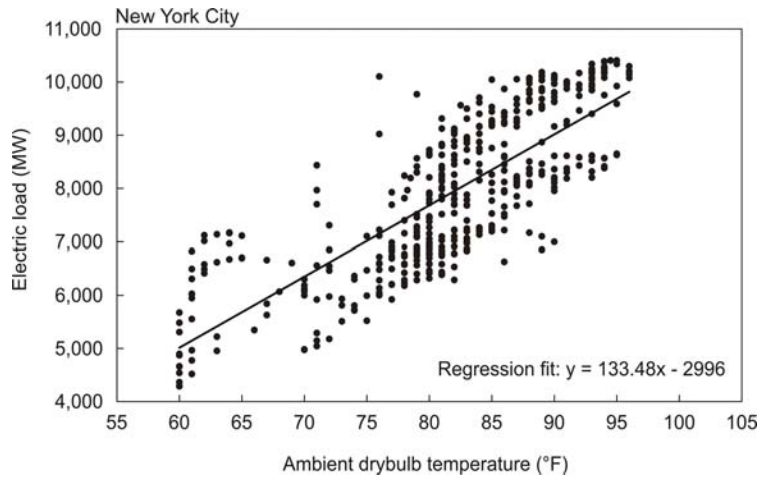


Figure 5-2. Electric load and temperature data for New York City.

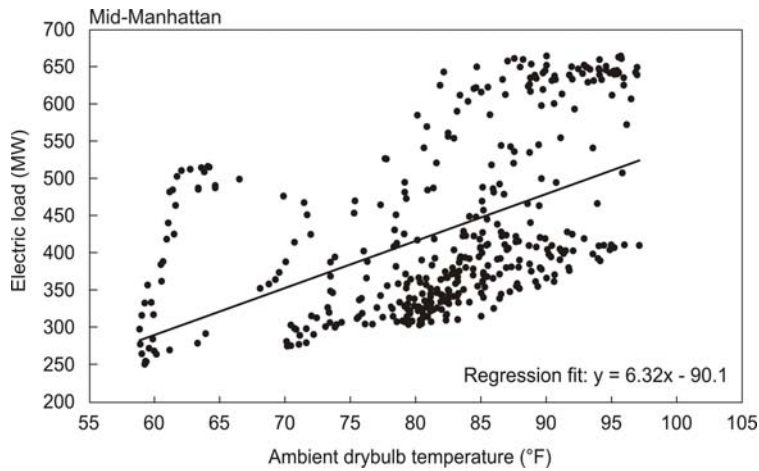


Figure 5-3. Electric load and temperature data for Mid-Manhattan West.

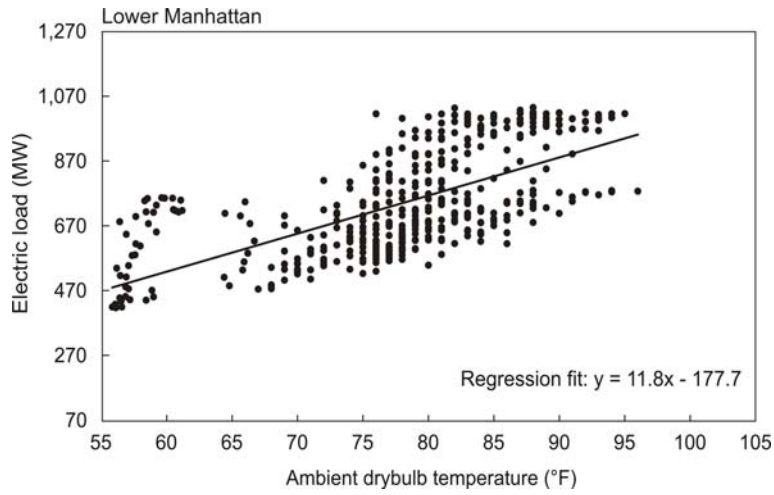


Figure 5-4. Electric load and temperature data for Lower Manhattan East.

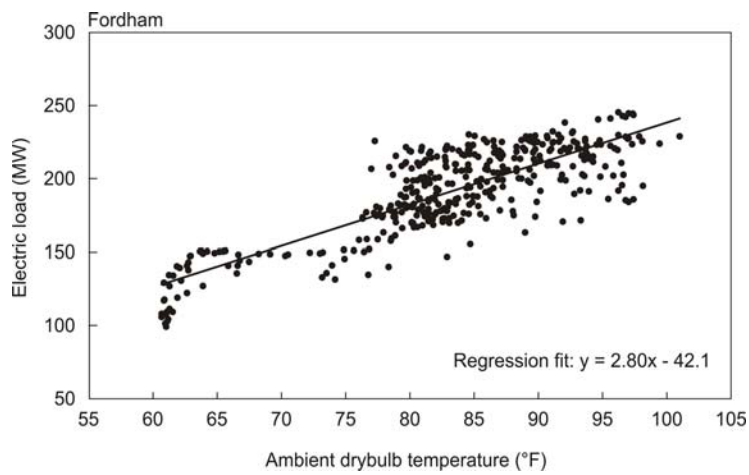


Figure 5-5. Electric load and temperature data for Fordham.

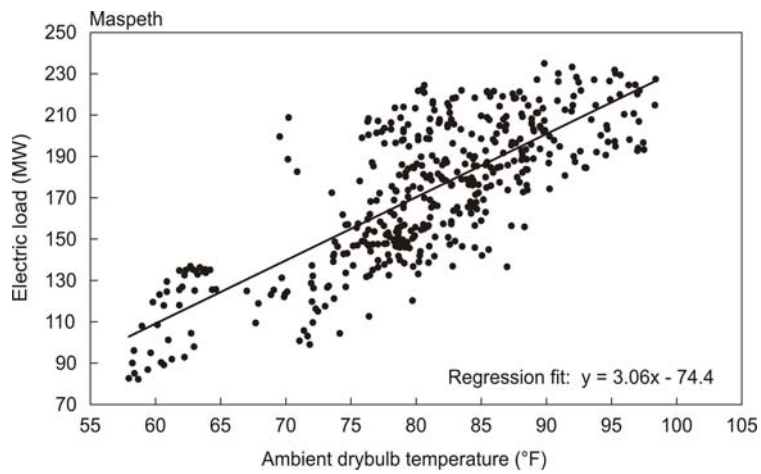


Figure 5-6. Electric load and temperature data for Maspeth.

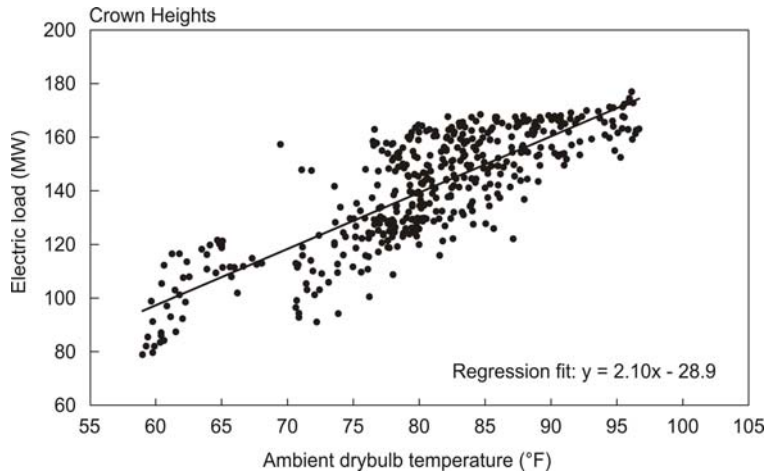


Figure 5-7. Electric load and temperature data for Crown Heights.

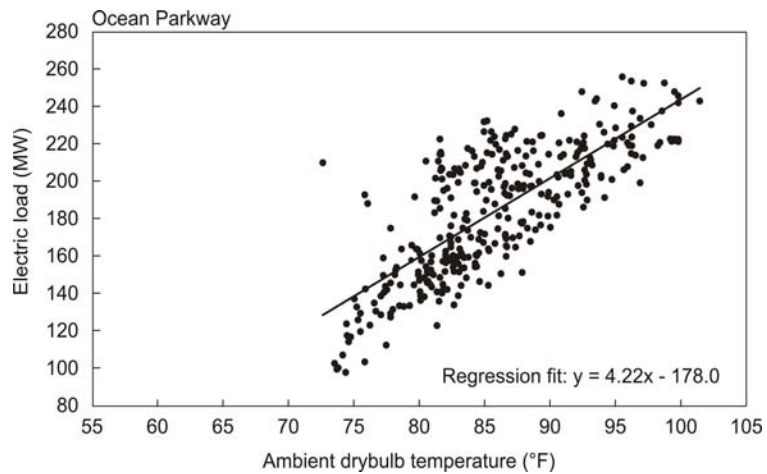


Figure 5-8. Electric load and temperature data for Ocean Parkway.

## MM5 TEMPERATURE IMPACTS

Changes in localized ambient temperature for each case study area were modeled using the MM5 results for each of the mitigation scenarios. Nine mitigation scenarios were selected for further study to determine the net benefits and costs associated with each (Table 6-3). A more detailed discussion of each mitigation scenario can be found in Section 2 and Table 2-9.

Table 5-3. Selected mitigation scenarios.

<b>Scenario</b>	<b>Description</b>
50% Open Space Planting	50% Urban Forestry, Grass-to-Trees
50% Curbside Planting	50% Urban Forestry Street-to-Trees
50% Urban Forestry	50% Urban Forestry Grass+Street-to-Trees
50% Living Roofs	50% Living Roofs
50% Light Roofs	50% Light Roofs
50% Light Surfaces	50% Light Surfaces
Ecological Infrastructure	100% Urban Forestry Grass+Street-to-Trees + 100% Living Roofs
Urban Forestry + Light Roofs	100% Urban Forestry Grass+Street-to-Trees + 100% Light Roofs
Urban Forestry + 25% Living Roofs + 25% Light Roofs	50% Urban Forestry Grass+Street-to-Trees + 25% Living Roofs + 25% Light Roofs

The hourly temperature impacts from the MM5 runs were analyzed for each of the selected mitigation scenarios. The MM5-modeled temperature changes were grouped to obtain a daily average, on-peak-period average, and maximum peak-period value. The on-peak period is defined by NYSERDA as non-holiday weekdays from 12 PM to 6 PM, May through October. A summary of the weighted air-temperature impacts is presented in Tables 5-4, 5-5, 5-6.

Table 5-4. Maximum on-peak temperature reduction (°F).

	<b>NYC</b>	<b>Mid-Manhattan</b>	<b>Lower Manhattan</b>	<b>Fordham</b>	<b>Maspeth</b>	<b>Crown Heights</b>	<b>Ocean Parkway</b>
50% Open Space Planting	0.10	0.04	0.05	0.13	0.15	0.09	0.09
50% Curbside Planting	0.22	0.26	0.30	0.31	0.20	0.46	0.45
50% Urban Forestry	0.32	0.30	1.34	0.44	0.35	0.55	0.54
50% Living Roofs	0.28	0.76	0.59	0.39	0.34	0.48	0.52
50% Light Roofs	0.29	0.67	0.55	0.32	0.34	0.45	0.47
50% Light Surfaces	0.39	0.78	0.66	0.42	0.42	1.55	0.58
Ecological Infrastructure	1.28	2.03	1.92	1.51	1.45	2.03	2.00
Urban Forestry + Light Roofs	1.23	1.89	1.82	1.44	1.44	1.99	1.95
Urban Forestry + 25% Living Roofs + 25% Light Roofs	0.60	0.97	0.91	0.75	0.69	1.00	1.00



Table 5-5. Average temperature reduction (°F).

	<b>NYC</b>	<b>Mid-Manhattan</b>	<b>Lower Manhattan</b>	<b>Fordham</b>	<b>Maspeth</b>	<b>Crown Heights</b>	<b>Ocean Parkway</b>
50% Open Space Planting	0.04	0.03	0.02	0.07	0.06	0.05	0.05
50% Curbside Planting	0.12	0.14	0.16	0.18	0.11	0.26	0.24
50% Urban Forestry	0.16	0.17	0.18	0.25	0.18	0.31	0.29
50% Living Roofs	0.15	0.44	0.32	0.22	0.18	0.27	0.29
50% Light Roofs	0.14	0.31	0.26	0.15	0.16	0.21	0.21
50% Light Surfaces	0.19	0.36	0.31	0.20	0.20	0.26	0.27
Ecological Infrastructure	0.70	1.15	1.06	0.85	0.81	1.16	1.09
Urban Forestry + Roofs	0.63	0.93	0.91	0.76	0.72	1.03	0.97
Urban Forestry + 25% Living Roofs + 25% Light Roofs	0.31	0.54	0.48	0.42	0.35	0.55	0.53

Table 5-6. Average on-peak temperature reduction (°F).

	<b>NYC</b>	<b>Mid-Manhattan</b>	<b>Lower Manhattan</b>	<b>Fordham</b>	<b>Maspeth</b>	<b>Crown Heights</b>	<b>Ocean Parkway</b>
50% Open Space Planting	0.07	0.03	0.04	0.10	0.11	0.07	0.07
50% Curbside Planting	0.19	0.22	0.25	0.27	0.17	0.40	0.39
50% Urban Forestry	0.26	0.25	0.28	0.37	0.29	0.47	0.46
50% Living Roofs	0.25	0.65	0.50	0.33	0.29	0.42	0.45
50% Light Roofs	0.22	0.48	0.41	0.24	0.26	0.34	0.35
50% Light Surfaces	0.31	0.56	0.49	0.31	0.32	0.42	0.44
Ecological Infrastructure	1.12	1.73	1.63	1.28	1.26	1.78	1.73
Urban Forestry + Light Roofs	1.01	1.43	1.43	1.16	1.14	1.62	1.57
Urban Forestry + 25% Living Roofs + 25% Light Roofs	0.51	0.81	0.75	0.63	0.57	0.85	0.84

## **ESTIMATING ELECTRIC LOAD IMPACTS**

Electric load and peak kW impacts were determined by inserting the temperature reduction values (Tables 6-4 through 6-6) into the load correlation equations. As can be seen in Figures 6-2 through 6-8, there was a wide range of ambient temperatures observed during the days used to develop the load correlation equations. Therefore, we felt confident that the correlation coefficients developed from the study days to estimate the electric load impact could be used over the entire cooling season (i.e., throughout the remainder of the summer including non-study days). To perform this task, the temperature changes shown in Tables 5-4, 5-5, and 5-6 were used in the equations shown in Table 5-2. The values in Table 5-5 were used to calculate the cooling season electric

energy (MWh) savings by multiplying the average daily MWh savings by the number of seasonal cooling days (153).

Table 5-7. Energy and demand reduction.

		NYC	Mid-Manhattan	Lower Manhattan	Fordham	Maspeth	Crown Heights	Ocean Parkway
50% Open Space Planting	Max MW	13.40	0.238	0.654	0.363	0.487	0.199	0.379
	Ave On-Peak MW	13.144	0.234	0.620	0.351	0.467	0.193	0.379
	MWh	19,122	594	831	765	728	350	769
50% Curbside Planting	Max MW	29.48	1.621	3.494	0.878	0.620	0.985	1.910
	Ave On-Peak MW	29.439	1.621	3.475	0.878	0.615	0.975	1.910
	MWh	59,177	3,325	7,002	1,826	1,259	2,019	3,781
50% Urban Forestry	Max MW	42.20	1.876	4.058	1.223	1.096	1.165	2.257
	Ave On-Peak MW	42.201	1.876	4.023	1.221	1.077	1.152	2.257
	MWh	77,991	3,930	7,776	2,595	1,986	2,359	4,553
50% Living Roofs	Max MW	37.88	4.844	6.967	1.091	1.034	1.023	2.196
	Ave On-Peak MW	37.876	4.819	6.922	1.083	1.026	1.014	2.196
	MWh	74,346	10,146	13,874	2,289	2,011	2,106	4,537
50% Light Roofs	Max MW	38.73	4.304	6.709	0.922	1.067	0.972	1.976
	Ave On-Peak MW	38.382	4.260	6.498	0.885	1.038	0.946	1.961
	MWh	68,518	7,235	11,215	1,552	1,766	1,648	3,298
50% Light Surfaces	Max MW	52.95	4.974	8.012	1.225	1.331	1.183	2.470
	Ave On-Peak MW	52.472	4.922	7.742	1.170	1.295	1.151	2.449
	MWh	94,291	8,377	13,436	2,073	2,249	2,028	4,162
Ecological Infrastructure	Max MW	170.49	12.895	22.699	4.222	4.464	4.330	8.411
	Ave On-Peak MW	170.486	12.841	22.546	4.222	4.431	4.272	8.411
	MWh	343,949	26,693	45,924	8,729	9,058	8,928	16,868
Urban Forestry + Light Roofs	Max MW	164.97	11.995	21.759	4.089	4.501	4.237	8.222
	Ave On-Peak MW	164.741	11.927	21.350	4.026	4.395	4.185	8.214
	MWh	308,555	21,601	39,310	7,780	8,097	7,988	15,034
Urban Forestry + 25% Living Roofs + 25% Light Roofs	Max MW	80.72	6.176	10.755	2.117	2.131	2.125	4.216
	Ave On-Peak MW	80.507	6.161	10.676	2.108	2.106	2.101	4.216
	MWh	153,490	12,431	20,660	4,331	3,980	4,232	8,241

The resultant maximum MW reduction, average on-peak MW reduction, and seasonal average MWh reduction are presented in Table 5-7. To account for the uncertainty resulting from the scatter in the electric load versus temperature data, the standard error on temperature dependency as presented in Table 5-2 can be applied to the values in Table 5-7.

All of the measures reduce summer peak demand, with an average summer peak demand reduction of less than 1 percent (Table 5-8). The largest impacts, both citywide and in individual case study areas, are seen for the measures that combine 100% urban forestry with either living roofs or light surfaces. The two scenarios that include 100% urban forestry average peak demand reductions of roughly 2%. The maximum on-peak demand reduction was 3.2% for both of these scenarios.

Table 5-8. Percentage reduction on peak electric load from mitigation scenarios.

	<b>NYC</b>	<b>Mid-Manhattan</b>	<b>Lower Manhattan</b>	<b>Fordham</b>	<b>Maspeth</b>	<b>Crown Heights</b>	<b>Ocean Parkway</b>
50% Open Space Planting	0.13%	0.04%	0.06%	0.15%	0.21%	0.11%	0.15%
50% Curbside Planting	0.28%	0.24%	0.34%	0.36%	0.26%	0.56%	0.75%
50% Urban Forestry	0.41%	0.28%	0.39%	0.50%	0.47%	0.66%	0.88%
50% Living Roofs	0.36%	0.73%	0.67%	0.44%	0.44%	0.58%	0.86%
50% Light Roofs	0.37%	0.65%	0.65%	0.38%	0.45%	0.55%	0.77%
50% Light Surfaces	0.51%	0.75%	0.77%	0.50%	0.57%	0.67%	0.97%
Ecological Infrastructure	1.64%	1.94%	2.19%	1.72%	1.90%	2.45%	3.29%
Urban Forestry + Light Roofs	1.59%	1.81%	2.10%	1.67%	1.92%	2.39%	3.21%
Urban Forestry + 25% Living Roofs + 25% Light Roofs	0.78%	0.93%	1.04%	0.86%	0.91%	1.20%	1.65%

## **Section 6**

### **COST – BENEFIT ANALYSIS**

A benefit-to-cost ratio in regard to wholesale energy and demand impacts was developed to evaluate selected mitigation opportunities.

#### **MITIGATION SCENARIO COSTS**

Implementation costs of the mitigation scenarios were estimated based on literature review, as well as materials vendors and other professionals involved with the technologies and materials used in the mitigation scenarios. The total cost of each mitigation scenario was determined based on the available area for implementation and cost per square foot of each mitigation scenario.

Different implementation costs apply to street trees versus trees planted in grassy or open areas. The average fully mature canopy of an individual tree is assumed to be 37.7-feet in diameter (1116 square feet). This applies to both street trees and trees planted in a park or other grassy area. This value was determined in consultation with the NYC Department of Parks and NYS Department of Environmental Conservation.

The average cost for a tree planted in a grassy or open area was calculated to be \$480. This was based on an assumed diversity of 25% @ 1.5-inch caliper, 25% @ 1.75-inch caliper, and 50% @ 2.5-inch caliper. The per tree costs used were \$315 for a 1.5-inch caliper tree, \$350 for a 1.75-inch caliper tree, and \$625 for a 2.5-inch caliper tree. This cost is an average that would apply citywide to any grassy or open area.

For trees planted in curbside locations the costs per tree are significantly higher. For street or curbside trees in Manhattan the cost is assumed to be \$1,400 per tree. In the boroughs of Brooklyn, Bronx, Queens, and Staten Island the cost per street tree is \$1,300. For curbside plantings the cost is based on the selection of only 2.5-inch caliper.

The costs for tree planting as required in the mitigation scenarios 50% open space planting, 50% curbside planting, and 50% urban forestry are shown in Table 6-1.

Table 6-1. Costs for tree-planting mitigation scenarios (\$millions).

Area	Cost for 50% Open Space Planting	Cost for 50% Curbside Planting	Cost for 50% Urban Forestry
<b>New York City</b>	\$199.95	\$341.12	\$541.07
<b>Mid-Manhattan West</b>	\$0.31	\$3.78	\$4.09
<b>Lower Manhattan East</b>	\$1.34	\$5.94	\$7.28
<b>Fordham Bronx</b>	\$3.02	\$9.31	\$12.33
<b>Maspeth Queens</b>	\$10.67	\$11.27	\$21.94
<b>Crown Heights Brooklyn</b>	\$2.71	\$13.54	\$16.25
<b>Ocean Parkway Brooklyn</b>	\$1.20	\$8.40	\$9.60

There are two mitigation scenarios that deal exclusively with the roofs of buildings: living roofs and light roofs. The implementation costs for these scenarios are based on the incremental cost over a standard roofing project. Costs are shown in Table 6-2.

These costs are based on an incremental cost of \$10 per square foot for a living roof above the cost of a standard roof. The incremental cost for a light roof is assumed to be \$0.68 per square foot.

Table 6-2. Cost for living roofs and light surfaces mitigation scenarios (\$millions).

Area	Cost for 50% Living Roofs	Cost for 50% Light Roofs	Cost for 50% Light Surfaces
<b>New York City</b>	\$5,855.6	\$398.2	\$442.6
<b>Mid-Manhattan West</b>	\$127.3	\$8.7	\$9.1
<b>Lower Manhattan East</b>	\$143.2	\$9.7	\$10.3
<b>Fordham Bronx</b>	\$130.0	\$8.8	\$9.7
<b>Maspeth Queens</b>	\$257.5	\$17.5	\$18.9
<b>Crown Heights Brooklyn</b>	\$176.0	\$12.0	\$12.8
<b>Ocean Parkway Brooklyn</b>	\$116.8	\$7.9	\$8.6

The last type of mitigation scenario that was studied was the use of light surfaces (high-albedo roadways). The estimated incremental cost for this measure was assumed to be \$0.03 per square foot for light-colored roadways. The light-colored roadway consists of the use of white aggregate in place of dark aggregate in a standard asphalt mix. The

incremental cost for the white aggregate, at \$0.03 per square foot of finished asphalt, is the only additional cost for this scenario. For the light surfaces measure, the light roadways would be implemented along with the light roofs.

The final three mitigation scenarios comprised various combinations of tree plantings, living roofs and light surfaces including 100% grass+street-to-trees along with 100% living roofs (ecological infrastructure), 100% grass+street-to-trees along with 100% light surfaces, and 50% grass+street-to-trees along with 25 % living roofs and 25% light roofs. The costs for these three scenarios are presented below in Table 6-3.

Table 6-3. Costs for combination mitigation scenarios (in \$millions).

<b>Area</b>	<b>Cost for 100% Urban Forestry + 100% Living Roofs</b>	<b>Cost for 100% Urban Forestry + 100% Light Roofs (Ecological Infrastructure)</b>	<b>Cost for 50% Urban Forestry + 25% Living Roofs + 25% Light Roofs</b>
<b>New York City</b>	\$12,793.3	\$2,927.8	\$3,667.9
<b>Mid-Manhattan West</b>	\$262.8	\$63.7	\$72.1
<b>Lower Manhattan East</b>	\$300.9	\$71.6	\$83.7
<b>Fordham Bronx</b>	\$284.6	\$65.0	\$81.7
<b>Maspeth Queens</b>	\$558.9	\$128.8	\$159.5
<b>Crown Heights Brooklyn</b>	\$384.5	\$88.0	\$110.2
<b>Ocean Parkway Brooklyn</b>	\$252.8	\$58.4	\$72.0

The 50% open space planting scenario is the cheapest to implement city-wide (~\$200 million) and across all case study areas (~ \$0.3 million in Mid-Manhattan West to ~\$10 million in Maspeth). The two scenarios that include living roofs are the most expensive to implement city-wide and in each case study area. City-wide, the 50% living roofs and the ecological infrastructure scenarios would respectively cost ~\$5,855 million and ~\$12,793 million to implement. For the six case study areas, the costs for 50% living roofs ranges from ~\$116 million in Ocean Parkway to ~\$257 million in Maspeth. The cost for the ecological infrastructure scenario ranges from ~\$252 million in Ocean Parkway to ~\$558 million in Maspeth.

## **COST-BENEFIT MODELING**

To determine the cost effectiveness of the mitigation scenarios, we applied a simplified approach to the methodology used by NYSERDA for many of its energy programs. The wholesale energy demand benefits of each scenario were compared to its cost. A ratio greater than one suggests that from a societal perspective the opportunity provides a greater value of energy benefit than its cost.

The benefits used in this analysis were limited to the avoided or reduced electric energy and capacity requirements. These benefits were valued using wholesale electric and demand costs. The costs evaluated in this analysis were those for implementation, without accounting for ongoing annual or semi-annual costs such as maintenance. In addition, the benefits were based on assumptions of fully mature and implemented scenarios.

We used a benefit-to-cost model developed for the New York State Energy Research and Development Authority. Specific inputs to the model were based on avoided wholesale electric energy and capacity costs for the Con Edison service territory. The useful life of each measure was assumed to be 35 years. Summaries of the net benefits and benefit-to-cost (B/C) ratio for each scenario in each case study area are presented in Table 6-4 and 6-5. In Table 6-5, uncertainty levels are also shown based on the standard error on the dependency of electric MW load on ambient temperature as determined from the regression analysis.

The highest benefit-cost ratios are for Mid-Manhattan West, Lower Manhattan East, and Ocean Parkway. The 50% open space planting scenario in Mid-Manhattan West has the highest benefit-cost ratio (5.84), followed by the 50% light surfaces scenario in Lower Manhattan East (4.48). The results of the benefit-to-cost assessment suggest that in general, additional benefits beyond energy alone such as air quality, public health, reduction in the city's contribution to greenhouse gas emissions, and reduction in stormwater runoff must be considered to more fully assess the mitigation scenarios in a city-wide implementation.

Table 6-4. Net mitigation scenario benefits (\$millions).

	NYC	Mid-Manhattan	Lower Manhattan	Fordham	Maspeth	Crown Heights	Ocean Parkway
50% Open Space Planting	70.11	1.80	3.20	2.43	2.62	1.18	2.48
50% Curbside Planting	191.44	10.68	22.66	5.84	4.06	6.49	12.29
50% Urban Forestry	259.44	12.54	25.55	8.25	6.65	7.61	14.71
50% Living Roofs	242.29	32.37	45.00	7.30	6.57	6.76	14.54
50% Light Roofs	231.45	24.90	38.67	5.34	6.11	5.65	11.38
50% Light Surfaces	317.77	28.81	46.28	7.12	7.73	6.93	14.31
Ecological Infrastructure	1,110.82	85.49	148.18	27.97	29.20	28.63	54.58
Urban Forestry + Light Roofs	1,022.15	72.51	131.80	25.62	27.19	26.39	50.20
Urban Forestry + 25% Living Roofs + 25% Light Roofs	505.62	40.18	67.82	13.92	13.19	13.73	26.89

Table 7-5. Benefit-to-cost ratio for mitigation scenarios.

	NYC	Mid-Manhattan	Lower Manhattan	Fordham	Maspeth	Crown Heights	Ocean Parkway
50% Open Space Planting	0.350	<b>5.840</b>	<b>2.380</b>	0.810	0.250	0.440	<b>2.060</b>
	±0.013	±0.501	±0.133	±0.028	±0.010	±0.015	±0.094
50% Curbside Planting	0.560	<b>2.830</b>	<b>3.820</b>	0.630	0.360	0.480	<b>1.460</b>
	±0.020	±0.243	±0.213	±0.021	±0.014	±0.016	±0.066
50% Urban Forestry	0.480	<b>3.070</b>	<b>3.510</b>	0.670	0.300	0.470	<b>1.530</b>
	±0.018	±0.264	±0.196	±0.022	±0.012	±0.016	±0.069
50% Living Roofs	0.040	0.250	0.310	0.060	0.030	0.040	0.120
	±0.001	±0.021	±0.017	±0.002	±0.001	±0.001	±0.005
50% Light Roofs	0.580	<b>2.880</b>	<b>3.970</b>	0.600	0.350	0.470	<b>1.430</b>
	±0.021	±0.247	±0.222	±0.020	±0.014	±0.016	±0.065
50% Light Surfaces	0.720	<b>3.170</b>	<b>4.480</b>	0.730	0.410	0.540	<b>1.670</b>
	±0.026	±0.272	±0.250	±0.024	±0.016	±0.018	±0.076
Ecological Infrastructure	0.090	0.330	0.490	0.100	0.050	0.070	0.220
	±0.003	±0.028	±0.027	±0.003	±0.002	±0.002	±0.010
Urban Forestry + Light Roofs	0.520	<b>2.750</b>	<b>3.740</b>	0.580	0.330	0.450	<b>1.380</b>
	±0.019	±0.236	±0.209	±0.019	±0.013	±0.015	±0.063
Urban Forestry + 25% Living Roofs + 25% Light Roofs	0.140	0.560	0.810	0.170	0.080	0.120	0.370
	±0.005	±0.048	±0.045	±0.006	±0.003	±0.004	±0.017

## ANALYSIS ASSUMPTIONS AND LIMITATIONS

Within the analysis procedure there were several limitations:

- Interactive effects: Interactions between the individual mitigation scenarios and building energy use were not taken into account. For instance, light colored surfaces could be shaded by trees. The electric savings associated with the reduction of building cooling load when light roofs are implemented were not



considered. Likewise, the additional heating energy required as a result of the implementation of light colored roofs, for example, were not considered.

- Timeline of benefits: Benefits are assumed to accrue starting in year one of the analysis. Actual benefits from infrastructure improvements will depend on implementation rates. This study does not account for benefits from tree planting that will actually start out small and grow over time nor does it account for the fact that light surfaces will likely start out at their maximum benefit and degrade over time.
- On-going costs: On-going costs for items such as maintenance and the degradation on performance with time were not considered. Similarly, tree mortality rates and replanting costs were not included.
- Electric MW load versus temperature relationship: The regression analysis used to develop the electric load versus ambient temperature correlation used data from 19 days during the 2002 summer season. The correlation was assumed to hold true for the remaining days within the cooling season.

## **RESULTS**

The energy modeling and benefit-to-cost analysis is used to assess which mitigation scenarios offer wholesale energy and capacity benefits that exceed the cost to implement. As shown in Table 6-8, the implementation of mitigation scenarios yields moderate impacts on maximum electric demand. Implementation of the most effective scenarios on a broad scale throughout New York City is predicted to reduce maximum electric demand on the order of roughly 170 MW, a nearly 2% reduction in city-wide peak electric requirements. Using wholesale electric and capacity rates, the benefits of the two 100% urban forestry scenarios in the citywide case study area are valued at over \$1 billion each over the 35-year study period.

Average on-peak period temperature reductions were typically less than 0.5°F (0.3°C). However, for the two scenarios that included 100% urban forestry in combination with

either living roofs or light roofs, the temperature reductions were typically in excess of 1°F (0.6°C).

It is important to note that the cost-benefit analysis reflects up-front costs to implement mitigation strategies and does not fully account for all costs (such as ongoing maintenance or replacement costs required to assure long-term performance). It should also be noted that it did not include non-energy benefits such as urban beautification, stormwater management, health benefits, and air quality benefits. It also did not include possible benefits associated with market price effects or deferred electric distribution infrastructure costs.

The results of the benefit-to-cost assessment suggest that in general, additional benefits beyond energy alone should be considered to more fully assess the mitigation scenarios in a city-wide implementation.

## **ANSWERS TO KEY QUESTIONS ON COSTS AND BENEFITS**

### **5. What are the costs associated with each mitigation strategy?**

#### **City-Wide**

Given the cost assumptions of the study, the cost for combination mitigation scenarios implemented in all available areas ranges from \$2,927 million for urban forestry + light roofs to \$12,793 million for ecological infrastructure (Figure 6-1). Implementing the single strategy scenarios in 50% of the available area ranges in estimated cost from \$199 million for open space planting to \$5,855 million for living roofs.

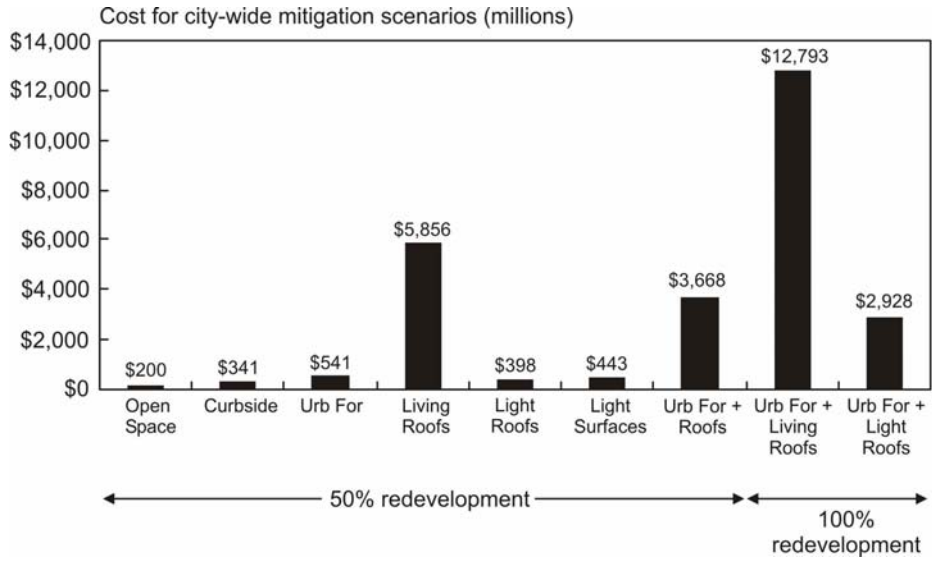


Figure 6-1. City-wide costs for selected mitigation scenarios (in millions). Note that urban forestry plus roofs represents mitigation scenario 9: 50% open space planting plus 50% curbside planting + 25% living roofs plus 25% light roofs.

### Case Study Areas

The estimated costs vary across mitigation scenarios and case study areas (Figure 6-2). Across all case study areas and all mitigation scenarios, the cost ranges from \$0.3 million for 50% open space planting in Mid-Manhattan West to \$588 million for ecological infrastructure in Maspeth.

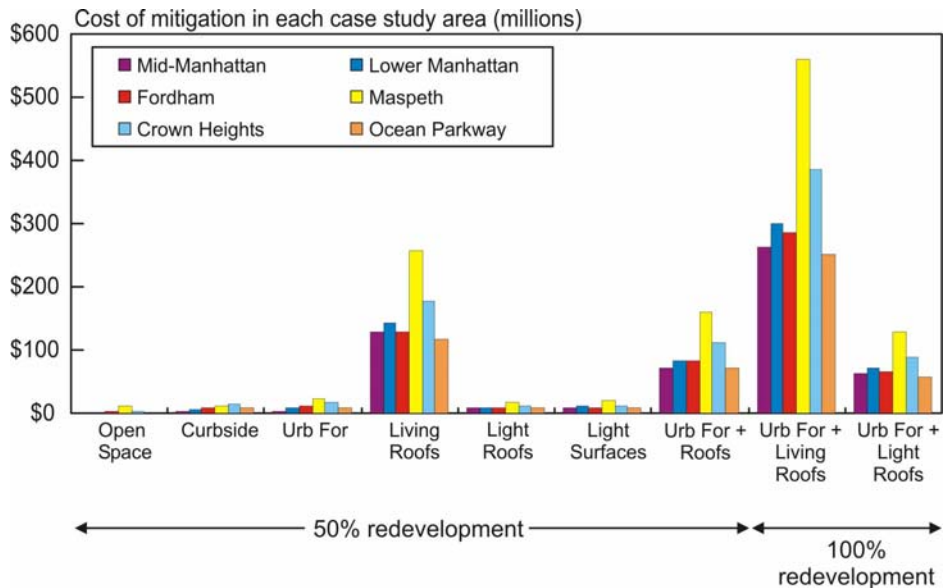


Figure 6-2. Costs for selected mitigation scenarios (in millions) by case study area.

## **6. Which mitigation strategies provide greater benefits in terms of reduced air temperature and demand for electrical energy for cooling at lower costs?**

### **City-Wide**

Light surfaces, light roofs, and curbside planting are more cost-effective than the other strategies. The estimated cost per 0.1°F (0.06°C) temperature reduction ranges from \$233 million for 50% light surfaces to \$3,904 million for 50% living roofs.

The peak load megawatt (MW) impacts of the mitigation scenarios are moderate. The largest city-wide impacts are seen for the measures that combine 100% urban forestry with either living roofs or light roofs. The two scenarios that include 100% urban forestry average peak demand reductions of approximately 2% (MW), over all heat-wave days. The maximum on-peak demand reduction (single largest value of demand between 12 and 6 PM on non-holiday weekdays) was 3.2% (MW) for both of these scenarios.

While all of the measures reduce summer peak demand, for individual scenarios the average summer peak demand reduction over all heat-wave days was less than 1%. Among these scenarios, light surfaces, light roofs, and living roofs can potentially reduce the summer peak electric load more than the other strategies. At 50% redevelopment of the available area, light surfaces can potentially reduce peak load by 0.51%, light roofs by 0.37%, and living roofs by 0.36%. Given cost and benefit assumptions (see Section 6 for details), the cost per MW reduction ranges \$8.4 for light surfaces to \$154 million for living roofs (Figure 6-3).

Tree-planting may have a greater impact on energy demand than was estimated by this study because the effect of shading the sides of buildings was not included in the MM5 simulated temperature impacts.

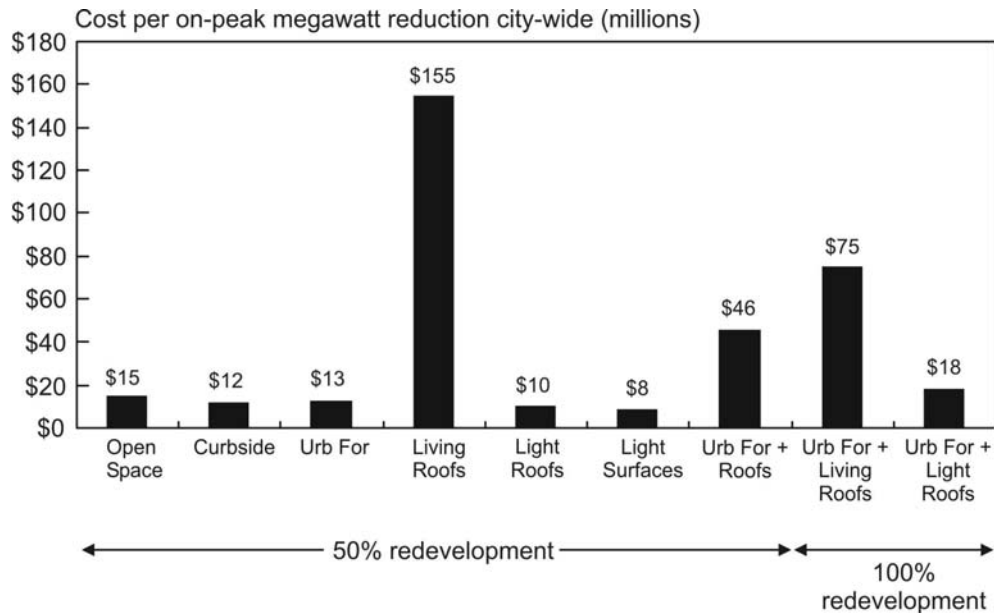


Figure 6-3. Cost per city-wide on-peak megawatt reduction (in millions).

### **Case Study Areas**

The cost per 0.1°F (0.06°C) temperature reduction is greater in Fordham, Maspeth, and Crown Heights and lower in Mid-Manhattan West, Lower Manhattan East, and Ocean Parkway. Differences are mainly result of the amount of redevelopment necessary to achieve comparable levels of cooling. The costs range from \$1 million per 0.1°F (0.06°C) temperature reduction for 50% open space planting in Mid-Manhattan West to \$143 million per 0.1°F (0.06°C) reduction for 50% living roofs in Maspeth.

The energy demand benefit exceeds the cost of implementation for all individual scenarios in Lower Manhattan, Mid-Manhattan West and Ocean Parkway. Although costs exceed the benefit in the remaining case study areas, as well as city-wide, it is likely that if additional benefits such as air quality, public health, reduction in the city's contribution to greenhouse gas emissions, and reduction in stormwater runoff were also taken into account, in many cases the benefit-cost ratio city-wide and for all case study areas would be positive. This is an important area for further study.

For all case study areas, 50% living roofs is the most expensive strategy per on-peak MW reduction (Figure 6-4). All other 50% implementation scenarios have approximately

equal costs per on-peak MW reduction. Maspeth, Crown Heights, and Fordham have higher costs per on-peak MW reduction, partly because these case study areas tend to have more available area for open space planting, which has a lesser temperature impact, and less available area for living roofs.

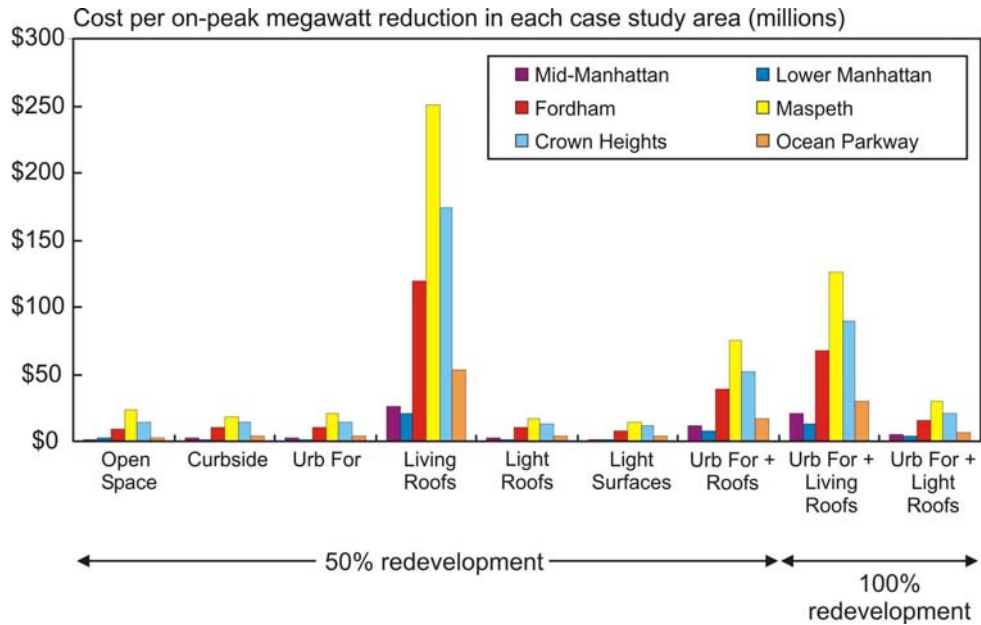


Figure 6-4. Cost per on-peak megawatt reduction (in millions) for case study areas.

## **Section 7**

### **OTHER BENEFITS OF MITIGATION STRATEGIES**

In addition to reduced energy demand, mitigation of New York City's heat island could improve air quality and public health, as well as reduce the city's contribution to greenhouse gas emissions. Reduced energy demand could also reduce the cost of air conditioning for both residential and commercial customers.

#### **AIR QUALITY AND PUBLIC HEALTH**

The study results show that the mitigation strategies can significantly reduce surface temperatures and that these surface temperature reductions are likely to reduce near-surface air temperatures. This could improve public health by reducing heat stress and by reducing the build-up of temperature-dependent pollutants such as ground-level ozone. This is described further below.

Urban heat islands are associated with a range of health hazards, with heat stress the most significant threat. Heat stress potential increases dramatically when daily high temperatures are elevated and when the diurnal temperature range is reduced, such as during summer heat-wave periods. These conditions also encourage a build-up of temperature-dependent secondary air pollutants and resulting acute and chronic exposure impacts. These include a range of respiratory problems including asthmatic attacks requiring hospitalization.

Heightened heat-related mortality tends to occur several days into a heat-wave period after several nights of elevated temperatures and associated physiological stress (Klinenberg, 2002). Heat-related health impacts are most threatening to vulnerable populations – the very young, very old, poor, health-compromised and disabled (Kinney et al., 2001). In the future, health-related impacts of the urban heat island may increase due to climate change (Rosenzweig et al., 2005).

A study of the effect of urban trees on air quality in New York City found that a 10 – 32% increase in canopy cover could reduce near-surface air temperatures by about 1.8°F (1°C) and ozone concentrations by about 4 parts per billion (ppb) (Luley and Bond, 2002). Another study simulated the effect of increasing albedo and vegetation in Salt Lake City, Baton Rouge, and Sacramento; ozone reductions were on the order of 3-5 ppb in Salt Lake City and Baton Rouge and 10 ppb for Sacramento (Taha et al., 2000). However, the selection of low-VOC-emitting trees for planting is essential to achieving the ozone reductions. In addition to reducing ozone concentrations, trees can improve air quality by reducing human exposure to dry deposition (a process through which gases and particles settle out of the atmosphere onto the tree canopy surface) (Taha, 1996; see also Rosenthal et al., 2006).

The two factors determining which mitigation scenario offers greater health benefits are the magnitude of the potential cooling with the scenario and non-temperature-dependent benefits of the scenario. The health benefits of light surfaces are essentially a function of the first factor – the amount of cooling they provide. However, vegetation, and particularly trees, also plays a role in improving air quality through the direct uptake of pollutants. Trees can also play a role in reducing the quantity and temperature of stormwater runoff. The volume of runoff can stress public infrastructure. Both the volume and temperature of runoff can stress aquatic ecosystems.

In most of the case study areas, curbside planting provides greatest cooling potential. Since tree-planting has additional non-temperature-dependent public health benefits, planting street trees is the mitigation strategy that offers the greatest health benefits. Living roofs is the second-best strategy from a health perspective, for similar reasons.

## **GREENHOUSE GAS EMISSIONS**

Heat island mitigation strategies can reduce atmospheric concentrations of greenhouse gases. Urban trees can sequester carbon dioxide through the creation of carbohydrates in the process of photosynthesis, subsequently storing it in trunks as wood. For trees to



remain effective, however, they must be properly maintained and periodically replaced, since actively growing trees are needed to sequester carbon. If there are dead or dying trees in an area, the site could become a source of carbon dioxide rather than a sink (Nowak, 1994). A loss of urban trees can also be an indirect source of atmospheric carbon dioxide because tree loss will lead to increased energy demand for cooling. Reducing energy demand will also reduce the amount of carbon dioxide emissions from fossil fuel burning power plants. One study has suggested that if all urban tree spaces in the United States were filled, and if rooftops and parking lots were covered with lighter colors, electricity use would be reduced by 50 billion kilowatt hours each year, reducing the amount of carbon dioxide released into the atmosphere by as much as 35 million tons per year (EREC, 1995).

## Section 8 CONCLUSIONS

Results of this study show that all mitigation strategies have a significant temperature impact, but there is substantial variability in the magnitude of their effects across scenarios, case study areas, and heat-wave days. A combined strategy that maximizes the amount of vegetation in New York City by planting trees along streets and in open spaces, as well as by building living (or green) roofs (i.e. ecological infrastructure), offers more potential cooling than any individual strategy. The choice of a strategy should consider the characteristics and priorities of the neighborhood, including benefit/cost factors and the available area for implementation of each strategy.

Vegetation cools more effectively than changes in albedo and the street trees scenarios have the greatest temperature impact per unit area. Taking available areas in the city for each strategy into account, curbside planting, living roofs, and light roofs and surfaces have comparable cooling effects. (Note that light surfaces require an area many times greater than the area for street trees needed to achieve comparable cooling.)

There is potential for cooling in all case study areas; however, Mid-Manhattan West, Lower Manhattan East, and Ocean Parkway have greater potential for both temperature and cost-effective energy reduction. Light surfaces, light roofs, and curbside planting tend to have lower costs per 0.1°F (0.06°C) temperature reduction as well as per on-peak MW reduction.

It is important to note that our assessment of benefits and costs did not address non-energy or market benefits. It is likely that if additional benefits such as air quality, public health, reduction in the city's contribution to greenhouse gas emissions, and reduction in stormwater runoff were also taken into account, the benefit-cost ratio would be positive in all case study areas. Reduced energy demand could also reduce the cost of air conditioning for all New York City electricity consumers and possibly defer the cost of utility distribution upgrades. Furthermore, planting trees and building living roofs can be

expected to have a positive impact on quality of life in New York City as a result of increased interaction with vegetation in the urban environment.

## Section 9

### FURTHER RESEARCH

Further research suggested by this study includes:

- Incorporate the effect of shading into MM5 to more accurately represent the full cooling potential of urban forestry.
- Couple MM5 to an urban boundary layer model to better capture the effects of land-surface cover and building height on near-surface air temperature.
- Incorporate building height directly into simulations of living roofs.
- Improve the soil-moisture specification in MM5.
- Test the effects of the mitigation strategies on humidity and wind fields with MM5.
- Verify assumption of linearity of temperature impacts from mitigation scenarios.
- Investigate extent to which a minimum scale of mitigation strategy is required for a measurable impact.
- Determine the per-tree cooling effect using a three-dimensional microclimate model that simulates surface-air interactions in an urban environment. ENVI-MET is one example of such a technology that does so with a spatial resolution of 0.5 to 10 meters and a temporal resolution of 10 seconds.
- Create a 3-D model of one or more case study areas to create more explanatory variables (i.e., building shading, wind direction) to refine the neighborhood-scale statistical models.
- Evaluate the net benefits and entire life-cycle costs of each mitigation scenario to better assess the benefit-to-cost ratio.
- Characterize the electric MW load relationship on ambient temperature and other independent variables more fully.
- Include non-energy benefits such as urban beautifications, stormwater management, and health benefits in a more comprehensive benefit-to-cost analysis.

## **Section 10**

### **RECOMMENDATIONS**

Results of this study indicate that policy-makers should consider the following measures:

- 1) Develop urban heat island mitigation strategies appropriate to priorities and conditions in individual neighborhoods and communities.
- 2) Implement urban heat island strategies at large enough spatial extents to be temperature and cost-effective.
- 3) Maximize the temperature impact of urban heat island mitigation through combination strategies, and particularly by planting trees along streets and in open spaces, as well as by building living roofs (i.e. ecological infrastructure).
- 4) Develop and implement cost-effective strategies for light-colored surfaces, light roofs, and curbside planting for reducing on-peak energy use.
- 5) Conduct ongoing analyses and monitoring of tree-planting programs, living roofs, and light surfaces to observe actual mitigation levels over time and use results to improve calibration and validation of regional climate models for further documentation of heat island mitigation.
- 6) Conduct additional analyses to value benefits of the mitigation scenarios, and include appropriate non-energy benefits of mitigation strategies in cost-benefit analyses.

**Section 11**  
**REFERENCES**

- Akbari, H. (2002) Shade trees reduce building energy use and CO<sub>2</sub> emissions from power plants. *Environmental Pollution*. 116, S119-S126 Suppl. 1 2002
- Bass, B., E.S. Krayenhoff, A. Martilli, R.B. Stull, and Auld, H. (2003) The impact of green roofs on Toronto's urban heat island. *Proceedings of Greening Rooftops for Sustainable Communities*, Chicago, 2003.
- Bretz, S. and B. Pon (1994), Durability of High Albedo Coatings, Recent Research in the Building and Energy Analysis Group at Lawrence Berkeley Laboratory, Issue # 4, <http://eetd.lbl.gov/Buildings/RResearch/Albedo.html>, accessed June 2006.
- Childs, P. P. and Raman, S. (2005) Observations and Numerical Simulations of Urban Heat Island and Sea Breeze Circulations Over New York City, *Pure and Applied Geophysics*, v. 162, p. 1955-1980.
- Davis, S., Martien, P., and Sampson, N. (1992) Planting and light-colored surfacing for energy conservation in *Cooling our Communities: A Guidebook on Tree Planting and Light-Colored Surfacing*. EPA Guidebook. 1992, 93-110.
- Dandou, A., Tombrou, M., Akylas, E., Soulakellis, N. and E. Bossioli (2005) Development and Evaluation of an Urban Parameterization Scheme in the Penn State/NCAR Mesoscale Model (MM5), *J. of Geophys. Res.*, v. 110 D 10102.
- Gaffin, S. R., Rosenzweig, C., Parshall, L., Beattie, D., Berghage, R., O'Keeffe, G., and Braman, D. (2005) Energy Balance Modeling Applied to a Comparison of Green and White Roof Cooling Efficiency, in *Proceedings of the 3<sup>rd</sup> Annual Greening Rooftops for Sustainable Cities Conference*, May 4-6, 2005, Washington, DC.

- Gedzelman, S.D., Austin, S., Cermak, R., Stefano, N., Partridge, S., Quesenberry, S., and Robinson, D.A. (2003) Mesoscale aspects of the urban heat island around New York City. *Theoretical Applied Climatology*. 75(1-2), 29-42
- Grell, G.A., Dudhia, J., and Stauffer, D. (1994) A Description of the Fifth-Generation Penn State/NCAR Mesoscale Model (MM5). NCAR Technical Note TN-398+STR. Boulder, CO: National Center for Atmospheric Research.
- Grimmond, C.S.B and T.R. Oke (1999) Heat Storage in Urban Areas: Observations and Evaluation of a Simple Model, *J. of Applied Meteorology*, v. 28, 922-940.
- Heat Island Group (2006a) Wash Your Roof,  
<http://eetd.lbl.gov/heatisland/CoolRoofs/Wash/>, accessed January 2006.
- Heat Island Group (2006b) Pavement Albedo,  
<http://eetd.lbl.gov/heatisland/Pavements/Albedo/>, accessed January 2006.
- Heat Island Group (2006c) Painting the Town White – and Green, accessed January 2006.
- Hogrefe , C., Lynn, B. Civerolo, K., Ku, J.Y., Rosenthal, J.E., Rosenzweig, C. Goldberg, R., Gaffin, S. Knowlton, K. and P.L. Kinney (2004) Simulating changes in regional air pollution over the eastern United States due to changes in global and regional climate and emissions, *Journal of Geophysical Research*, v. 109, D22301.
- Knowlton, K., Hogrefe, C., Lynn, B., Rosenzweig, C., Rosenthal, J.E., Gaffin, S., Goldberg, R., Civerolo, K., Ku, J.Y., and P.L. Kinney (2004), Climate-Related Changes in Ozone Mortality Over the Next 50 years in the New York City Metropolitan Region, *Environmental Health Perspectives*, v. 112, n. 15.

Kirkpatrick, J.S. and M.D. Shulman (1987) A statistical evaluation of the New York City – Northern New Jersey urban heat island effect on summer daily minimum temperature. *National Weather Digest*, 12(1), 12.

Kinney, P., Shindell, D., and Chae, E. (2001) Climate change and public health: Impact assessment for the NYC metropolitan region. In: Rosenzweig, C. and W.D. Solecki, eds. (2001) *Climate Change and a Global City: An Assessment of the Metropolitan East Coast Region* (pp. 103-147). Columbia Earth Institute, New York, 210 pages.

Klinenberg, E. (2002) *Heat-wave: A Social Autopsy of Disaster in Chicago*. University of Chicago Press, Chicago, 320 pages.

Kunkel, K. E., Changnon, S. A., Reinke, B. C. and R. W. Arritt (1996) The July 1995 Heat-wave and Critical Weather Factors, *Bulletin of the American Meteorological Society*, v. 77(7), p. 1507-1518.

Lu, J. (2005) Personal communication, July 27, 2005.

Luley, C.J. and Bond, J. (2002) *A Plan to Integrate Management of Urban Trees into Air Quality Planning: A Report to the North East State Foresters Association*. 61pages. Available at:  
[http://www.fs.fed.us/ne/syracuse/Pubs/Downloads/Final\\_report\\_March2002\\_Davey.pdf](http://www.fs.fed.us/ne/syracuse/Pubs/Downloads/Final_report_March2002_Davey.pdf)

Martelli, A., Roulet, Y-A, Junier, M., Kirchner, F., Rotach, M. W. and A. Clappier (2003), On the Impact of Urban Surface Exchange Parameterizations On Air Quality Simulations: the Athens Case, *Atmospheric Environment*, v. 37, p. 4217-4213.



- Mertens, B. and Lambin, E.F. (2000) Land-cover trajectories in Southern Cameroon..  
Annals of the Association of American Geographers, 90, 467-495.
- Myeong, S., Nowak, D.J, Hopkins, P.F., and Brock, R.J. (2003) Urban cover mapping using digital, high-spatial resolution aerial imagery, Urban Ecosystems, 5, 243-256.
- Nowak, D. (2005) Personal Communications.
- Oke, T. R. (1987) Boundary Layer Climates, 2<sup>nd</sup> Edition, Routledge Press.
- Rosenfeld, A.H., Akbari, H., Bretz, S., Fishman, B.L., Kurn, D. M., Sailor, D. and H. Taha (1995) Mitigation of Urban Heat Island: Materials, Utility Programs, Updates, Energy and Buildings, v. 22, p. 255-265.
- Rosenfeld, A.H. Romm, J.J., Akbari, H., Pomerantz, M. and H.G. Taha (1996) Policies to Reduce Heat Islands: Magnitudes of Benefits and Incentives to Achieve Them, in *Proceedings of the 1996 ACEEE Summer Study on Energy Efficiency in Buildings*, Pacific Grove, CA, v.9, p.177-191.
- Rosenthal, J., Pena Sastre, M., Rosenzweig, C., Knowlton, K., Goldberg, R., and Kinney, P. (2003) One hundred years of New York City's "urban heat island": temperature trends and public health impacts. *Eos Trans. AGU*, 84(46), Fall Meet. Suppl., Abstract U32A-0030.
- Rosenthal, J., Crauderueff, R., and Carter, M. (2006) Urban Heat island Mitigation Research and Strategies for New York City. Sustainable South Bronx. Upcoming, January 2006.

- Rosenzweig, C., Solecki, W.D., Parshall, L., Chopping, M., Pope, G., and Goldberg, R. (2005) Characterizing the Urban Heat Island Effect in Current and Future Climates in Urban New Jersey. *Environmental Hazards*, 6, 51-62.
- Rosenzweig, C., Gaffin, S., and Solecki, W.D. (Eds.) (2006) Green Roofs in the New York Metropolitan Region: Research Report. A Joint Publication of NASA/Goddard Institute for Space Studies, Columbia Center for Climate Systems Research of the Earth Institute at Columbia University, and Hunter College, City University of New York. 62 pp.
- Sailor, D. J. (1995) Simulate Urban Climate Response to Modifications in Surface Albedo and Vegetative Cover, *J. Appl. Met.*, v. 34, 1694-1704.
- Sailor, D. J., Kalkstein, L. S. and E. Wong (2002) Alleviating Heat-Related Mortality Through Urban Heat Island Mitigation, *Bulletin of the American Meteorological Society*, v. 83(5), p. 663-664.
- Small, C. (2001) Estimation of urban vegetation abundance by spectral mixture analysis. *International Journal of Remote Sensing*. 22(7), 1305-1334.
- Small, C. (2003) High spatial resolution spectral mixture analysis of urban reflectance. *Remote Sensing of Environment*. 88, 170-186.
- Solecki, W.D., Rosenzweig, C., Parshall, L., Pope, G., Clark, M., and Wiencke, M. (2005) Mitigation of the Heat Island Effect in Urban New Jersey. *Environmental Hazards*, 6, 39 – 49.
- Taha, H. (1996) Modeling impacts of increased urban vegetation on ozone air quality in the south coast air basin. *Atmospheric Environment*. 30(20), 3423-3430.

- Taha,H. (1997) Urban Climates and Heat Islands: Albedo, Evapotranspiration and Anthropogenic Heat, Energy and Buildings, v. 25, p. 99-103
- Taha, H., S. Douglas, J. Haney (1997) Mesoscale Meteorological and Air Quality Impacts of Increased Urban Albedo and Vegetation, Energy and Buildings, v. 25, p. 169-177.
- Taha, H., Akhari, H. and A. Rosenfeld (1991) Heat Island and Oasis Effects of Vegetative Canopies: Micrometeorological Field Measurements, Theoret. Appl. Climatology, v. 44 p. 123.
- Taha, H., Chang, S., and Akbari, H. (2000) Meteorological and Air Quality Impacts of Heat Island Mitigation Measures in Three U.S. Cities. Lawrence Berkley National Laboratory, Berkley, CA. LBNL-44222.
- Terjung, W. H. and O'Rourke, P.A. (1980), Simulating the Causal Elements of Urban Heat Islands, Boundary Layer Meteorology, v. 19, p. 13-118.
- United States Department of Energy, Energy Information Administration (US DOE EIA) (1997) Residential Energy for New York State 1997.
- United States Department of Energy, Energy Information Administration (US DOE EIA) (1999) 1999 Commercial Building Energy Consumption Survey for Buildings in the Northeast.
- Unwin, D. J. (1980) The Synoptic Climatology of Birmingham's Urban Heat Island, Weather, v. 35(2), p. 43-50.
- Zaengl, G. (2002) An improved method for computing horizontal diffusion in a sigma-coordinate model and its application to simulations over mountainous topography. *Monthly Weather Review*, v. 130, p. 1423 – 1432.

Zehnder, J.A. (2002) Simple Modifications to Improve Fifth-Generation Pennsylvania University – National Center for Atmospheric Research Mesoscale Model Performance for the Phoenix, Arizona Metropolitan Area. *Journal of Applied Meteorology*. 41, 971 – 979.



## **APPENDIX A: TREE SPECIES SELECTION LIST FOR NEW YORK CITY**

David J. Nowak  
USDA Forest Service, Northeastern Research Station  
5 Moon Library, SUNY-ESF, Syracuse, NY 13210

### **INTRODUCTION**

To optimize particular environmental benefits of trees planted in urban reforestation efforts, an appropriate list of tree species needs to be identified based on the desired environmental effect. In addition to optimizing tree performance and increasing tree longevity, the species must also be properly matched to the site conditions where it will be planted. To help determine the most appropriate tree species for various urban forest functions, a data base of several thousand tree species was developed by the USDA Forest Service in cooperation with Horticipia, Inc. This database along with additional information on tree characteristics and site requirements was used to determine the most appropriate species for curbside and open space locations in New York City. Input from NYSERDA/DEC and/or other project team members on desired functions were used to help determine weighting functions of values to develop this recommended species list.

### **PURPOSE**

Develop a list of approximately 200 tree species appropriate for New York City and rank these species based on identified functional attributes that optimize selected environmental functions, in this case urban heat island mitigation.

### **Functions Evaluated**

- Air pollution removal
- Air temperature reduction
- Tree shade
- Building energy conservation
- Carbon storage
- Pollen allergenicity
- Life span

### **METHODS**

In developing this species recommendation list for New York City, the following tasks were conducted:

#### ***1) Reduce the species list down to approximately 200 appropriate species for New York City.***

Based on data base variables, the complete list of about 5,000 tree and shrub species was reduced down to about 1,500 species based on tree winter hardiness characteristics (what species are hardy to New York City: USDA hardiness zone 6b). This list was further reduced to 179 species based on trees that are available from local nursery stock.

Available nursery stock is defined as plant materials that can be acquired from reputable growers, which meet American Nurseryman Association growing standards, within a 350 mile radius of New York City. Availability of growing stock was determined by cross referencing plant availability of the three largest growers who are members of New York State Nurserymen and Landscape Association, Pennsylvania Landscape and Nursery Association, Maryland Nursery and Landscape Association or New England Nursery Association. Plant availability from these nurseries was determined using online sources such as [www.plantlocator.net](http://www.plantlocator.net).

**2) *Quantify the relative functional value of each of the appropriate tree species.***

To evaluate the relative functional ability of each species, a data base was compiled on tree attributes, including tree crown height and width at maturity, water use, total leaf area and biomass, leaf characteristics, and species allergenicity ratings. For each environmental function, these base tree data were used to develop a standardized index score between 0-100 (0 = greatest negative effect of all species analyzed; 100 – greatest positive effect).

**Tree Information**

Information about the plant dimensions, physical leaf characteristics, and hardiness zones of 5,380 trees, shrubs, cactus and palms trees were derived from the Horticipia database ([www.horticipia.com](http://www.horticipia.com)). Based on the Horticipia database and literature searches, the plants were classified by type and all plants that were not classified as a tree or large shrub / small tree were removed, leaving 2,236 plants classified as trees. Of these trees, data (either from the species itself, or genera, family, order or class averages) were obtained for all variables for about 1,600 species.

**Tree size and shading coefficients.** Maximum tree height and width were derived from the Horticipia database. Crown height of each tree was estimated as 0.78 of median tree height based on field measurements of urban trees.

Species shading coefficients (percent light intensity intercepted by foliated tree crowns) were derived from Nowak (1996). If data on individual species were not known, genera averages were applied. If genus data were not available, family average data were applied.

**Leaf area and leaf biomass.** Leaf area and leaf biomass of individual trees were calculated using regression equations for deciduous urban species (Nowak 1996). For deciduous trees that were too large to be used directly in the regression equation, average leaf-area index (LAI:  $m^2$  leaf area per  $m^2$  projected ground area of canopy) was calculated by the regression equation for the maximum tree size based on the appropriate height-width ratio and shading coefficient class of the tree. This LAI was applied to the ground area ( $m^2$ ) occupied by the tree to calculate leaf area ( $m^2$ ). For deciduous trees with height-to-width ratios that were too large or too small to be used directly in the regression equations, tree height or width was scaled downward to allow the crown to reach maximum (2) or minimum (0.5) height-to-width ratio. Leaf area was calculated using the regression equation with the maximum or minimum ratio; leaf area was then

scaled back proportionally to reach the original crown volume. Leaf area index was not allowed to exceed 15 or be less than 1.

For conifer trees (excluding pines), average LAI per height-to-width ratio class for deciduous trees with a shading coefficient of 0.91 were applied to the tree's ground area to calculate leaf area. The 0.91 shading coefficient class is believed to be the best class to represent conifers as conifer forests typically have about 1.5 times more LAI than deciduous forests (Barbour et al. 1980), the average shading coefficient for deciduous trees is 0.83 (Nowak 1996); 1.5 times the 0.83 class LAI is equivalent to the 0.91 class LAI. Because pines have lower LAI than other conifers and LAI that are comparable to hardwoods (e.g., Jarvis and Leverenz 1983; Leverenz and Hinckley 1990), the average shading coefficient (0.83) was used to estimate pine leaf area.

Leaf biomass was calculated by converting leaf-area estimates using species-specific measurements of g leaf dry weight/m<sup>2</sup> of leaf area based on the literature and field measurements (e.g., Bacon and Zedaker, 1986; Box, 1981; Cregg, 1992; Gacka-Grzesikiewicz, 1980; McLaughlin and Madgwick, 1968; Monk et al., 1970; Reich et al., 1991; Shelton and Switzer, 1984)

Species crown width x species shading coefficient was used to develop a standardized shading score.

**Relative transpiration rates.** As actual transpiration rates are highly variable depending upon site or species characteristics, and very limited data exist on transpiration rates for various species under comparable conditions, relative transpiration factors were determined for each species based on estimated monthly water use (Costello and Jones, 1994). Each species were classified into one of seven categories in a "water need" classification scheme: High water need (H); High to Moderate need (MH); Moderate need (M); Moderate to Low need (ML); Low need (L); Low to Very Low need (LVL); and Very Low need (VL). If the species was not included on water use species list, the water need was estimated from water use classifications of other species in the same genus or family.

A relative transpiration factor scale (Table A) was developed, following an assumption that trees requiring greater amounts of water (e.g., species in "H" or "MH" water use classes) transpire at higher rates than those needing less water ("L" to "VL" classes). The relative transpiration factors were generated from the maximum estimated species water need (inches per month) associated with each water use classification (Costello and Jones, 1994). The tree transpiration factor x LAI was used to calculate a standardized air temperature score.



Table A-1. Relative transpiration factors corresponding to tree species' water use classification.

Water Use Classification	Max. Water Use (in. per month)	Relative Transpiration Rate	Transpiration Factor
High need (H)	0.9	High	1.50
High to moderate need (MH)	-	Moderate to high	1.25
Moderate need (M)	0.6	Moderate	1.00
Moderate to low need (ML)	-	Moderate to low	0.75
Low need (L)	0.3	Low	0.50
Low to very low need (LVL)	-	Low to very low	0.35
Very low need (VL)	0.1	Very low	0.20

**Species VOC emissions.** Base genera emission factors (isoprene and monoterpene) were derived from Geron et al (1994) with updated emission factors from (Guenther et al 1996; Isebrands et al 1999; Owen and Hewitt 2000; Steinbrecher et al. 1993; Zimmerman 1979). Species leaf biomass was multiplied by genus-specific emission factors to produce emission levels standardized to 30°C and photosynthetically active radiation (PAR) flux of 1,000  $\mu\text{mol m}^{-2} \text{s}^{-1}$ . If genus-specific information is not available, median emission values for the family, order, or class were used. Standardized emissions are converted to actual emissions based on light and temperature correction factors (Geron et al. 1994) based on average in-leaf daytime weather and pollution concentration data from 53 U.S. cities in 1994 (Table B).

VOC emission (E) (in  $\mu\text{gC tree}^{-1} \text{hr}^{-1}$  at temperature T (K) and PAR flux L ( $\mu\text{mol m}^{-2} \text{s}^{-1}$ )) for isoprene and monoterpenes are estimated as:

$$E = B_E \times B \times \gamma$$

where  $B_E$  is the base genus emission rate in  $\mu\text{gC (g leaf dry weight)}^{-1} \text{hr}^{-1}$  at 30°C and PAR flux of 1,000  $\mu\text{mol m}^{-2} \text{s}^{-1}$ ;  $B$  is species leaf dry weight biomass (g) and:

$$\gamma = [\alpha \cdot c_{L1} L / (1 + \alpha^2 \cdot L^2)^{\frac{1}{2}}] \cdot [\exp[c_{T1}(T - T_S) / R \cdot T_S \cdot T] / (0.961 + \exp[c_{T2}(T - T_M) / R \cdot T_S \cdot T])]$$

for isoprene where L is PAR flux;  $\alpha = 0.0027$ ;  $c_{L1} = 1.066$ ; R is the ideal gas constant ( $8.314 \text{ K}^{-1} \text{ mol}^{-1}$ ), T(K) is leaf temperature, which is assumed to be air temperature,  $T_S$  is standard temperature (303 K), and  $T_M = 314\text{K}$ ,  $C_{T1} = 95,000 \text{ J mol}^{-1}$ , and  $C_{T2} = 230,000 \text{ J mol}^{-1}$  (Geron et al. 1994; Guenther et al. 1995; Guenther 1997).

For monoterpenes:  $\gamma = \exp[\beta(T - T_S)]$  where  $T_S = 303 \text{ K}$ , and  $\beta = 0.09$ .

**Tree temperature effect.** As the emission of volatile organic compounds from a species varies with air temperature, the extent to which a tree lowers air (canopy, and therefore leaf) temperatures through transpiration can have a direct effect on its VOC emissions. The change in air temperature per hour due to transpiration (in degrees Celsius) was

estimated, and the adjusted temperature was used to recalculate the net emission of VOCs from each species.

To estimate differences in individual species temperate effects, an estimate of average tree cover effects on air temperature was used. Given reported reductions in mid-day air temperatures from an aggregate effect of all trees in a local area ranging from 0.04°C to 0.2°C per percent increase in cover (Simpson 1998) and an a national average urban tree cover of 27.1% (Nowak et al. 2001), the average decrease in mid-day air temperatures due to urban tree canopies, assuming the minimum estimate of 0.04°C, would be 1.08°C. The base estimate of change of 1.08°C assumes an average species transpiration factor of 1 and an average leaf area index (LAI) of 6 (Nowak 1994).

To adjust for temperature changes due to individual species, the temperature change was adjusted based in individual species transpiration factors and LAI, such that:

$$\text{NewTempAdj} = -1.08^{\circ}\text{C} \times (\text{LAI}/6) \times (\text{TF})$$

Where NewTempAdj = the new temperature adjustment; and TF = transpiration factor (Table A-1).

The new air temperatures were input into the calculations for isoprene and monoterpene emission equations for the species.

**Physical characteristics of leaves.** To help rate relative differences in particulate pollution removal by trees, leaf and crown characteristics of each species were summarized from the literature and given a score between 0 and 2, with the higher the score indicating a higher probability of particle capture. The basic premise was that dense and fine textured crowns, and complex, small, and rough leaves would capture and retain more particle than open and coarse crowns, and simple, large, smooth leaves. Six crown and leaf characteristics were assessed:

Crown density (from Horticipia database): Open crown = 0; medium density = 1; dense crown = 2.

Crown texture (from Horticipia database): Coarse = 0, Medium = 1, Fine = 2.

Leaf complexity (from Horticipia database): Simple = 0, pinnately or palmately compound, trifoliolate, or palmate = 1, bi- or tri-pinnately compound = 2

Leaf Size (from Horticipia database): Median leaf size was calculated as the average of the minimum and maximum leaf size classes. If leaf size > 4" = 0; 2-4" = 1, <2" = 2

Leaf Surface Roughness (Dirr 1990; Elias 1980; Stein et al 2003; Williamson et al 1985; University of Connecticut 2005): For surface ratings, the upper surface characteristics were considered twice as important lower surface characteristics with average conditions

used if surface characteristics differed between young and old leaves. Dull, smooth, glossy, lustrous, shiny, glabrous = 0; Ciliate, silky, velvety, pubescent, glaucous, pilose, felty, waxy, downy, sometimes hairy, slightly hairy, fuzzy = 1; Rough, resinous, hairy, tomentose, scabrous, sticky, sticky hairs, setose, floccose, scaly, villous, scurfy, glutinous, tufts (in axils of veins), “with hairs”, long hair, or densely hairy = 2. Conifers were given a score of 1, unless noted as shiny or notably smooth surface (0) or scale-like, ridged or glaucous (2).

Leaf Margins (from Horticipia database): Entire, terminal spine, spiny, sinuate, or undulate = 0;  
Cleft, crenate, dentate, incised, lobed, parted, pectinate, revolute, serrate, or unknown = 1; Ciliate, serrulate, double serrate, or filamentous = 2.

Leaf and crown scores were added to produce a potential leaf score between 0 and 12. Leaf scores were standardized between 0 and 100.

### **Particle Pollution Removal**

Because the removal of particulate matter by trees is influenced by the physical characteristics of their leaves (i.e., the size, complexity, and surface features), the U.S. average PM-10 flux (from the Urban Forests Effect (UFORE) model: Nowak et. al. 2000, 2001, 2002, 2003; Nowak and Crane, 2000, 2002) had to be adjusted to reflect the leaf characteristics of each evaluated species. Thus, overall leaf scores were assigned corresponding particle deposition rates ( $V_d$ ), based on values from Little (1977). Average deposition velocities for Nettle, Beech, and White poplar were used to develop a scale of relative particle deposition velocities, based on their respective leaf characteristics. Nettle represented the tree species with the stickiest/hairiest leaf surface, and had the highest overall leaf score (81-100). Beech represented the species with the smoothest leaf surface, and had the lowest overall leaf score (0-20). White poplar was given an overall leaf score of 41-60. The average particle deposition velocities for these three species were standardized to the particle deposition velocity for Beech to determine a weighting factor (Table A-2).

The U.S. average PM<sub>10</sub> flux represents the PM<sub>10</sub> removal rate for a species with average leaf characteristics (i.e., moderate leaf size, surface, and complexity) and a leaf area index of 6. To determine the appropriate PM<sub>10</sub> removal rate for trees with different leaf characteristics (and therefore different deposition velocities), the U.S. average PM<sub>10</sub> flux was weighted by the weighting factor for each species based on the species leaf score (Table A-2).

Table A-2. Range of overall leaf scores and the development of their associated relative particle deposition rates ( $V_d$ ).

Species	Leaf Score	Avg. $V_d$ (cm/sec)	Weight Factor	PM <sub>10</sub> Removal Rate (g/m <sup>2</sup> /hr, LAI = 6)
Nettle	81-100	1.24	1.5	0.00111
	61-80		1.25	0.00093
White poplar	41-60	0.82	1.0	<b>0.00074</b>
	21-40		0.64	0.00047
Beech	0-20	0.23	0.28	0.00021

The final PM<sub>10</sub> removal rate (g/tree/hr) was determined for each species by multiplying the tree's canopy area ( $\pi r^2$ ) and leaf area index by the PM<sub>10</sub> removal rate corresponding to its relative particle deposition rate factor:

$$\text{PM}_{10} \text{ removal (g/tree/hr)} = (\text{Tree canopy area, m}^2) \times (\text{PM-10 removal rate, g/m}^2/\text{hr}) \times (\text{LAI}/6)$$

PM<sub>10</sub> removal for the species was then adjusted based on whether the tree was evergreen or deciduous. Evergreen trees were multiplied by a factor of 1; deciduous trees were multiplied by a factor of length of in-leaf season (days) / 365 to account for period when deciduous trees are leaf-off.

### **Sulfur Dioxide, Ozone, and Nitrogen Dioxide Removal**

The removal rates for NO<sub>2</sub>, O<sub>3</sub>, and SO<sub>2</sub> were determined for each species by using the average pollutant flux from 53 cities using the UFORE model (Table A-3); relative transpiration factor (Table A); total tree canopy area; and leaf area index (LAI). The U.S. average pollutant flux (g/m<sup>2</sup>/hr) was used to represent the pollutant removal rate for a species with an average transpiration rate (Table A; TF = 1) and a leaf area index of 6. This base pollutant removal rate was multiplied by each tree's relative transpiration factor to yield appropriate pollutant removal rates for trees with different transpiration rates (Tables A-3, A-4, A-5).

Table A-3. NO<sub>2</sub> removal rates based on relative transpiration rate.

Water Use Classification	Relative Transpiration Factor	NO <sub>2</sub> Removal Rate (g/m <sup>2</sup> /hr)
High need (H)	1.50	0.00067
High to moderate need (MH)	1.25	0.00056
Moderate need (M)	1.00	<b>0.00045</b>
Moderate to low need (ML)	0.75	0.00033
Low need (L)	0.50	0.00022
Low to very low need (LVL)	0.35	0.00016
Very low need (VL)	0.20	0.00009

Table A-4. O<sub>3</sub> removal rates based on relative transpiration rate.

Water Use Classification	Relative Transpiration Factor	O <sub>3</sub> Removal Rate (g/m <sup>2</sup> /hr)
High need (H)	1.50	0.00194
High to moderate need (MH)	1.25	0.00162
Moderate need (M)	1.00	<b>0.00129</b>
Moderate to low need (ML)	0.75	0.00097
Low need (L)	0.50	0.00065
Low to very low need (LVL)	0.35	0.00045
Very low need (VL)	0.20	0.00026

Table A-5. SO<sub>2</sub> removal rates based on relative transpiration rate.

Water Use Classification	Relative Transpiration Factor	SO <sub>2</sub> Removal Rate (g/m <sup>2</sup> /hr)
High need (H)	1.50	0.00044
High to moderate need (MH)	1.25	0.00037
Moderate need (M)	1.00	<b>0.00030</b>
Moderate to low need (ML)	0.75	0.00022
Low need (L)	0.50	0.00015
Low to very low need (LVL)	0.35	0.00010
Very low need (VL)	0.20	0.00006

The final pollutant removal (g/tree/hr) was determined by multiplying the tree's canopy area and LAI by the pollutant removal rate corresponding to its relative transpiration factor:

$$\text{Pollutant removal (g/tree/hr)} = (\text{pollutant removal rate (g/m}^2\text{/hr)}) \times (\text{tree canopy area}) \times (\text{LAI}/6)$$

### **Carbon Monoxide Removal**

CO removal was estimated for each species based on average CO flux of the 53 U.S. cities (0.00007 g/m<sup>2</sup>/hr); total tree canopy area; and LAI. The final CO removal rate (g/tree/hr) was calculated for each tree by multiplying the tree's canopy area (m<sup>2</sup>) and leaf area index by the average CO flux of the 54 U.S. cities (0.00007 g/m<sup>2</sup>/hr):

$$\text{CO removal rate for tree (g/tree/hr)} = (\text{CO flux}) \times (\text{Tree canopy area}) \times (\text{LAI}/6)$$

CO removal for the species was then adjusted based on whether the tree was evergreen or deciduous. Evergreen trees were multiplied by a factor of 1; deciduous trees were multiplied by a factor of length of in-leaf season (days) / 365 to account for period when deciduous trees are leaf-off.

### **Net Carbon Monoxide and Ozone Effects**

The emission of both carbon monoxide and ozone were determined by combining the total emission of isoprene, and monoterpenes with their reactivity coefficients (yielding the potential of the VOC to form into either carbon monoxide or ozone) (Carter 1998; Madronovich, pers. comm., 1997).

**Carbon Monoxide.** The VOC potential to form carbon monoxide is likely near 10% (Madronovich, pers. comm. 1997). Thus, the carbon monoxide forming potential (COFP) is:

$$\text{COFP (g CO/tree/hr)} = [0.1 * (\text{VOC in g C/tree/hr}) * (28 \text{ g CO/mol CO}) / (12 \text{ g C/mol CO})]$$

Net CO removal rate was then calculated as:

$$\text{Net CO removal rate (g CO/tree/hr)} = \text{CO removal (g CO/tree/hr)} - \text{COFP.}$$

**Ozone.** VOC to ozone conversion was based on Maximum Ozone Incremental Reactivity (MOIR) scenarios (Carter 1998). Base reactivity scales used were 3.85 g O<sub>3</sub> / g isoprene, 1.4 g O<sub>3</sub> / g monoterpene, and 0.04 g O<sub>3</sub> / g CO. These base scales were based on a NO<sub>x</sub>/VOC ratio of 8. Average NO<sub>x</sub>/VOC ratios for 22 cities (National Research Council 1991) was 10.6. Data from Maximum Incremental Reactivity (MIR) scenarios (NO<sub>x</sub>/VOC ratio = 4) and Equal Benefit Incremental Reactivity (EBIR) scenarios (NO<sub>x</sub>/VOC ratio = 15) were used to adjust the reactivity scale to the national average NO<sub>x</sub>/VOC ratio (3.23 g O<sub>3</sub> / g isoprene, 1.23 g O<sub>3</sub> / g monoterpene, and 0.036 g O<sub>3</sub> / g CO).

VOC and CO emissions per tree/hr were multiplied by the appropriate reactivity scale to estimate O<sub>3</sub> formation due to tree VOC emissions and consequent CO formation. Net O<sub>3</sub> removal rate was then calculated as:

$$\text{Net O}_3 \text{ removal rate (g O}_3\text{/tree/hr)} = \text{O}_3 \text{ removal} - \text{O}_3 \text{ formation.}$$

### **Overall Pollutant Rating**

Each species received an overall pollutant rating, based on its estimated effect for each pollutant. The overall score were based on removal values for particulate matter, sulfur dioxide, nitrogen dioxide; and the net removal/emission values for carbon monoxide and ozone. The net effect for each pollutant was weighted by the relative effect of each pollutant based on California Ambient Air Quality Standards (California Air Resources Board 2005) for the same measurement period (Table A-6).

Table A-6. California ambient air quality standards. Weight was based on referencing against the 1-hour ozone standard.

<i>Standards</i>	<i>Ozone</i>	<i>Particulate Matter (PM<sub>10</sub>)</i>	<i>Nitrogen Dioxide</i>	<i>Sulfur Dioxide</i>	<i>Carbon Monoxide</i>
1-hour	180 $\mu\text{g}/\text{m}^3$		470 $\mu\text{g}/\text{m}^3$	655 $\mu\text{g}/\text{m}^3$	23,000 $\mu\text{g}/\text{m}^3$
24-hour		50 $\mu\text{g}/\text{m}^3$		105 $\mu\text{g}/\text{m}^3$	
Weight*	1.00	0.58	0.38	0.27	0.01

\* weight = 180 / 1-hour standard. PM<sub>10</sub> 1-hour standard was estimated as 312  $\mu\text{g}/\text{m}^3$  based on the ratio of 1-hour to 24-hour standard of sulfur dioxide.

The overall pollutant score was calculated as:

$$\text{Overall Score} = [(\text{O}_3 \text{ effect (g/tree/hr)} * 1.0) + (\text{PM}_{10} \text{ effect} * 0.58) + (\text{NO}_2 \text{ effect} * 0.38) + (\text{SO}_2 \text{ effect} * 0.27) + (\text{CO effect} * 0.01)]$$

All trees not listed as adapted to New York City's hardiness zone were removed and the overall score was standardized to values between 0 and 100.

### **Carbon Storage**

Carbon storage estimates were based on estimated tree diameter at maturity (from tree height data using equations in Frelich, 1992), tree height, and species allometric equation for biomass (in Nowak et al., 2002). Carbon storage at maturity was then standardized to a score of 0 -100.

### **Allergenicity**

Species allergenicity was based on species allergenicity rating (1-10) (Ogren 2000) times total leaf area. Allergenicity score was then standardized to a score of 0 -100.

### **Energy conservation (summer-time)**

Summer energy scores were based on a combination of air temperature reduction and shading. Based on McPherson and Simpson (2000), the average tree effect on carbon emission reductions due to energy conservation was 2.3 times greater than the climate effect for tree cover at 30%. Thus standardized shading was weighted by 2.3 and added to the standardized temperature effect (x 0.3 for 30% cover) to produce the summer energy score, which was subsequently standardized to a scale of 0 – 100.

For species that have missing data (e.g., VOC base emission rates may not have been measured), the program will allocate information from the closest botanical relative. For example, a genera average may be used if species information is not available, or if no other species exist in the same genera, then family average will be used, and so on.

***3) Collect, identify, and analyze additional information on appropriate species to aid in developing species recommendations.***

A few additional attributes were determined for each species to aid in species selection for New York City:

**Growth habit**

Tree height and width information were derived from the species data base to determine which tree at maturity would fit within various site constraints: open space (no site constraints) and street trees (some street trees were eliminated from the street tree list based on size (if tree was larger than the largest tree on the NYC approved list) and type (various conifer species were removed).

**Relative species longevity**

Relative species longevity was based primarily on the Urban Forest Ecosystems Institute website (UFEI, 2005) where species longevity was rated as:

- Very short: < 50 years
- Moderately short: 40 – 60 years
- Average: 50 -150 years
- Moderately long: 100 - 175 years
- Very long: > 150 years

If more than one category was listed per species, an average or the most appropriate category was used. If data were not available at UFEI (2005), then other citations were used to determine longevity using the same categories (Hightshoe 1978; Burns and Honkala 1990a, b; Collingwood and Brush 1964; Stein et al. 2003; Elias 1980).

***4) Determine the best species based on the tree functions that are desired and the local planting / landscape conditions.***

For each of the 179 species that were considered adapted to New York City's hardiness zone and available from local nurseries, as standardized score (0-100) was created for each of the tree functions. Based on relative weightings of each tree function for park (Table A-7) and street (Table A-8) trees provided by NYSERDA/DEC, a cumulative index score was produced for each species (Sum of index score times weighting). The final cumulative score was then sorted to produce the final order species recommendation list (Table A-9).



Table A-7. Weighting of tree functions by NYSERDA/DEC for park trees.

<u>Weight</u>	<u>Function</u>	<u>NYSERDA scoring (A=highest; D= lowest)</u>			
		<u>A</u>	<u>B</u>	<u>C</u>	<u>D</u>
61.2	Total Air Quality	1	3	2	
89.0	Air Temperature Reduction	4	2		
83.5	Shading/Leaf Area	3	3		
80.0	Energy Conservation	3	1	1	
33.3	Carbon Storage	1	1	1	3
44.2	Low Allergenicity	1		5	
89.0	Long Relative Life Span	4	2		

A = 100; B = 67; C = 33; D = 0.

Table A-8. Weighting of tree functions by NYSERDA/DEC for street trees.

<u>Weight</u>	<u>Function</u>	<u>Numbers scoring (A=highest; D= lowest)</u>			
		<u>A</u>	<u>B</u>	<u>C</u>	<u>D</u>
72.3	Total Air Quality	2	3	1	
83.5	Air Temperature Reduction	3	3		
100.0	Shading/Leaf Area	6			
100.0	Energy Conservation	5			
27.7	Carbon Storage	1		2	3
61.2	Low Allergenicity	2	2	1	1
83.5	Long Relative Life Span	3	3		

A = 100; B = 67; C = 33; D = 0.

Table A-9. Ranked tree species list for NYC based on weighting factors by NYSERDA/DEC

Scientific Name	Common name	Park Score	Street Tree Score	Approved NYC List <sup>a</sup>	Quarantine <sup>b</sup>	ALB Genus Susceptible <sup>c</sup>
<i>Abies balsamea</i>	Balsam fir	174.7	NR			
<i>Abies concolor</i>	White fir	276.0	NR			
<i>Abies fraseri</i>	Fraser fir	174.7	NR			
<i>Acer buergerianum</i>	Trident maple	131.2	141.1			ALB
<i>Acer campestre</i>	Hedge maple	123.4	137.5	NYC-S	ALB	ALB
<i>Acer freemanii(x)</i>	Freeman maple	223.0	245.5			ALB
<i>Acer ginnala</i>	Amur maple	144.9	166.8	NYC-S	ALB	ALB
<i>Acer griseum</i>	Paperbark maple	96.2	107.2			ALB
<i>Acer negundo</i>	Boxelder	159.5	175.1			ALB
<i>Acer nigrum</i>	Black maple	151.4	165.6			ALB
<i>Acer palmatum</i>	Japanese maple	130.3	144.2			ALB
<i>Acer pensylvanicum</i>	Striped maple	139.3	151.5			ALB
<i>Acer pseudoplatanus</i>	Sycamore maple	212.2	231.7			ALB
<i>Acer rubrum</i>	Red maple	242.3	267.6	NYC-M	ALB	ALB
<i>Acer saccharum</i>	Sugar maple	250.1	268.9			ALB
<i>Acer truncatum</i>	Purple blow maple	152.8	167.2	NYC-S	ALB	ALB
<i>Aesculus carnea(x)</i>	Red horsechestnut	160.7	176.1			ALB
<i>Aesculus flava</i>	Yellow buckeye	189.0	205.2			ALB
<i>Aesculus hippocastanum</i>	Horsechestnut	254.8	277.5			ALB
<i>Aesculus parviflora</i>	Bottlebrush buckeye	167.6	183.9			ALB
<i>Aesculus pavia</i>	Red buckeye	104.6	118.2			ALB
<i>Amelanchier arborea</i>	Downy serviceberry	126.3	142.3			
<i>Amelanchier canadensis</i>	Eastern service berry	144.7	159.1	NYC-S		
<i>Amelanchier laevis</i>	Smooth service berry	146.5	161.0			
<i>Asimina triloba</i>	Pawpaw	135.3	150.1			
<i>Betula lenta</i>	Black birch	155.5	168.9			ALB
<i>Betula nigra</i>	River birch	169.8	181.3			ALB
<i>Betula papyrifera</i>	Paper birch	202.8	214.1			ALB
<i>Betula pendula</i>	European white birch	122.7	130.6			ALB
<i>Betula platyphylla</i>	Asian white birch	132.2	140.1			ALB
<i>Carpinus betulus</i>	European hornbeam	179.2	195.8	NYC-M		
<i>Carpinus caroliniana</i>	American hornbeam	143.3	150.4	NYC-M		
<i>Carya aquatica</i>	Water hickory	264.9	283.0			
<i>Carya cordiformis</i>	Bitternut hickory	230.4	243.6			
<i>Carya glabra</i>	Pignut hickory	199.3	206.4			
<i>Carya illinoensis</i>	Pecan	227.4	237.5			
<i>Carya laciniosa</i>	Shellbark hickory	246.7	264.4			
<i>Carya ovata</i>	Shagbark hickory	225.3	236.5			
<i>Castanea mollissima</i>	Chinese chestnut	200.9	212.0			
<i>Catalpa speciosa</i>	Northern catalpa	134.7	149.8			
<i>Cedrus atlantica</i>	Atlas cedar	293.5	328.1			
<i>Cedrus deodara</i>	Deodar cedar	284.6	316.5			
<i>Cedrus libani</i>	Cedar of lebanon	273.4	303.3			
<i>Celtis occidentalis</i>	Northern hackberry	238.3	261.9	NYC-M	ALB	
<i>Cercidiphyllum japonicum</i>	Katsura tree	141.0	155.6	NYC-M		
<i>Cercis canadensis</i>	Eastern redbud	129.1	146.9			

<i>Chamaecyparis thyoides</i>	Atlantic white cedar	193.1	205.4		
<i>Chionanthus virginicus</i>	Fringe tree	37.2	33.5		
<i>Cladrastis kentukea</i>	Yellowwood	197.7	222.2		
<i>Clerodendrum trichotomum</i>	Harlequin glorybower	53.2	65.0		
<i>Clethra acuminata</i>	Mountain sweetpepperbush	54.1	67.9		
<i>Cornus florida</i>	Flowering dogwood	142.8	154.9		
<i>Cornus foemina</i>	Stiff dogwood	136.7	150.0		
<i>Cornus mas</i>	Cornelian cherry	123.8	135.6		
<i>Corylus colurna</i>	Turkish hazelnut	187.3	197.3		
<i>Cotinus coggygria</i>	Smoke tree	78.0	84.6		
<i>Crataegus aestivalis</i>	May hawthorn	133.8	144.7		
<i>Crataegus crus-galli</i>	Cockspur hawthorn	146.3	159.6	NYC-S	
<i>Crataegus laevigata</i>	Smooth hawthorn	146.3	159.6		
<i>Crataegus phaenopyrum</i>	Washington hawthorn	145.9	159.1		
<i>Crataegus viridis</i>	Green hawthorn	174.8	193.1		
<i>Cryptomeria japonica</i>	Japanese red cedar	186.0	192.4		
<i>Eucommia ulmoides</i>	Hardy rubber tree	151.5	170.6	NYC-L	
<i>Euonymus atropurpurea</i>	Eastern wahoo	89.0	95.6		
<i>Fagus grandifolia</i>	American beech	295.0	324.8		
<i>Fagus sylvatica</i>	European beech	260.1	284.5		
<i>Franklinia alatamaha</i>	Franklin tree	106.6	119.8		
<i>Fraxinus pennsylvanica</i>	Green ash	228.3	244.6	NYC-L	ALB
<i>Ginkgo biloba</i>	Ginkgo	234.2	255.9	NYC-L	
<i>Gleditsia triacanthos</i>	Honeylocust	214.3	239.6	NYC-L	
<i>Gymnocladus dioica</i>	Kentucky coffeetree	204.3	223.2	NYC-L	
<i>Halesia carolina</i>	Snowdrop tree	160.6	183.1		
<i>Halesia tetraptera</i>	Mountain silverbell	187.5	217.7		
<i>Hamamelis vernalis</i>	Ozark witchhazel	112.5	127.1		
<i>Hippophae rhamnoides</i>	Seabuckthorn	125.9	137.6		
<i>Ilex opaca</i>	American holly	131.7	142.0		
<i>Juglans cinerea</i>	Butternut	254.8	281.6		
<i>Juglans nigra</i>	Black walnut	307.3	331.3		
<i>Juniperus chinensis</i>	Chinese juniper	73.2	81.1		
<i>Juniperus virginiana</i>	Eastern red cedar	165.5	171.2		
<i>Koelreuteria bipinnata</i>	Chinese flame tree	165.9	187.1		
<i>Koelreuteria paniculata</i>	Goldenrain tree	190.1	218.3	NYC-M	
<i>Larix decidua</i>	European larch	210.2	236.9		
<i>Liquidambar styraciflua</i>	Sweetgum	235.4	255.4	NYC-L	
<i>Liriodendron tulipifera</i>	Tulip tree	364.4	393.2	NYC-L	
<i>Magnolia acuminata</i>	Cucumber tree	267.9	294.2		
<i>Magnolia denudata</i>	Chinese magnolia	162.8	178.3		
<i>Magnolia grandiflora</i>	Southern magnolia	338.4	368.0		
<i>Magnolia soulangiana</i> (x)	Chinese magnolia	139.1	151.9		
<i>Magnolia tripetala</i>	Umbrella magnolia	188.5	209.4		
<i>Malus angustifolia</i>	Southern crabapple	166.2	182.9		
<i>Malus baccata</i>	Siberian crabapple	159.7	173.7		
<i>Malus floribunda</i>	Japanese flowering crabapple	148.2	161.8		
<i>Metasequoia glyptostroboides</i>	Dawn redwood	250.2	268.3	NYC-L	
<i>Morus alba</i>	White mulberry	143.6	156.5		
<i>Nyssa sylvatica</i>	Black tupelo	214.9	222.4		

<i>Ostrya virginiana</i>	Eastern hophornbeam	175.1	192.6	NYC-M	
<i>Oxydendrum arboreum</i>	Sourwood	147.4	167.7		
<i>Parrotia persica</i>	Persian ironwood	139.4	157.2		
<i>Phellodendron amurense</i>	Amur corktree	167.7	187.4		
<i>Picea abies</i>	Norway spruce	261.9	NR		
<i>Picea glauca</i>	White spruce	198.7	NR		
<i>Picea omorika</i>	Serbian spruce	231.1	NR		
<i>Picea pungens</i>	Blue spruce	234.3	NR		
<i>Pinus albicaulis</i>	Whitebark pine	158.9	NR		
<i>Pinus aristata</i>	Bristlecone pine	171.3	NR		
<i>Pinus armandii</i>	David's pine	209.4	NR		
<i>Pinus banksiana</i>	Jack pine	172.8	NR		
<i>Pinus cembra</i>	Swiss stone pine	160.5	174.0		
<i>Pinus densiflora</i>	Japanese red pine	225.1	NR		
<i>Pinus elliottii elliottii (v)</i>	Slash pine	209.4	234.1		
<i>Pinus flexilis</i>	Limber pine	202.7	NR		
<i>Pinus monticola</i>	Western white pine	246.4	NR		
<i>Pinus nigra</i>	Austrian pine	205.2	NR		
<i>Pinus parviflora</i>	Japanese white pine	210.4	NR		
<i>Pinus resinosa</i>	Red pine	215.1	NR		
<i>Pinus strobiformis</i>	Southwestern white pine	211.0	NR		
<i>Pinus strobus</i>	Eastern white pine	246.6	NR		
<i>Pinus sylvestris</i>	Scotch pine	223.6	NR		
<i>Pinus taeda</i>	Loblolly pine	208.5	NR		
<i>Pinus thunbergiana</i>	Japanese black pine	229.0	NR		
<i>Pinus virginiana</i>	Virginia pine	192.0	NR		
<i>Pistacia atlantica</i>	Mt. Atlas mastic tree	150.1	166.2		
<i>Pistacia chinensis</i>	Chinese pistache	192.3	204.4		
<i>Platanus hybrida</i>	London planetree	316.8	349.5		ALB
<i>Platanus occidentalis</i>	American sycamore	332.4	365.4		ALB
<i>Platycladus orientalis</i>	Oriental arbor vitae	72.2	76.7		
<i>Populus nigra</i>	Black poplar	159.5	181.7		
<i>Prunus cerasifera</i>	Cherry plum	120.6	134.6	NYC-S	
<i>Prunus persica</i>	Nectarine	102.9	120.3		
<i>Prunus sargentii</i>	Sargent cherry	175.5	194.9		
<i>Prunus serrulata</i>	Kwanzan cherry	121.3	133.1	NYC-S	
<i>Prunus yedoensis(x)</i>	Yoshino flowering cherry	120.0	133.7		
<i>Pseudotsuga menziesii</i>	Douglas fir	259.4	287.3		
<i>Pyrus calleryana</i>	Callery pear	170.3	187.4	NYC-M	
<i>Pyrus communis</i>	Common pear	162.6	178.5		
<i>Quercus acutissima</i>	Sawtooth oak	243.8	265.5	NYC-M	
<i>Quercus alba</i>	White oak	271.2	297.8		
<i>Quercus bicolor</i>	Swamp white oak	243.8	261.1	NYC-L	
<i>Quercus coccinea</i>	Scarlet oak	241.7	254.7		
<i>Quercus hemisphaerica</i>	Darlington oak	253.9	274.1		
<i>Quercus imbricaria</i>	Shingle oak	216.8	228.5		
<i>Quercus laurifolia</i>	Laurel oak	246.1	264.8	NYC-L	
<i>Quercus lyrata</i>	Overcup oak	200.5	217.7		
<i>Quercus macrocarpa</i>	Bur oak	271.1	297.6		
<i>Quercus michauxii</i>	Swamp chestnut oak	223.9	237.3		

<i>Quercus nigra</i>	Water oak	272.8	300.2			
<i>Quercus palustris</i>	Pin oak	240.4	253.7	NYC-L		
<i>Quercus phellos</i>	Willow oak	212.1	229.6	NYC-L		
<i>Quercus prinoides</i>	Dwarf chinkapin oak	232.3	251.3			
<i>Quercus prinus</i>	Chestnut oak	265.8	286.6			
<i>Quercus robur</i>	English oak	271.1	295.2	NYC-M		
<i>Quercus rubra</i>	Northern red oak	270.5	294.6	NYC-L		
<i>Quercus shumardii</i>	Shumard oak	270.7	287.6			
<i>Quercus stellata</i>	Post oak	204.0	216.9			
<i>Quercus velutina</i>	Black oak	236.5	248.7			
<i>Rhododendron catawbiense</i>	Catawba rosebay	105.2	118.5			
<i>Robinia pseudoacacia</i>	Black locust	204.5	231.3			
<i>Salix alba</i>	White willow	152.7	185.5			ALB
<i>Salix matsudana</i>	Corkscrew willow	64.5	83.2			ALB
<i>Salix nigra</i>	Black willow	56.1	66.6			ALB
<i>Salix purpurea</i>	Purpleosier willow	94.9	112.5			ALB
<i>Salix sericea</i>	Silky willow	76.7	87.1			ALB
<i>Sophora japonica</i>	Japanese pagoda tree	232.2	265.1			
<i>Stewartia koreana</i>	Stewartia	124.0	140.1			
<i>Syringa reticulata</i>	Japanese tree lilac	93.8	99.7	NYC-S		
<i>Taxodium distichum</i>	Baldcypress	207.3	221.9	NYC-L		
<i>Taxus cuspidata</i>	Japanese yew	223.9	244.1			
<i>Thuja occidentalis</i>	Northern white cedar	107.5	111.6			
<i>Tilia cordata</i>	Littleleaf linden	252.6	275.8	NYC-L		
<i>Tsuga canadensis</i>	Eastern hemlock	299.0	NR			
<i>Ulmus americana</i>	American elm	314.9	337.5	NYC-L	ALB	ALB
<i>Ulmus glabra</i>	Wych elm	324.2	348.5			ALB
<i>Ulmus parvifolia</i>	Chinese elm	188.7	202.2	NYC-L	ALB	ALB
<i>Ulmus pumila</i>	Siberian elm	250.0	267.9			ALB
<i>Vaccinium arboreum</i>	Sparkleberry	93.8	104.9			
<i>Viburnum obovatum</i>	Small-leaf arrowwood	101.8	115.4			
<i>Viburnum sieboldii</i>	Siebold's arrowwood	88.1	99.1			
<i>Zelkova serrata</i>	Japanese zelkova	202.0	222.4	NYC-L		

“NR” – not rated. These trees were eliminated from the street tree list based on size (if tree was larger than the largest tree on the NYC approved list) and type (various conifer species were removed by Frank Dunstan).

<sup>a</sup> Approved NYC street tree list – notes if species in on NYC street tree list (from Frank Dunstan). Note most species on the NYC list are on the functional scoring list. However, some species did not make the scoring list as they were removed based on availability from major local nurseries.

<sup>b</sup> species listed ALB restricted based on list from Frank Dunstan

<sup>c</sup> list the genera that are noted to be “good” or “very good” hosts to ALB based on information from APHIS (Nowak et al., 2001)

## **CONCLUSION**

This report details recommended tree species for New York City based on standardized tree functions and weightings of tree functions provided by NYSERDA/DEC. This list is not based on adaptability of species to the street tree or park environment in New York. The list was limited to plants available in local nurseries and adapted to New York City's hardiness zone. Many factors that are critical to selecting species are not considered by this list (e.g., invasiveness, survivability under New York conditions, various pest or disease problems). Thus, local experience with these trees should be used to determine if listed trees are suitable for the demands and priorities of the site specific urban environment.

## APPENDIX B: EVALUATION OF WEATHERBUG DATA QUALITY

WeatherBug® distributes data from commercial weather stations, many of which are located at schools. The quality of the data from each of these stations was evaluated against NWS stations at JFK, La Guardia, and Central Park. Table B-1 lists the NWS and WeatherBug stations with the quality ratings developed for this report.

Table B-1. NWS and WeatherBug stations with data quality ratings. Tier I indicates the data is from an NWS station. Tier II indicates high confidence in a WeatherBug station. Tier III indicates some confidence in a WeatherBug station and Tier IV indicates that the data were not useable.

Case study area	Name	County	Latitude	Longitude	Rating
JFK	JFK	Kings	40.650	-73.783	Tier I
La Guardia (LGA)	LGA	Queens	40.767	-73.900	Tier I
Central Park	Central Park	New York	40.783	-73.967	Tier I
Mid-Manhattan	NWYK1	New York	40.767	-73.987	Tier II
Maspeth	CORNA	Queens	40.747	-73.853	Tier II
Crown Heights	BKLN1	Kings	40.639	-73.941	Tier II
Fordham	BRNX6	Bronx	40.863	-73.881	Tier III
Ocean Parkway	BKBHS	Kings	40.616	-73.979	Tier III
Lower Manhattan	BRKL2	Kings	40.689	-73.977	Tier IV

The evaluation included comparisons between summer 2002 mean temperatures, mean temperatures during the heat waves, hourly maps and graphs of near-surface air temperature, and maps of other variables. In comparing between NWS and WeatherBug stations, it was assumed that equipment at different stations was placed uniformly at the same height on a surface type that was the same for each station – i.e. no correction was made for the fact that two of the NWS stations are located at airports while the WeatherBug stations are often located on rooftops. In evaluating the results, it was also assumed that it is generally cooler to the north and near the water given prevailing meteorological conditions in the region.

In addition to near-surface air temperature, tests comparing sea-level pressure, relative humidity, and winds were also performed. In general, it was found that the relative humidity and sea-level pressure at the WeatherBug stations were reasonable, but that wind data were erratic. The sea-level pressure data at the Mid-Manhattan site were biased; however, this was most likely a calibration problem because the data were highly correlated with the data from the other stations.

The Mid-Manhattan WeatherBug station is located close to Central Park and the Maspeth station is close to La Guardia. Detailed comparisons of the data from these two Weatherbug stations to nearby NWS stations indicate that the Weatherbug stations are collecting data of reasonable quality.

However, there are some exceptions. Crown Heights and Ocean Parkway are close to one another, but the mean summer 2002 temperatures were 3.8°F (2.1°C) higher at Ocean Parkway than at Crown Heights. By comparison, Central Park, La Guardia, and JFK had mean summer 2002 temperatures that were within 2.2°F (1.2°C) of one another. Thus it is unlikely that that the difference observed between Crown Heights and Ocean Parkway is realistic, especially given that there is little difference in elevation or distance to shore between the two sites. The most likely explanation is the location of the Ocean Parkway station on top of a dark-colored roof.



## APPENDIX C: ALGORITHM FOR GENERATING SURFACE TEMPERATURE FROM REMOTELY-SENSED LANDSAT DATA

The study uses three Landsat ET+ Images spanning the summer of 2002 from July to September (July 20th, August 14th, and September 8<sup>th</sup>). We utilize methodologies detailed by Voogt and Oke (2003) in their review of the satellite-based surface temperature studies, and by Aniello et al. (1995) who discuss surface temperature GIS-map generation for micro-climate urban heat islands. Using the TIR (60 meter resolution), surface temperature maps were derived using the following model. The first step is to convert the DN thermal band 6 L (low gain) to radiance from the following equations.

$$L_{\lambda} = ((L_{MAX\lambda} - L_{MIN\lambda}) / (QCAL_{MAX} - QCAL_{MIN})) * (QCAL - QCAL_{MIN}) + L_{MIN\lambda}$$

where

$L_{\lambda}$  = spectral radiance in  $W * m^{-2} * ster^{-1} * \mu m$

$L_{min}$  = min spectral radiance at  $QCAL = 0$  DN in  $W * m^{-2} * ster^{-1} * \mu m$

$L_{max}$  = max spectral radiance at  $QCAL = 255$  DN in  $W * m^{-2} * ster^{-1} * \mu m$

Then convert band 6 radiance to the surface-leaving temperature with the atmospheric correction parameter calculator developed by Landsat Science team with

$$L_{TOA} = t \varepsilon L_T + L_u + (1 - \varepsilon) L_d$$

where

$L_u$  = upwelling or atmospheric path radiance,

$L_d$  = downwelling or sky radiance,

$t$  = atmospheric transmission,

$\varepsilon$  = emissivity of the surface,

$L_{TOA}$  = the space-reaching or TOA radiance measured by the instrument, and

$L_T$  = the radiance of a blackbody target of kinetic temperature T.

The last step is the conversion of the surface radiance to surface temperature in Kelvin using

$$T = K_2 / \ln((K_1/L) + 1)$$

where

T = Temperature (Kelvin)

K<sub>2</sub> = Calibration constant 2, 1282.71 Kelvin

K<sub>1</sub> = Calibration constant 1, 666.09 watts/ (meter squared \* ster \*  $\mu m$ ), and

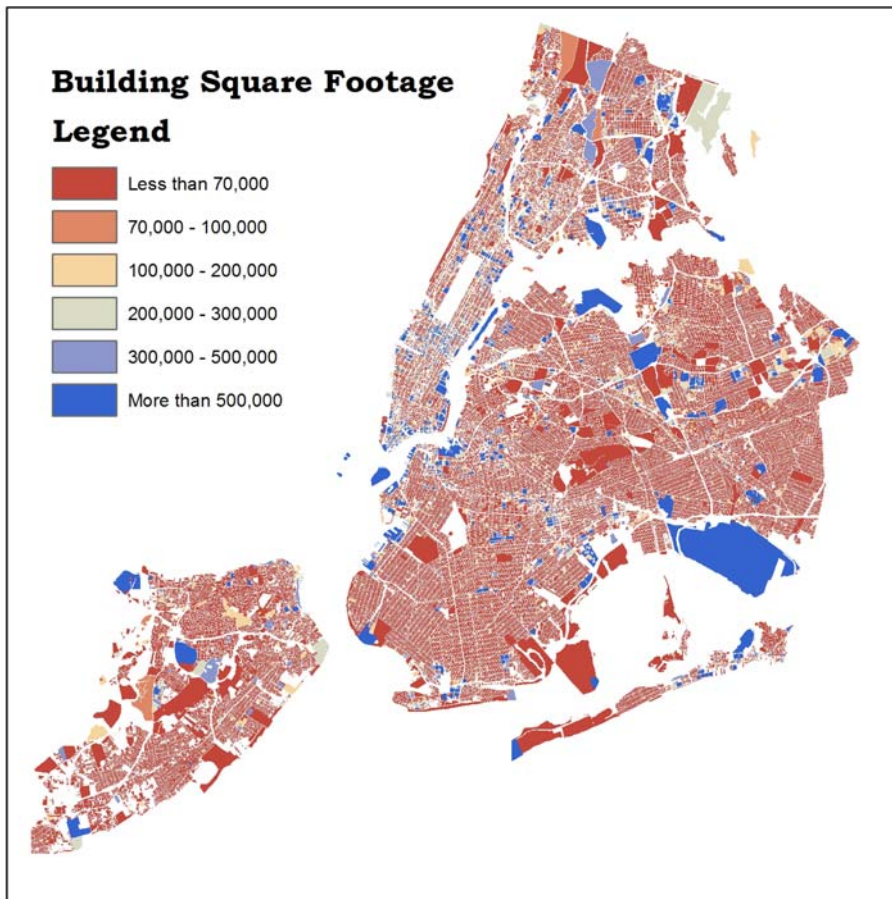
L = Spectral radiance in watts/(meter squared \* ster \*  $\mu m$ )

## APPENDIX D: ADDITIONAL GIS DATA

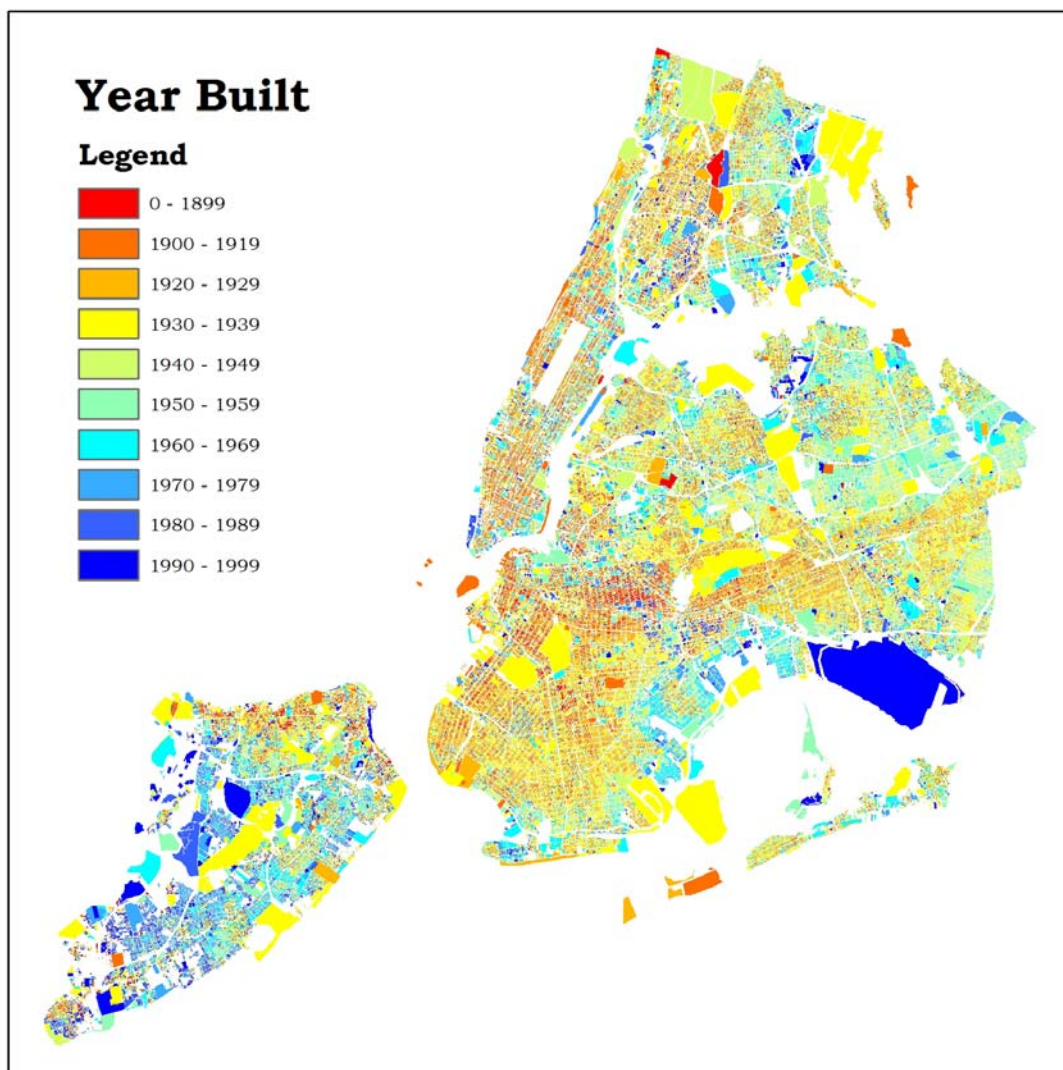
Building square footage and average year built are available from the real property database and were generated in the same way as the average building heights layer (Figures D-1 and D-2).

Urban function parameters include population density (Figure D-3), housing density, workday population density, electrical generators (points), and energy use constants (RASTER, in units of KBtu/ft<sup>2</sup>) (Figure D-4). GIS layers based on the former three parameters were created using CENSUS 2002 data available through the Regional Plan Association.

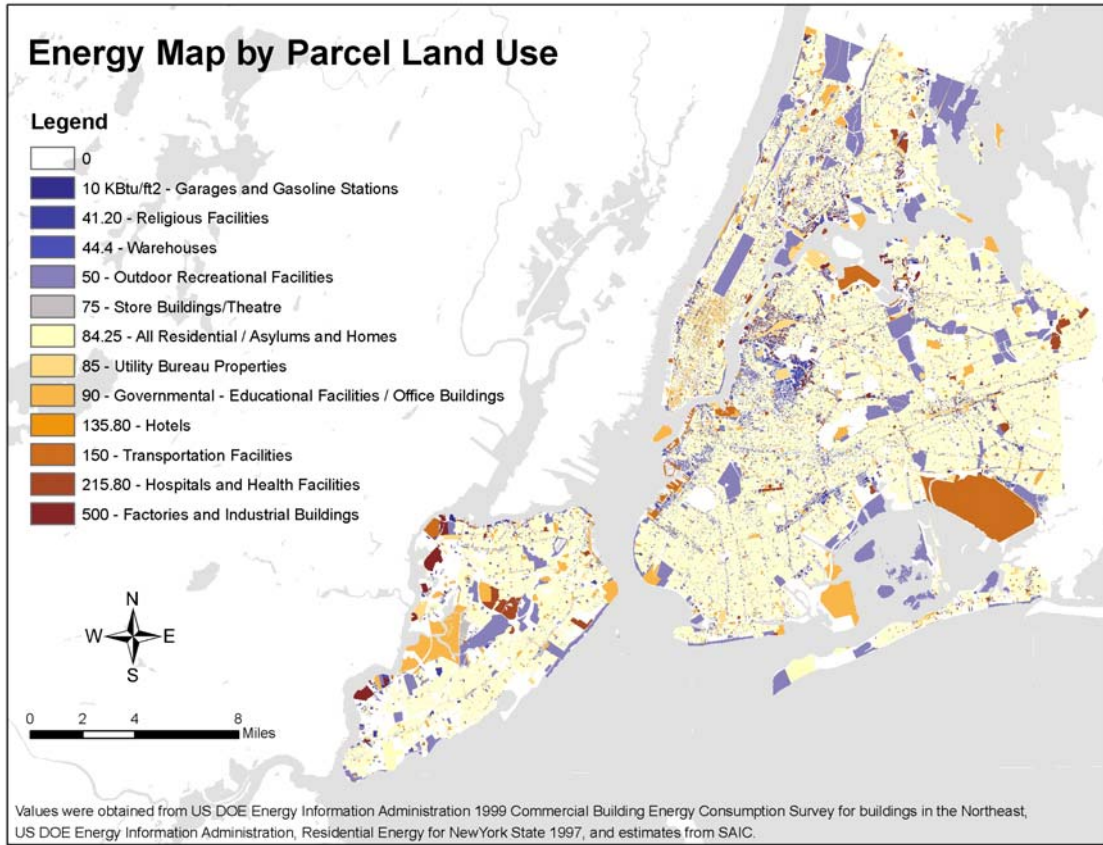
Energy use constants were assigned to each of New York City's 24 land use categories based on values published by the U.S. Department of Energy's Energy Information Administration and supplemented with values estimated by SAIC based on past experience (US DOE EIA, 1999 and US DOE EIA, 1997). The values were added to the real property database as a new field and a 10 meter RASTER data layer was created for the urban heat island database.



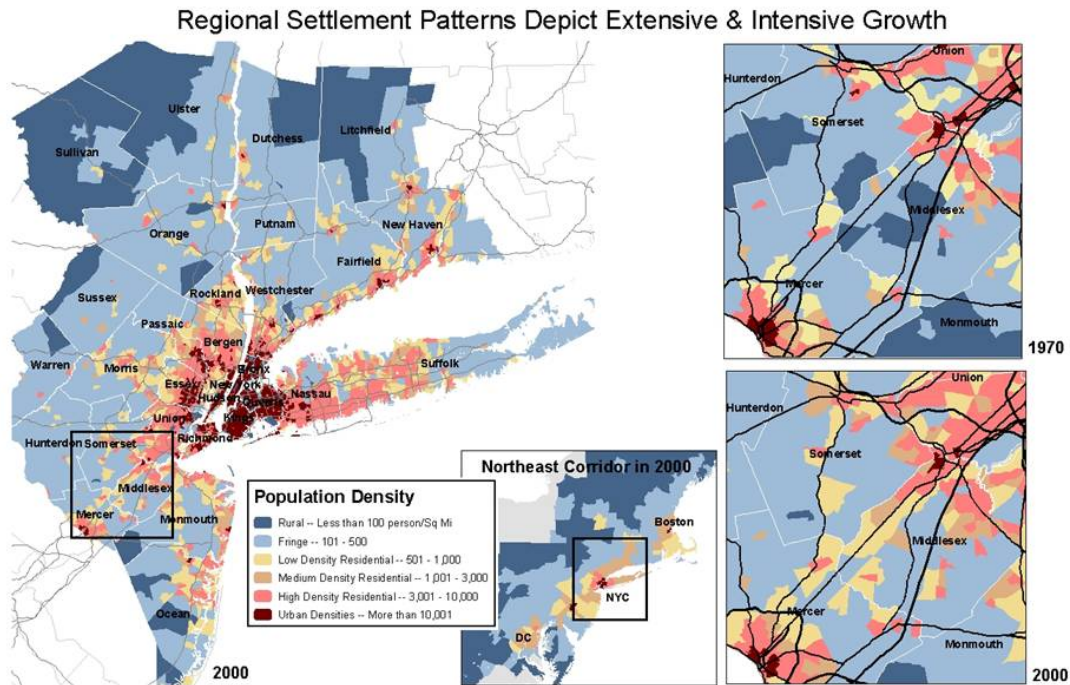
D-1 Building square footage.



D-2. Average year built.



D-3. Energy map by parcel land use



D-4. Population density



## APPENDIX E: BOROUGH-LEVEL STATISTICAL ANALYSIS

A statistical analysis was also performed over the five boroughs – Manhattan, Queens, the Bronx, Brooklyn, and Staten Island. Cells within the two major airports or an open space larger than 10 acres or within 100 meters of a large body of water were excluded (Figure E-1). Descriptive statistics are shown in Table E-1.

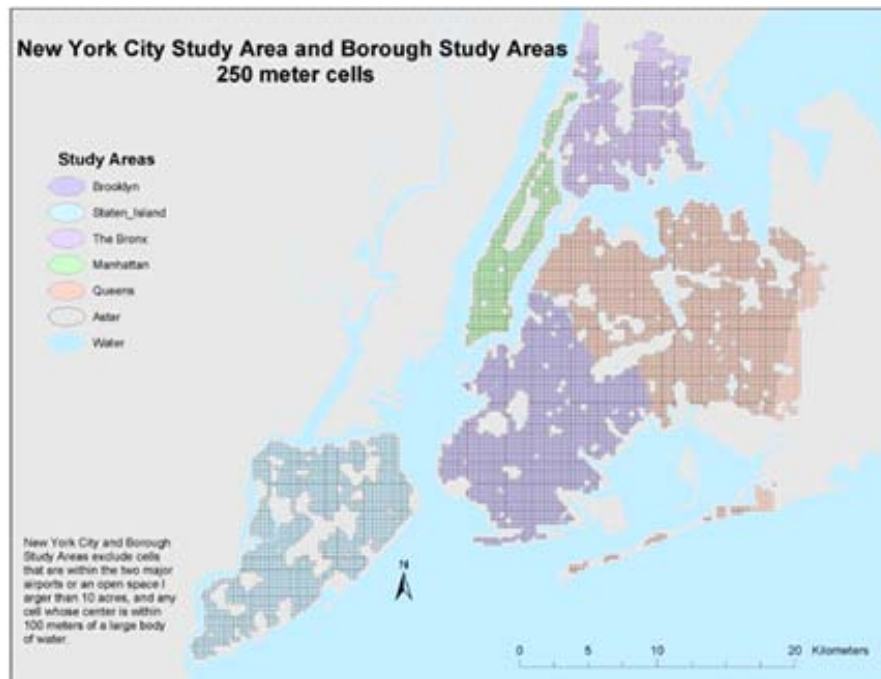


Figure E-1 Borough study areas with 250 meter grid cells.

As expected there is surface temperature variation between the different days. Average surface temperatures range from 24.52 to 40.87 degrees Celsius among the four images for all of New York City. Tables E-1 shows the descriptive statistics for each of the images used in the analysis. Higher average temperatures were associated with greater levels of standard deviation. The variation among the temperatures across the five NYC boroughs (counties) was quite consistent. The borough of Brooklyn was the hottest and was 0.5 to 1.0 hotter than the average for the entire city. Manhattan and Staten Island were consistently among the coolest in temperature.

Table E-1. Descriptive statistics for New York City and the five boroughs.

		New York City	NYC	NYC - 8% randomly sampled	Manhattan	Bronx	Queens	Brooklyn	Staten Island
		Excluding all cells that are open space, airport, or coastal							
ETM 7/22/02	Number of cells (N)	11992	7573	635	519	998	2800	2053	1502
	<b>Mean</b>	<b>40.87</b>	<b>41.77</b>	<b>41.75</b>	<b>41.06</b>	<b>41.85</b>	<b>41.39</b>	<b>42.74</b>	<b>40.96</b>
	Median	41.60	41.60	41.60	40.71	41.60	41.60	42.48	41.60
	Standard Deviation	3.26	2.45	2.41	1.94	2.54	2.16	2.12	3.28
ETM 8/14/02	Number of cells (N)	11992	7573	635	519	998	2800	2053	1502
	<b>Mean</b>	<b>29.05</b>	<b>29.50</b>	<b>29.46</b>	<b>29.12</b>	<b>29.96</b>	<b>29.45</b>	<b>29.97</b>	<b>28.60</b>
	Median	29.51	29.51	29.51	29.03	30.00	29.51	30.00	28.55
	Standard Deviation	1.96	1.53	1.52	1.14	1.55	1.36	1.36	1.92
ETM 9/8/02	Number of cells (N)	11992	7573	635	519	998	2800	2053	1533
	<b>Mean</b>	<b>35.33</b>	<b>36.01</b>	<b>35.99</b>	<b>35.47</b>	<b>36.07</b>	<b>35.72</b>	<b>36.74</b>	<b>35.40</b>
	Median	35.87	35.87	35.87	35.20	35.87	35.87	36.54	35.87
	Standard Deviation	2.45	1.85	1.82	1.46	1.92	1.63	1.60	2.47
Aster 9/8/02	Number of cells (N)	11431	7219	361	519	857	2527	2053	1502
	<b>Mean</b>	<b>24.52</b>	<b>25.34</b>	<b>25.41</b>	<b>25.36</b>	<b>26.60</b>	<b>25.31</b>	<b>25.88</b>	<b>23.74</b>
	Median	24.83	25.37	25.45	25.37	26.67	25.21	25.83	24.04
	Standard Deviation	2.65	2.13	2.18	1.66	2.03	1.89	1.78	2.45

The results for each borough (Table E-2) begin to show the complex nature of the urban heat islands within the city. NDVI is the strongest predictor of surface temperature for all boroughs except Manhattan. Albedo is a strong predictor in Queens and Staten Island and slightly weaker for the Bronx. Population density, road density and average building height account for a small amount of the variation of surface temperature in two of the boroughs. None of the remaining variables – building square footage, average year built, and energy use – were significant predictors of surface temperature over any of the boroughs.

The borough level statistical results show the characteristics of the heat island at a finer level of detail. Albedo, for instance, accounts for 41% of the variability of surface temperature in Staten Island and 15% of the variability city-wide. As did the case study analysis, the borough analysis indicates that different variables are driving the surface temperature in different areas of the city. According to the borough statistical analysis, in Staten Island and Queens, planting street trees and changing to light surfaces would be the best urban heat island mitigation scenario. None of the variables are significant in the Manhattan analysis, so no recommendations can be made.

Table E-2. Bivariate OLS regression results – New York City and boroughs derived from September 8, 2002 Landsat EM+ Image

	New York City (8% sampled) n = 635	Manhattan (40% sampled) n = 208	Bronx (25% sampled) n = 239	Queens (10% sampled) n = 277	Brooklyn (9% sampled) n = 185	Staten Island (13% sampled) n = 195
	R2 (S.E.)	R2 (S.E.)	R2 (S.E.)	R2 (S.E.)	R2 (S.E.)	R2 (S.E.)
	Moran's I (Sig.)	Moran's I (Sig.)	Moran's I (Sig.)	Moran's I (Sig.)	Moran's I (Sig.)	Moran's I (Sig.)
NDVI	.30 (1.52)		.38 (1.20)	.48 (1.06)	.17 (1.37)	.57 (1.74)
	I = .07 (.20)		I = .01 (.84)	I = .05 (.32)	I = .03 (.56)	I = -.07 (.35)
Albedo Composite	.15 (1.67)		.08 (1.80)	.17 (1.34)		.41 (2.03)
	I = .04 (.20)		I = .07 (.25)	I = .15 (.00)		I = .10 (.15)
Road Density	.07 (1.75)		.09 (1.79)			
	I = .02 (.46)		I = .05 (.35)			
Population Density						.08 (2.55)
						I = .02 (.67)
Average Building Height		.06 (2.01)				
		I = .08 (.26)				

## APPENDIX F: EVALUATION OF MM5 V3.7+SEBM

MM5 was forced with NCEP re-analysis data and was also initialized with radiosonde data. It was run over a domain encompassing the area surrounding New York City at grid resolutions of 36, 12, and 4 km to obtain boundary conditions (Figure F-1). The NCEP data was refreshed every six hours at the boundaries of the 36 km domain. Each nested grid box was driven by the input from the coarser nest surrounding it at every time step. The MRF physics scheme was used, which includes both local and non-local mixing. Turbulence was parametrized using first order closure. Surface temperature was initialized from the climatology.

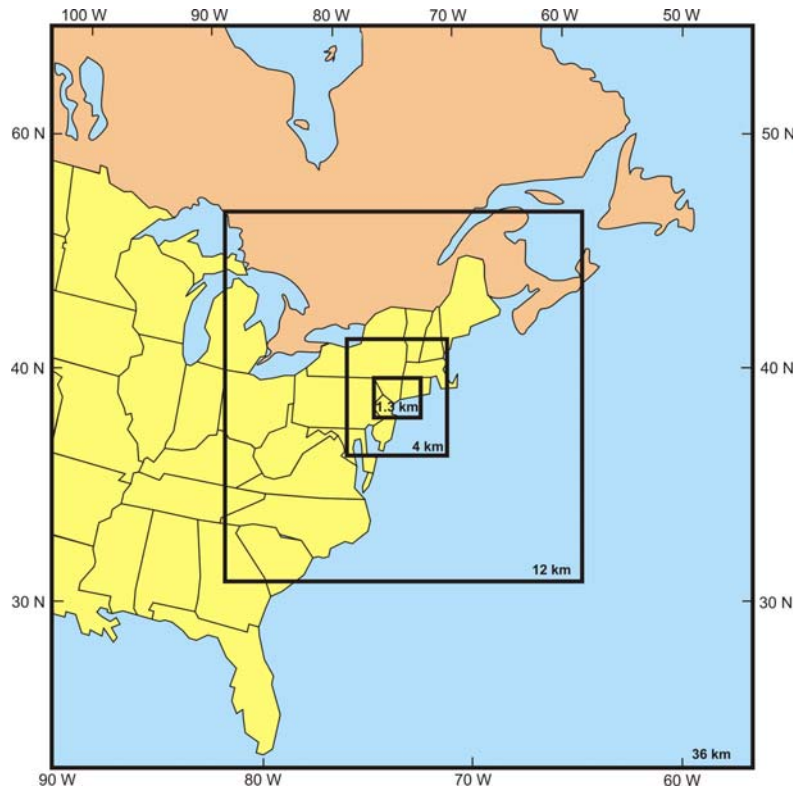


Figure F-1. MM5 36 km, 12 km, 4 km, and 1.3 km domains.

The standard MM5 input files for the land surface module (i.e. USGS, 1993) assign each grid box a single land surface type. Within vegetated grid boxes, a vegetation fraction intensity – a measure of the intensity of vegetative processes such as photosynthesis – was specified according to a vegetated fraction dataset developed by Chris Small of Lamont Doherty Earth Observatory (Small, 2001) (Table F-1). Note that this dataset serves as a proxy for vegetation fraction intensity, as it actually represents the fractional area of a pixel that is vegetated and not the intensity of the vegetated area. Furthermore,



the values represent only illuminated vegetation not actual vegetation because optical satellite sensors can only measure reflected light.

Table F-1. MM5 vegetation specification

	Land Surface	Vegetation Intensity
Outside NYC	USGS, 1993	Chris Small
Inside NYC	EMERGE database	Trees=0.9/Grass=0.5

Within New York City, MM5 was run at 1.3 km grid resolution (initialized and forced with input from the 4 km domain) and the Myeong et al. (2003) database was used to specify a percent area *impervious*, a percent area *grass*, a percent area *trees*, and a percent area *water* within each grid box to achieve sub-grid resolution of the different land surface types. The Myeong et al. (2003) database has a resolution of 3 meters and separate categories for grass and trees. All trees were assumed to be deciduous and the vegetation fraction intensity of tree cover was assumed to be 90%. The vegetation fraction intensity of grass was assumed to be 50%. The selected intensities were intended to capture the greater amount of evapotranspiration from a tree-covered surface as compared to a grass-covered surface. A comparison of the model parameters used in this study and model parameters from previous studies is given in Table F-2.

A weighted average of MM5 surface temperature and 2-meter air temperature was compared to observations. Based on RMSE optimization, surface temperature was assigned a weight of 30% and air temperature a weight of 70%. Comparisons between the simulations and observations showed that the model did an excellent job of simulating temperatures over the heat wave days (Figure F-2; Tables F-3, F-4, and F-5). At Central Park for example, the average error for HW3 hours is +1.8°F (1.0°C), the RMSE is 3.0°F (1.7°C) and the correlation over time is 0.94. There are larger errors at JFK due to problems with the simulation of sea-breezes. JFK is situated just off the ocean and thus is subjected to more sea-breezes than the other stations used in this study. For example, during HW1, a sea-breeze was simulated on July 4<sup>th</sup> which kept the temperatures down, but the observations did not show much of a sea-breeze on that day. MM5 is known to have a sea-breeze bias and the model warms and cools early. During model evaluation, less emphasis was placed on the WeatherBug data relative to the NWS sites because there is a lack of uniformity in the WeatherBug data (see Appendix B).

Table F-2. Comparison of model parameters from published urban heat island mitigation studies.

Parameter	Surface Type	Current Study, 2006	Luley & Bond, 2002	Taha et al. 2000
Grid cell size		1.3 km	4 km	4 km
Domain				
Leaf area index (LAI)	Trees	6		
Leaf area index (LAI)	Grass	1		
Leaf area index (LAI)	Impervious	0		
Vegetated fraction intensity	Trees	0.9		0.50
Vegetated fraction intensity	Grass	0.5		0.60
Vegetated fraction intensity	Impervious	0.0		0.05-0.20
Minimum canopy resistance	Trees	100 s m-1		
Minimum canopy resistance	Grass	40 s m-1		
Minimum canopy resistance	Impervious	X		
Shortwave albedo	Trees	0.16	0.16	0.15
Shortwave albedo	Grass	0.27	0.18	0.18
Shortwave albedo	Impervious	0.15	0.118 – 0.145	0.14-0.20
Longwave emissivity	Trees	0.93	0.93	
Longwave emissivity	Grass	0.985	0.92	
Longwave emissivity	Impervious	0.88	0.93 – 0.94	
Roughness length	Trees	50 cm	50 cm	350 cm
Roughness length	Grass	12 cm	20 cm	12 cm
Roughness length	Impervious	5 cm	60 – 200 cm	35 – 150 cm
Initial soil moisture (L& B: moisture availability)	Trees	all layers 90% saturation (v/v)	30%	0.20 (20%)
Initial soil moisture (L& B: moisture availability)	Grass	top layer 50% saturation; others 90% (v/v)	25%	0.30 (20%)
Initial soil moisture (L & B: moisture availability)	Impervious	all layers desiccated	11.9 – 16.8%	

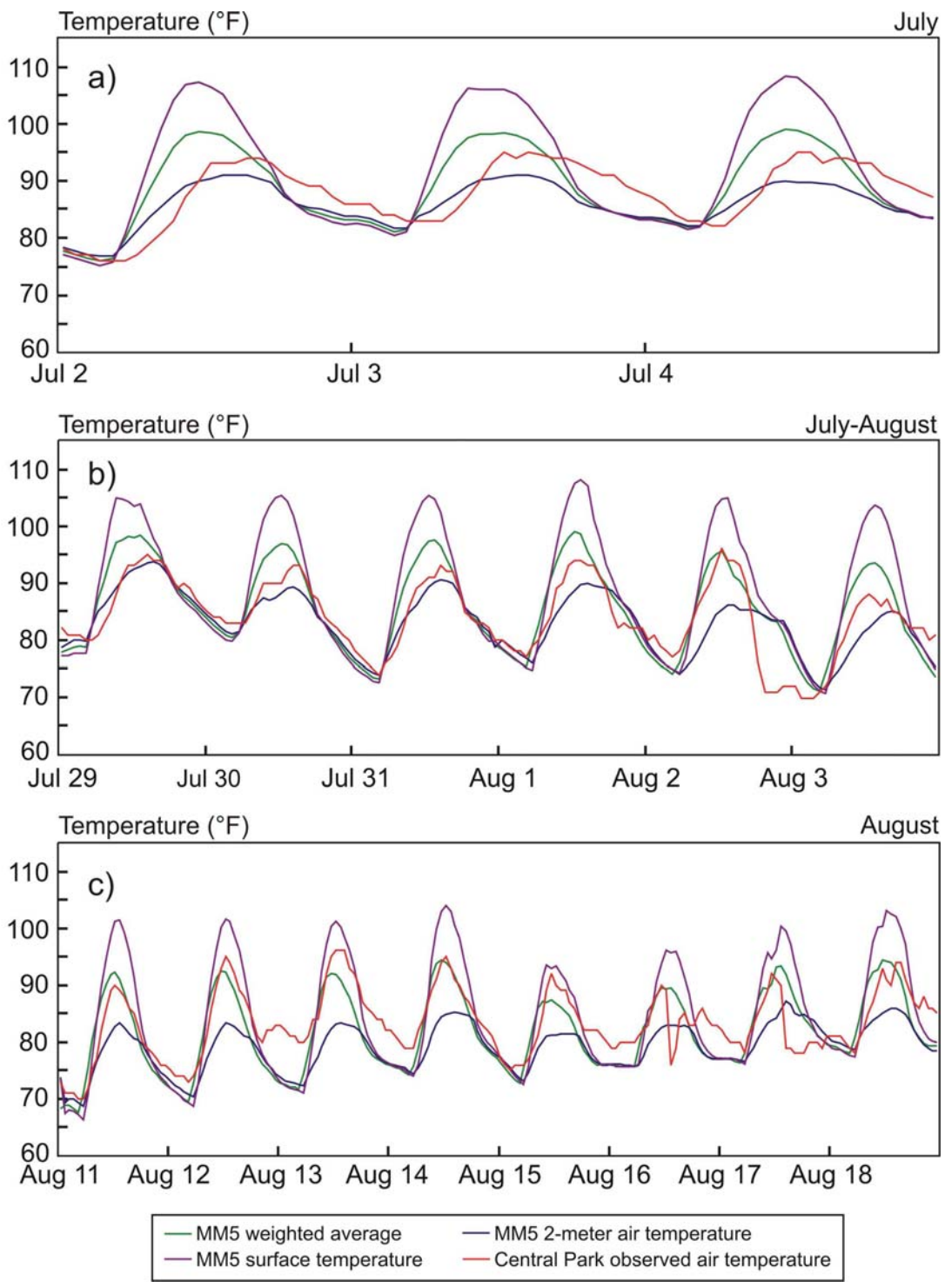


Figure F-2. Observed Central Park data and MM5 base weighted average near-surface air temperatures.

Table F-3. Evaluation of MM5 results for HW1, July 2-4, 2002.

<b>Weighted Average Near-Surface Air Temperature (°F)</b>	<b>MM5 1km</b>	<b>Observed</b>	<b>Ave. Error</b>	<b>RMSE</b>	<b>Correlation Coefficient</b>
Central Park	89.44	87.75	1.69	4.21	.75
LGA	89.53	88.32	1.21	4.70	.70
JFK	86.50	86.05	0.45	4.79	.71
Riverside/Mid-Manhattan	90.36	88.74	1.62	4.03	.81
Maspeth	88.84	89.71	-0.86	4.03	.78
Fordham	87.87	90.19	-2.32	4.45	.76
Crown Heights	88.02	89.08	-1.06	4.25	.76
Ocean Parkway	88.03	91.85	-3.82	6.12	.71
Lower Manhattan East	88.56	85.69	2.86	4.61	.83
Mean	88.57	88.59	-0.02	4.57	.76

Table F-4. Evaluation of MM5 results for HW2, July 29 – August 3, 2002.

<b>Weighted Average Near-Surface Air Temperature (°F)</b>	<b>MM5 1km</b>	<b>Observed</b>	<b>Ave. Error</b>	<b>RMSE</b>	<b>Correlation Coefficient</b>
Central Park	84.38	83.91	0.47	3.89	.82
LGA	84.47	84.76	-0.29	3.96	.81
JFK	84.40	82.63	1.76	4.03	.85
Riverside/Mid-Manhattan	85.33	84.43	0.90	4.52	.76
Maspeth	83.73	83.01	0.72	4.36	.78
Fordham	83.84	86.41	-2.57	3.64	.84
Crown Heights	83.75	83.30	0.45	3.94	.81
Ocean Parkway	83.61	87.21	-3.60	3.92	.85
Lower Manhattan East	M	M	M	M	M
Mean	84.18	84.45	-0.27	4.03	.82

Table F-5. Evaluation of MM5 results for HW3, August 11 – 18, 2002.

<b>Weighted Average Near-Surface Air Temperature (°F)</b>	<b>MM5 1km</b>	<b>Observed</b>	<b>Ave. Error</b>	<b>RMSE</b>	<b>Correlation Coefficient</b>
Central Park	84.90	83.14	1.76	2.99	.94
LGA	84.79	82.98	1.82	3.35	.93
JFK	82.78	77.85	4.93	5.24	.96
Riverside/Mid-Manhattan	85.71	83.03	2.68	4.61	.86
Maspeth	84.18	80.44	3.74	4.95	.89
Fordham	82.89	84.61	-1.73	3.51	.90
Crown Heights	83.17	79.81	3.37	4.79	.85
Ocean Parkway	83.39	82.83	0.56	3.49	.84
Lower Manhattan East	81.99	79.56	2.43	4.27	.77
Mean	83.75	81.59	2.18	4.14	.88